TRACER DIFFUSION IN WHISKER-PRONE TIN PLATINGS

Thomas A. Woodrow, Ph.D.
Boeing Phantom Works
Seattle, WA, USA
thomas.a.woodrow@boeing.com

ABSTRACT

Surprisingly, after almost 60 years of research into the causes of tin whisker formation, very little experimental evidence exists to verify some of the basic mechanisms believed to be involved in whisker growth. Long range diffusion of tin is thought to occur in order to supply the amount of tin required to form a whisker, however, no direct experimental data to support the long range diffusion hypothesis has been generated. The objective of this study was to use tin isotopes and secondary ion mass spectroscopy (SIMS) to evaluate the room temperature self-diffusion of tin within whisker-prone tin platings (bright and matte tin). Tin diffusion was monitored through the plating thickness and also parallel to the substrate by using SIMS surface analysis and depth profiling techniques. The amount of each isotope that was incorporated into the whiskers that formed and variations in the isotopic percentages along the length of each whisker were quantified (before and after sputtering of the whiskers).

Key Words: tin whiskers, isotopes, diffusion

BACKGROUND

The propensity of pure tin platings to form tin whiskers has been known since the 1940's[1,2]. Tin whiskers have been found to form on a wide variety of tin-plated substrates under a wide range of environmental conditions[1,2,3,4].

Numerous mechanisms for whisker formation and growth have been postulated[5-19]. The earlier publications focused on dislocation theories to explain whisker growth[5,6,7,11] while more recent publications tend to focus on recrystallization events to explain whisker growth[17,18]. One major driving force for whisker growth is believed to be compressive stress within the tin plating. One source of compressive stress (at least for copper alloy substrates) is believed to be the formation of a tin-copper intermetallic at the tin plating/copper substrate interface[12,14,15,16]. The relative importance of micro- and macro-stresses within tin platings is not well understood and is still the topic of much debate[2].

Surprisingly, after almost 60 years of research into the causes of tin whisker formation, very little experimental evidence exists to verify some of the basic mechanisms believed to be involved in whisker growth. Long range diffusion of tin is thought to occur in order to supply the amount of tin required to form a whisker, however, no direct experimental data to support the long range diffusion hypothesis has been generated. It is not clear if movement of tin to the whisker occurs by lattice diffusion, grain boundary diffusion, surface diffusion or a combination thereof. Diffusion rates of tin within whisker-prone systems have not been measured nor have the effects of intermetallic growth on diffusion of tin within the plating been explored. It is not clear if whisker growth is initiated within the plating or occurs only on the surface of the plating.

An elegant study by Kehrer and Kadereit[20] in 1970 explored diffusion within tin platings on glass substrates. A continuous layer of inactive tin was deposited in a vaccum (5 x 10^{-7} Torr) on top of a spot of radioactive tin. The radioactive tin was observed to diffuse towards the surface of the plating after 20 hours at 60°C. No large scale diffusion parallel to the substrate was observed and no whiskers grew on this plating. In contrast, tin layers deposited at higher pressures (1 x 10^{-4} Torr) showed no diffusion of radioactive tin towards the surface of the plating even after an annealing time of 80 hours at 60°C. Tin whiskers did grow on the tin deposited at the higher pressure, however, and these whiskers did contain radioactive material even though no diffusion of radioactive tin within the plating was detected.

Additional studies of tin self-diffusion using tin isotope tracers should be conducted as such studies may verify many of the assumptions that have been made concerning the basic mechanisms underlying tin whisker growth. Development of more sophisticated technologies for conducting tracer diffusion studies (such as secondary ion mass spectroscopy (SIMS) imaging and depth profiling) have made it possible to carry the concepts developed by Kehrer and Kadereit to the next level.

OBJECTIVE

The objective of this study was to use tin isotopes and SIMS to evaluate the room temperature self-diffusion of tin within whisker-prone tin platings (bright and matte tin). Tin diffusion was monitored through the plating thickness and also parallel to the substrate by using SIMS surface analysis and depth profiling techniques. The amount of each isotope that was incorporated into the whiskers that formed and variations in the isotopic percentages along the length of each whisker were quantified (before and after sputtering of the whiskers).

APPROACH AND RESULTS

The coupons to be electroplated were sheared from brass Hull Cell cathodes (Kocour Company, Chicago, IL, Part No.

050062). Each coupon was 1.5 in. long by 0.25 in. wide by 0.015 inches thick. The composition of the brass was 69.325% Cu; 30.500% Zn; 0.007% Pb; and 0.038% Fe. The brass sheet comes from the manufacturer highly polished on one side and was used without further polishing. Before electroplating, the coupons were degreased by rinsing with methylene chloride.

Tin isotopes (Sn^{120} and Sn^{118}) were purchased from a commercial source and fashioned into anodes for electroplating. After fabrication, the anodes were analyzed by time-of-flight secondary ion mass spectroscopy (TOF-SIMS) to verify their isotopic composition. Before TOF-SIMS analysis, each anode was lightly sputtered with a Ga^+ beam to remove tin hydrides from the surface. The relative amount of each tin isotope in the anodes was then determined by analyzing the secondary positive ions produced from rastering a 50 micron by 50 micron area with the Ga^+ beam for four minutes. The isotopic composition of the anodes is given in Table 1.

In this study, time-of-flight secondary ion mass spectroscopy was performed using a Physical Electronics PHI TRIFT III equipped with a pulsed Ga^+ liquid metal ion gun operated at 12 kV (with a DC current of 600 pA) and a Cs^+ sputtering gun operated at 2 kV (with a current of 200 nA). The Ga^+ beam was used for surface analyses and was rastered over a 50 micron by 50 micron area with a penetration depth of approximately 10 Angstroms. The Cs^+ beam was used for sputtering and was rastered over a 400 micron by 400 micron area. Depth profiles were done by alternating the Cs^+ sputtering beam with the Ga^+ analysis beam. The secondary ions were accelerated to ±3kV by applying a bias on the sample. The charging effect was neutralized by a pulsed low-energy electron flood gun. The Cs^+ beam was positioned 42 degrees off normal; the Ga^+ beam was positioned 35 degrees off normal; and the two beams were 180 degrees opposed to each other.

The tin isotopes were electroplated onto the brass coupons in a 10 ml cell with magnetic stirring. Sulfuric acid based electrolytes were used and the tin was plated directly from the anodes onto the coupons without addition of tin salts to the electrolytes.

Matte tin platings were produced by using the following electrolyte formulation[21] and a current density of 4.6 A/sq.ft.

   5 grams conc. sulfuric acid
   6.15 grams 4-hydroxybenzenesulfonic acid
   0.2 grams gelatin
   0.1 grams 2-naphthol
   95 ml deionized water

Bright tin platings were produced by using the following electrolyte formulation and a current density of 9.2 A/sq.ft. A proprietary grain refiner from Benchmark Products (Indianapolis, IN) was used.

   10 ml conc. sulfuric acid
   2.0 ml Benchbrite® T-150
   0.75 ml Benchbrite® T-151
   93 ml deionized water

A positive photoresist was used to mask the coupons so that only the end of each coupon (0.25 in. by 0.25 in.) was plated. The coupons were then plated with approximately one micron of Sn^{118} isotope and the resist was removed using acetone. This process resulted in a very straight line of tin where the resist had been.

Plater's tape was then used to mask off the same end of each coupon so that only a 0.375 in. by 0.25 in. area would be plated. The coupons were then plated with a second layer of tin (Sn^{120} isotope) to a thickness of approximately one micron. This process yielded a double layer of the two tin isotopes next to a single layer of Sn^{120} on the same coupon (see Figure 1).

The thickness of each plating layer was determined by one or more of the following techniques: profilometer measurements of the as-plated layer; profilometer measurements of a crater sputtered through the layer; microsections made by focused ion beam (FIB); and sputtering times combined with the sputtering rate for tin as measured in this study (4.5 Angstroms/sec). All thicknesses reported are as-plated. The thicknesses reported for the matte tin platings are an average since the plating surfaces were very irregular.

The bright tin plating was very shiny to the naked eye. An SEM photo of the bright tin plating surface is shown in Figure 2. After aging at 23°C for 109 days, a FIB was used to create a microsection of the plating which revealed that the grains of the bright tin were columnar (Figure 3). In addition, both layers of the tin isotope bilayer can be seen upon close inspection of Figure 3. Some voiding can also be seen (predominately at the intermetallic/brass interface).

An Auger map of a second FIB microsection on a bright tin plated specimen (67 days after plating) revealed that zinc had migrated to the surface of the tin from the brass substrate and verified that an irregular intermetallic layer had formed between the tin and the brass substrate (see Figures 4 and 5). Interestingly, nodules of tin formed on the wall of the FIB microsection within 30 minutes (under vacuum) and continued to grow over the next 18 hours (see Figures 6 and 7). It is possible that the Ga^+ FIB beam (25 kV, 10-1000 pA) or the SEM electron beam (10 kV, 10 nA) created nucleation sites for nodule formation on the fresh tin surface.

Whiskers began to grow on the bright tin platings within 10 days. Ultimately, only a few whiskers grew on each coupon but they tended to be very long (up to 2000 microns in length). The bright tin whiskers emanated from large nodules which were believed to have formed prior to whisker growth.

2

TOF-SIMS depth profiling of the bright tin plating was performed using a Cs^+ beam for the sputtering and a Ga^+ beam for production of secondary ions as described above. The Cs^+ beam was on for 30 seconds followed by 7 seconds of analysis using the Ga^+ beam. The beams were alternated until the desired crater depth was achieved.

The secondary positive ion yields of tin under Ga^+ bombardment were too low to give optimum depth profiles. Much better results were obtained by analyzing for $SnCs^+$ ions. These ions are generated by the combination of a secondary neutral Sn^0 with a resputtered Cs^+ ion in the near surface region above the specimen. This technique also has the advantage in that it minimizes the matrix effect. A matrix with a non-uniform composition can cause the ion yield of a given sputtered element to vary by several orders of magnitude as the matrix is sputtered (i.e., the matrix effect). When working in the $SnCs^+$ mode, the emission process for Sn^0 is decoupled from the subsequent $SnCs^+$ ion formation resulting in a drastic decrease in the matrix effect[22].

The first data point for each depth profile was discarded when the data was plotted. Since the first data point was generated using the Ga^+ beam only, there was no Cs^+ present to generate $SnCs^+$ ions for detection.

Figure 8 shows the results of the depth profiling of the isotope double layer on a bright tin specimen (Sample 90) three days after plating. Figure 9 is the same profile but only the tin isotope data is shown. Note that zinc has already migrated to the surface of the tin from the brass substrate. This migration of zinc probably occurred via the grain boundaries as no significant amount of zinc was detected in the tin lattice. Interestingly, Sn^{118} can already be found through the entire depth of the upper Sn^{120} layer and Sn^{120} can be found through the entire depth of the lower Sn^{118} layer. The Sn^{118} must have diffused up the grain boundaries and then diffused into the tin lattice to give a relatively constant concentration of Sn^{118} within the grains of the upper Sn^{120} layer (see Figure 9, Line DE). Similarly, Sn^{120} must have diffused down the grain boundaries and then diffused into the grains of the lower Sn^{118} layer. Diffusion of tin along the grain boundaries is known to be very rapid with a diffusion coefficient[23] of 1.3×10^{-8} cm^2/sec at 25°C. The time required for tin to penetrate a distance x into the grain boundaries at 25°C can be estimated from x = $(2Dt)^{1/2}$ where x is the mean diffusion length in one dimension, t is the time in seconds and D is the grain boundary diffusion coefficient. Using D = 1.3×10^{-8} cm^2/sec and x = 3.1 microns (the approximate thickness of the bright tin plating), t equals 3.7 seconds.

Figure 9 also shows that a large amount of Sn^{118} has already migrated to the surface of the double layer via the grain boundaries and has begun to diffuse down into the lattice of the Sn^{120} layer (see Figure 9, Line AB). Diffusion along a surface is known to be more rapid than diffusion along a grain boundary, therefore, any Sn^{118} that reached the surface

would rapidly diffuse to cover the surface of the adjacent grains with a relatively constant concentration of Sn^{118}.

Similarly, Sn^{120} diffused to the brass/Sn^{118} interface via the grain boundaries and then diffused up into the lattice of the Sn^{118} layer.

Figure 10 shows a schematic of how the two tin isotopes have diffused along the grain boundaries, along the plating surface and into the grains. The corresponding idealized depth profile is also shown.

From Figure 9, we can see that the near surface concentration of Sn^{118} is approximately 43%. This is the relative percentage expected when the two isotope layers are completely mixed. It is believed that this near surface concentration of Sn^{118} was attained in less than two hours after plating. Assuming that a constant near surface composition was achieved soon after plating, the lattice diffusion coefficient of the bright Sn can be approximated[24] by Equation 1 where c is the concentration of the diffusing Sn^{118} at time t and penetration distance x; c_s is the constant surface concentration of the Sn^{118}; and c_o is the original concentration of Sn^{118} in the Sn^{120} layer (i.e., zero). The diffusion coefficient of the diffusing tin is D_t.

$$\text{Equation 1} \qquad \frac{c - c_o}{c_s - c_o} = 1 - erf\left(\frac{x}{2(D_t t)^{1/2}}\right)$$

In Figure 9, at the point where the concentration of the diffusing Sn^{118} falls to zero (Point B), $(c - c_o)/(c_s - c_o) = 0$ and $D_t = \{(x/4.8)^2\}/t$. At this zero concentration point, the sputter depth (x) is 9×10^{-5} cm and the diffusion time (t) is $2.6 \times 10^{+5}$ sec (i.e., 3 days). This yields a room temperature lattice diffusion coefficient of 10^{-15} cm^2/sec which is two to three orders of magnitude larger than the lattice diffusion coefficient of tin (10^{-17} to 10^{-18} cm^2/sec at 25°C) as reported in the literature [25,26,27,28]. It should be noted that the metals that commonly form whiskers (i.e., Sn, Zn and Cd) have room temperature lattice diffusion coefficients in the range of 10^{-15} to 10^{-18} cm^2/sec. Other common metals that do not normally form whiskers have exceedingly low room temperature lattice diffusion coefficients[29] in the range of 10^{-33} to 10^{-75} cm^2/sec (see Table 2). Although it is probable that diffusion of tin to the whisker takes place through the grain boundaries, the tin must first diffuse from the lattice into the boundaries. Therefore, whisker growth rates may ultimately be controlled by the lattice diffusion rate.

Figures 12 and 13 show depth profile data for the bright tin double layer (Sample 90) after it was aged at room temperature for 66 days. The two isotope layers are almost completely mixed. The expected relative percent of each isotope after complete mixing occurs is shown by the dashed lines in Figure 13 (i.e., 57% Sn^{120} and 43% Sn^{118}). The relative percent of each isotope present was calculated by measuring the areas under the depth profile plots. The depth profiling data demonstrates how quickly tin can

diffuse within the lattice of the bright tin plating. In addition, the mixing of the isotopes within the grains did not appear to be accompanied by an obvious change in the size of the grains.

Figures 14 and 15 show depth profile data for a bright tin isotope double layer on a different sample (Sample 89) after it was aged at room temperature for 187 days. The two isotope layers on this specimen are completely mixed. The relative percent of each isotope in this sample (Sample 89) was not the same as for Sample 90 since the thicknesses of the original plated layers were not identical.

Depth profiling was also conducted on the bright Sn^{120} single layer in order to determine if diffusion of Sn^{118} occurred parallel to the coupon surface (from the double isotope layer into the single isotope layer).

Figures 16 and 17 show the depth profile data for a single bright tin layer at 3 days after plating (Sample 90). The point of analysis was centered 220 microns from the single layer/double layer interface. The average amount of Sn^{118} in the plating (relative to total Sn^{120} plus Sn^{118}) was 1.1±0.6%. This number was obtained by averaging 34 data points. The amount of Sn^{118} detected was slightly higher than the percent of Sn^{118} in the Sn^{120} anode used to plate the single layer (i.e., 0.13±0.3% per Table 1). This suggests that a small amount of Sn^{118} may have diffused into the Sn^{120} single layer from the interface. Unfortunately, as the quantity of Sn^{118} measured was at the detection limits of the depth profiling technique, it can not be said with confidence that any significant lateral diffusion of Sn^{118} occurred.

Figures 18 and 19 show a depth profile on the same coupon at 66 days after plating (centered 280 microns from the interface). After 66 days, the average amount of Sn^{118} in the plating (relative to Sn^{120}) was 1.2±0.6%, which is essentially unchanged from the analysis conducted at 3 days.

An SEM photograph of the matte tin plating surface is shown in Figure 20. The matte tin had a very irregular surface composed of striated grains with a diameter of approximately 2 microns. Short whiskers were already growing on the matte tin within 20 days after plating (see Figure 21) and profuse whisker growth was noted within 44 days. The whiskers had a diameter equivalent to the grain size and no nodule growth prior to the formation of whiskers was observed.

After aging at 23°C for 158 days, a FIB was used to create a microsection of the matte tin double layer which revealed that the grains of the matte tin were approximately equiaxed (Figure 22). The matte tin differed from the bright tin in that separate isotope layers could not be visually distinguished even though mixing of the isotopes was incomplete at this time.

Additional FIB microsections of whiskers on the matte tin platings are shown in Figure 23. The whiskers appear to emanate from the surface of the platings and not from the plating/substrate interface.

An Auger map of a second FIB microsection on the matte tin plating (116 days after plating) revealed that zinc had migrated into the grain boundaries of the tin from the brass substrate and also verified that a very thick and irregular intermetallic layer had formed between the tin and the brass substrate (see Figures 24 and 25). Some zinc was noted on the plating surface and on the surface of a whisker adjacent to the FIB microsection (Figure 26). Also of note is the layer of tin between the intermetallic layer and the brass substrate. It is not clear how this layer formed. One explanation would be the formation of Kirkendall voids which later became filled with tin either by diffusion or by ablated material produced during the FIB processing.

Auger analysis of a whisker and of the adjacent matte tin plating surface showed no zinc on either at 26 days after plating but oxygen was detected on both (see Figure 27).

TOF-SIMS depth profiling of the matte tin plating was also conducted, again analyzing for $SnCs^+$ ions. The first data point for each depth profile was again discarded when the data was plotted since there was no Cs^+ present to generate $SnCs^+$ ions for detection.

Figure 28 shows the results of the depth profiling of the isotope double layer on a matte tin specimen (Sample 52) ten days after plating. Figure 29 is the same profile but only the tin isotope data is shown. The matte tin depth profile looks remarkably similar to that from the bright tin double layer, especially when you consider the non-uniform thickness of the matte tin plating. Note that zinc has already migrated into both isotope layers from the brass substrate (with the Zn probably residing mainly between the grains). As with the bright tin depth profiles, Sn^{118} can already be found through the entire depth of the upper Sn^{120} layer and Sn^{120} can be found through the entire depth of the lower Sn^{118} layer. Again, the Sn^{118} must have diffused up the grain boundaries and then diffused into the tin lattice to give a relatively constant concentration of Sn^{118} within the upper Sn^{120} layer. Similarly, Sn^{120} must have diffused down the grain boundaries and then diffused into the lower Sn^{118} layer.

As with the bright tin, a large amount of Sn^{118} has already migrated to the surface of the double layer and has begun to diffuse down into the lattice of the Sn^{120} layer (see Figure 29). The lattice diffusion coefficient of the matte tin was estimated as 10^{-17} cm^2/sec by the same method used for the bright tin.

Figures 30 and 31 show depth profile data for the matte tin isotope double layer (Sample 52) after it was aged at room temperature for 117 days. In contrast to the bright tin plating, the two isotope layers are far from being completely mixed. Due to the larger dimensions of the matte tin grains compared to the bright tin grains, it takes much longer for

4

tin to diffuse from the grain boundaries and through the entire thickness of a grain. The relative percent of each isotope in the Sample 52 double layer after complete mixing occurs is expected to be 48% Sn^{120} and 52% Sn^{118} based on the areas under the depth profile isotope plots (at 10 days after plating).

Figures 32 and 33 show the depth profile data for a single matte tin layer at 10 days after plating (Sample 52). The point of analysis was centered 2650 microns from the single layer/double layer interface. The average amount of Sn^{118} in the plating (relative to Sn^{120}) was 0.7±0.6%. This number was obtained by averaging 34 data points. The amount of Sn^{118} detected was slightly higher than the percent of Sn^{118} in the Sn^{120} anode used to plate the single layer (i.e., 0.13±0.3% per Table 1) but it could not be unequivocally determined if Sn^{118} had diffused into the Sn^{120} single layer from the interface due to the error in the measurements.

Figures 34 and 35 show a second depth profile on the same coupon (Sample 52) at 10 days after plating (this time centered 290 microns from the interface). The average amount of Sn^{118} in the single layer (relative to Sn^{120}) at this location was 0.6±0.6%. Again, it could not be determined if Sn^{118} had diffused into the Sn^{120} single layer from the interface due to the error in the measurements .

Figures 36 and 37 show a depth profile on the same coupon (Sample 52) at 117 days after plating (centered 315 microns from the interface). After 117 days, the average amount of Sn^{118} in the single layer (relative to Sn^{120}) was 0.8±0.6%, which was essentially the same as the concentration detected at 10 days and 290 microns from the interface.

Figures 38 and 39 show depth profile data for a second matte tin isotope double layer (Sample 62) at 3 days after plating. The relative percent of each isotope in the Sample 62 double layer after complete mixing occurs is expected to be 41% Sn^{120} and 59% Sn^{118} based on the areas under the depth profile isotope plots.

Figure 40 shows a long whisker on the matte Sn^{120}/Sn^{118} double layer (Sample 62). An ion image of this whisker (Figure 41) was generated by rastering the Ga^+ beam over the analysis area (150 microns by 150 microns) for 4 minutes and creating a false color map of the positive ions detected. The Ga^+ liquid metal ion gun was operated at 22 kV (with a DC current of 600 pA) for the creation of the ion image because these conditions allowed better focusing of the Ga^+ ion beam. Although Figure 41 only shows where Sn^{120} is present on the surface, a complete record of all masses detected for each pixel of the image was stored for later processing. Note than the whisker is much brighter than the plating surface due to an enhanced ion yield from the whisker. No explanation for this phenomenon can be offered at this time.

Line scans were drawn across the ion image near the base and the tip of the whisker (see the green lines in Figure 41).

The ion counts for Sn^{120} and Sn^{118} along the length of each line scan are shown in Figures 42 and 43. Interestingly, the relative percentages of the two isotopes were the same at the base and the tip of the whisker (with a distance of 80 microns between the measurement points).

Similar measurements were made on eight more whiskers growing on the double layer of two different matte tin coupons (Samples 62 and 52). These whiskers were located well away from the single layer/double layer interface. In every case, the relative percentages of the two isotopes were the same at the base and tip of each whisker (see Table 3 and Figure 44). The absolute experimental error in the line scan measurements was estimated to be ±2 percent.

In addition to having a consistent isotopic composition along the length of each whisker, the relative percentages of each isotope on the surface of each whisker was the same as the percentages expected within the double layer when the two isotope layers become completely mixed. This was true even though the isotope layers within the matte tin double layers were far from being completely mixed when these whiskers formed (see Figure 31). This observation suggests that the tin diffused to the whiskers via grain boundary diffusion which allowed the tin isotopes to mix before becoming part of the whisker.

Similar measurements on four whiskers on a bright tin plating double layer also showed that the relative percentages of the two isotopes were the same at the base and the tip of each whisker (Table 3 and Figure 44). However, it should be noted that the bright tin platings did not grow whiskers in the same manner as the matte tin platings. The bright tin whiskers emanated from large nodules which were believed to have formed prior to whisker growth. Figure 45 shows an FIB microsection of a nodule on the bright tin plating. The grains composing the nodule are much larger than the grains in the plating and appear to contain more material than could be supplied by the plating directly under the nodule. This implies that the nodule was formed by the long range migration of tin and could be considered a form of recrystallization. This is not a new observation. Gaylon and Palmer have published a very instructive series of photographs that clearly show the same phenomenon on bright tin[30]. The fact that the bright tin whiskers in this study grew from large nodules that were formed by a recrystallization process implies that the isotopes should be well mixed within the nodules and any whiskers growing from the nodule might be expected to have the same isotopic composition along their entire length. Data from the surface analyses of several nodules on the bright tin plating can be found in Table 4.

Positive ion scans were also generated for whiskers on the Sn^{120} single layer (both matte and bright tin). As with the whiskers on the double layer, the isotopic composition at the base and the tip of each whisker was the same (Table 5 and Figure 46). The amount of Sn^{118} in each whisker was determined by the distance between the whisker base and

5

the single layer/double layer interface (i.e., the source of the Sn^{118}).

Figure 47 is an SEM image of nine whiskers growing on the matte tin plating. Whiskers 3A, 3F, 3G and 3I were fully formed at 45 days after plating. Some of the whiskers are growing on the single isotope layer and some on the double isotope layer. The interface between the single and double isotope layers is shown by the dashed white line and the base of each whisker is indicated with a green arrow.

Figures 48 and 49 show the Sn^{120} and Sn^{118} positive ion images of the nine whiskers, respectively. Figure 50 shows Sn^{120} and Sn^{118} line scan data for Whiskers 3C (the tip) and 3D (the base). Notice that Whisker 3C contained much less Sn^{118} than Whisker 3D since the base of Whisker 3C is on the single layer far from the single layer/double layer interface which was the source of the Sn^{118}.

Figure 51 shows a plot of the amount of Sn^{118} on the surface of each whisker versus its distance from the interface as determined by TOF-SIMS analysis. The analyses were conducted 108 days after plating of the sample. Not surprisingly, the whiskers on the double isotope layer had significant amounts of Sn^{118} on their surfaces.

The whiskers on the single layer also had Sn^{118} on their surfaces and the amount of Sn^{118} decreased rapidly as the distance from the double layer increased (see Figure 51). This demonstrates that diffusion of Sn^{118} parallel to the substrate did occur. The amount of Sn^{118} detected on the whiskers appeared to plateau at approximately 5% as the distance from the single layer/double layer interface increased. The amount of Sn^{118} found on the whiskers at 108 days after plating was larger than the amount of Sn^{118} found within the matte tin plating by depth profiling. The depth profiling could not be performed on the same specimen used for the whisker analyses due to concerns about contaminating the whiskers during the sputtering process. Therefore, the depth profiling of the matte tin single layer was conducted on a second (comparable) specimen (at 117 days after plating and 315 microns from the single layer/double layer interface). The amount of Sn^{118} detected in the bulk of the plating (0.8±0.6%, see Figure 37) was much less than that detected on the whiskers. This suggests that the Sn^{118} reached the whiskers on the single layer by diffusion through the grain boundaries or across the plating surface and not by lattice diffusion.

A similar analysis of whiskers on the bright tin plating was not conducted because there were not enough whiskers to do so. In addition, the longer whiskers on the bright tin specimens were lost during the TOF-SIMS analysis. It is believed that the 3000V bias between the sample and the first lens within the mass spectrometer caused the longer whiskers to bend and then break off. This phenomenon was not as prevalent during analysis of the matte tin specimens.

It should be noted that depth profiling was conducted on some of the specimens (Samples 52 and 62) before whiskers had formed and were analyzed. There was no indication that the sputtering contaminated the surfaces of any whiskers that subsequently grew. After whiskers grew on a specimen, no further depth profiling was done until all whisker analyses were complete.

Surface analyses and depth profiles of both the matte and the bright tin were conducted between 254 and 337 days after plating to provide a better picture of how the Sn^{118} was diffusing parallel to and normal to the substrate. During the surface analyses, Sn^{118} and Sn^{120} positive ions were detected and quantified. These metallic ions were presumably formed by fragmentation of a surface oxide layer.

TOF-SIMS surface analyses were conducted at eleven separate locations (each 50 microns by 50 microns) on a matte tin specimen at 299 days after plating. This specimen (Sample 63) had not been exposed to any prior sputtering. Each spot was rastered with the Ga^+ beam for four minutes with positive ion detection (absolute experimental error was ±0.3%). The results of the surface analyses are shown in Figure 52. Large amounts of Sn^{118} were detected on the surface of the matte tin single layer which demonstrates that long range diffusion of Sn^{118} (over a distance of 3000 microns) had taken place.

Four depth profiles (each 400 microns by 400 microns) were then performed on the same matte tin specimen by sputtering with the Cs^+ beam and periodically analyzing for $SnCs^+$ ions. Each analysis was done by rastering the center of each depth profile crater with the Ga^+ beam for four minutes to yield sufficient ions. The amount of Sn^{118} within the single layer grains was less than the amount on the surface of the single layer (see Figures 52 and 53). This strongly suggests that the Sn^{118} must have reached the surface of the single layer by diffusion through the grain boundaries or across the plating surface and not by lattice diffusion. The amount of Sn^{118} detected increased greatly after sputtering of the double layer (to the level expected after both isotope layers had almost completely mixed, see Figures 52, 53 and 56). This suggests that the outer surface of the double isotope layer formed an oxide layer after plating which froze the relative percentage of Sn^{118} on the surface by inhibiting further diffusion. In addition, any isotopes that had rapidly diffused across the surface from the double layer onto the single layer were probably also frozen in composition by the formation of an oxide layer.

Similarly, TOF-SIMS surface analyses were conducted at ten separate locations (each 50 microns by 50 microns) on a bright tin specimen at 254 days after plating. This specimen (Sample 91) had not been exposed to any prior analysis or sputtering. Each spot was rastered with the Ga^+ beam for four minutes with positive ion detection (absolute experimental error was ±0.3%). The results of the surface analyses are shown in Figure 54.

Four depth profiles (each 400 microns by 400 microns) were then performed on the same bright tin specimen by sputtering with the Cs^+ beam and periodically analyzing for $SnCs^+$ ions. Each analysis was done by rastering the center of each depth profile crater with the Ga^+ beam for four minutes to yield sufficient ions. As with the matte tin, the amount of Sn^{118} detected increased greatly after sputtering of the double layer (see Figures 54, 55 and 57). This again suggests that the outer surface of the double isotope layer formed an oxide layer after plating which froze the relative percentage of Sn^{118} on the surface by inhibiting further diffusion. Not surprisingly, the amount of Sn^{118} within the double layer was lower in the area immediately adjacent to the single layer/double layer interface presumably due to lateral diffusion of Sn^{120} from the single isotope layer. After sputtering the single layer for 270 seconds, the amount of Sn^{118} detected increased greatly in the area adjacent to the single layer/double layer interface (from 0.8% to 6.1%, see Figures 54, 55 and 57). Again, we can speculate that removal of an oxide layer was required to reveal that substantial diffusion of Sn^{118} from the double layer into the single layer grains had taken place (over a distance of 580 microns). In contrast, comparable amounts of Sn^{118} were not observed within the matte tin single layer grains since there were far fewer grain boundaries to transport Sn^{118} from the double layer into the matte tin single layer and diffusion into the matte tin grains would take longer due to the larger size of the grains.

Unfortunately, detailed surface analyses were not conducted immediately after plating of the samples. The few additional surface analyses that were conducted during the course of this study are shown in Table 6. At the time the data was collected, the specimens had not been exposed to any prior analysis or sputtering. Again, each spot was rastered for four minutes using the Ga^+ beam with positive ion detection (absolute experimental error was ±0.3%). The data from these additional surface analyses corroborate the data from the more detailed maps conducted at 254 to 337 days after plating (Figures 56 and 57). We can see from the data in Table 6 that Sn^{118} has diffused to the surface of the matte tin double layer within a few days after plating. The amount of Sn^{118} detected on the surface of the matte tin double layer (Sample 63) at 3 days after plating was the same as the quantity detected at 299 days after plating (Figure 52). This supports the hypothesis that the isotopic composition on the surface was frozen by an oxide layer.

We have seen that the relative percentages of Sn^{120} and Sn^{118} on the surface of all whiskers analyzed remained relatively constant from the base of each whisker to its tip. In addition, we have seen that the isotopic percentages on the surface of the whiskers appear to be the same as the percentages expected within the double layer when the two isotope layers become completely mixed. This is true even when diffusion within the double layer is known to be incomplete. The question remains, "What are the isotopic percentages deep inside the whisker?" To answer this question, whiskers on both the matte and bright tin were sputtered and analyses conducted.

Whiskers on the matte tin double and single layers (Sample 62) were sputtered with the Cs^+ beam for 640 seconds. The sputtering removed 0.29 microns of tin from the surface of each whisker (based on the measured sputter rate for tin of 4.5 Angstroms/sec). Ion yields fell dramatically after sputtering which meant that the ion images of the whiskers were poor. It is not understood why the ion yields fell after sputtering but it may be due to the removal of the surface oxide layer or some surface contaminate that enhanced the ion yields. The poor ion yields required that a new technique for post-sputter analysis of the whiskers be developed. By alternating the Cs+ sputtering beam (10 seconds) with the Ga^+ analysis beam (7 seconds) over a four minute period and combining the negative ion counts, good ion images were obtained. This technique subjected each whisker analyzed to an additional 140 seconds of sputtering (i.e., a total sputtering time of 780 seconds with a removal of 0.35 microns of tin). To ensure that the new analytical technique was capable of giving the same results as the old technique (i.e., analyzing for positive ions using a four minute Ga^+ beam raster), a piece of tin foil with a normal isotopic composition was analyzed by both methods. The percent of Sn^{120} (relative to total Sn^{120} and Sn^{118}) as determined by the negative ion analysis was 57.9% which compared well to 57.7% as determined by the positive ion technique. The literature value for the relative percent of Sn^{120} in natural tin is 57.4%[31].

As with the pre-sputter analyses, line scans of the whisker ion images were performed. After sputtering, the relative percentages of Sn^{120} and Sn^{118} within many of the whiskers analyzed were still relatively constant from the base of each whisker to its tip (Table 7). However, for some of these whiskers, the isotopic percentages detected were no longer the same as the presputter percentages. The absolute experimental error in the line scan measurements was estimated to be ±2 percent (this error was due to the relatively low ion counts contained within the small area of the line scan).

Whiskers on the matte tin double layer (Whiskers 1, 5A, 5B and 5C) all showed a decrease in the percentage of Sn^{118} detected after sputtering. These whiskers were all located well away from the single layer/double layer interface and were all fully formed at 44 days after plating. The pre- and post-sputter data for these whiskers is also shown graphically in Figure 58.

Whiskers on the matte tin double layer that were located near the single layer/double layer interface (Whiskers 3B, 3D and 3E) also showed a decrease in the percentage of Sn^{118} detected after sputtering (Table 7).

In contrast, whiskers on the matte tin single layer that were located near the single layer/double layer interface (Whiskers 3F, 3G, 3H and 3I) showed little or no decrease

in the percentage of Sn^{118} detected after sputtering (Table 7). The pre- and post-sputter data for the whiskers located near the single layer/double layer interface is shown graphically in Figures 58 and 59.

The isotopic compositions of several whiskers and nodules on the bright tin plating were also determined after sputtering. These whiskers and nodules were sputtered for 1740 seconds (approx. 0.78 microns of tin removed) and then ion images of the isotopes were generated by alternating the Cs+ sputtering beam (10 seconds) with the Ga^+ analysis beam (7 seconds) over a four minute period and combining the negative ion counts. Line scans of the sputtered whisker and nodule ion images were conducted and the resulting data is shown in Tables 8 and 9 and in Figures 60-62.

For Whisker 7, the isotopic compositions before and after sputtering were very similar.

In contrast, the isotopic composition of Whisker 22 changed significantly after sputtering (however, the post-sputtering composition along the length of the whisker was constant).

DISCUSSION
A layer of Sn^{120} over a layer of Sn^{118} showed significant interdiffusion in just a few days. This interdiffusion of the double layer was observed for both the matte tin and the bright tin cases. The data suggested that Sn^{118} from the bottom layer diffused out of the grains and up the grain boundaries to the upper Sn^{120} isotope layer where it would enter the Sn^{120} grains by lattice diffusion (and vice versa for the Sn^{120}). This interdiffusion did not appear to be accompanied by a dramatic change in the size of the tin grains (matte or bright). The interdiffusion continued with time and the bright tin layers were close to an equilibrium mixture at 66 days after plating (Figure 13). In contrast, the matte tin layers were still not completely mixed at 117 days after plating (Figure 31). This behavior was to be expected as the bright tin plating had smaller grains than the matte tin and many more grain boundaries, both of which would allow the bright tin to reach an equilibrium mixture faster than the matte tin. In addition, significant amounts of Sn^{118} migrated to the surface of the Sn^{120} layer where it began to diffuse into the Sn^{120} lattice. An approximate room temperature lattice diffusion coefficient for the bright tin of 10^{-15} cm^2/sec was calculated which is two to three orders of magnitude larger than the lattice diffusion coefficient of tin in a near perfect crystal. Surface and depth profiling analyses of the double layer approximately three hundred days after plating revealed that the surface was deficient in Sn^{118} compared to the interior of the double layer. This was true for both the matte tin and bright tin cases (Figures 52-57). This suggests that the outer surface of the double isotope layer formed an oxide layer after plating which froze the relative percentage of Sn^{118} on the surface even though interdiffusion of the two isotope layers continued in the bulk of the plating. The amount of Sn^{118} detected on the surface of the matte tin double layer (Sample 63, Table 6) at 3 days

after plating was the same as the quantity detected at 299 days after plating (Figure 52). This supports the hypothesis that the isotopic composition on the surface was frozen by an oxide layer. If an oxide layer is indeed responsible for these observations, the depth profile data for bright tin shown in Figure 9 suggests that diffusion parallel to the substrate could still occur immediately under the oxide layer with subsequent diffusion into the lattice near the surface. This sub-oxide diffusion would explain the large concentrations of Sn^{118} found just below the surface of the bright tin double layer (Figure 9) compared to the smaller concentrations of Sn^{118} found on the surface of the bright tin double layer (Figure 54).

Lateral diffusion of Sn^{118} from the Sn^{120}/Sn^{118} matte double layer onto the matte Sn^{120} single layer was demonstrated by analyzing whiskers growing on the single layer. At 108 days after plating, Sn^{118} was detected on whiskers growing on the matte Sn^{120} single layer (Whiskers 3C, 3I, 3H, 3G and 3F in Figure 51) even though Sn^{118} levels within the single layer grains were much lower (Figure 37). Sputtering of the whiskers confirmed that large amounts of Sn^{118} were also present within the bulk of the whiskers (Figure 59). These findings demonstrated that not only did diffusion of Sn^{118} occur parallel to the substrate but the diffusion had to have occurred through the matte tin grain boundaries and not by lattice diffusion since the amount of Sn^{118} in the lattice was much less than in the whiskers. Long range diffusion of tin from many grains to supply tin for the growth of a whisker would explain why localized grain subsidence has rarely been observed. It should again be noted that no significant enlargement (recrystallization) of the matte tin grains was apparent before or after whisker formation.

Fisher, et. al.[32], proposed that the linear growth rate of a whisker was equal to $2DPV/(RTr_0)$ when the tin supplying the whisker was diffusing across a hemi-spherical shell with a large radius compared to the whisker radius. Setting $D=1.57 \times 10^{-18}$ cm^2/sec (the tin lattice diffusivity at $25°C^{[23]}$); P=1.47 psi (the pressure required for spontaneous whisker growth[32]); $V=16.3 cm^3$/mole; $R=1206$ psi·cm^3/mole·°K (the gas constant); T=298°K; and $r_0=1 \times 10^{-4}$ cm (the radius of a typical whisker), we get a growth rate of 2.1×10^{-10} Angstroms/sec at room temperature. This is many orders of magnitude less than the spontaneous growth rate actually observed for whiskers[3] (i.e., up to 0.4 Angstrom/sec). This supports the findings of this paper which suggest that the tin must be supplied to the whiskers by grain boundary or surface diffusion rather than by lattice diffusion.

Lateral diffusion of Sn^{118} into the grains of the Sn^{120} single layer (within both matte and bright tin) was also demonstrated by a series of surface and depth profile analyses (Figures 52-57) conducted approximately three hundred days after plating. The surface analyses proved that Sn^{118} had migrated a long distance (3000 microns) across the surface of the matte tin single layer. Depth profiling also found appreciable amounts of Sn^{118} in the

lattice of both the matte and bright tin single layers. The amount of Sn^{118} within the matte tin single layer lattice was less the amount on the surface of the matte tin single layer (see Figures 52 and 53). This strongly suggests that the Sn^{118} must have reached the surface of the matte tin single layer by diffusion through the grain boundaries or across the plating surface and not by lattice diffusion. In the case of the bright tin, the relative percent of Sn^{118} in the single layer lattice was very high (6.1%) near the single layer/double layer interface. This is not surprising as the small grain size and large number of grain boundaries in the bright tin plating would have facilitated diffusion of Sn^{118} from the double layer and into the single layer grains. It appears that large amounts of Sn^{118} penetrated farther into the matte tin single layer lattice (Figure 53) than into the bright tin single layer lattice (Figure 55), however. The surface analyses and depth profiles also revealed that the surface isotopic composition of the single layer was different from the lattice isotopic composition. This was true for both the matte tin and bright tin cases (Figures 52-57). This suggests that the outer surface of the tin formed an oxide layer after plating which froze the relative percentage of Sn^{118} on the surface even though diffusion of Sn^{118} continued in the bulk of the plating.

The isotopic compositions of whiskers that grew on the matte Sn^{120}/Sn^{118} double layer (**well away from the single layer/double layer interface**) were determined prior to and after sputtering. Surprisingly, the isotopic compositions found on the whiskers prior to sputtering were uniform from the base of the whiskers to their tips (Table 3 and Figure 44). The compositions were also very close to the equilibrium composition expected within the matte tin plating after complete mixing of the two isotope layers has occurred. This was true even though the depth profile data showed that when the whiskers formed on the matte tin double layer, complete mixing of the isotopes normal to the substrate had not occurred (Figure 31). Sputtering of Whiskers 1, 5A, 5B and 5C (all fully formed at 44 days after plating) revealed that the isotopic compositions of the interiors of the whiskers were also uniform from the base of the whiskers to their tips (Table 7 and Figure 58) but were not identical to the pre-sputtering compositions. In all cases, the internal compositions of the whiskers were deficient in Sn^{118} compared to the surface compositions. Different analytical techniques had to be used to determine the isotopic compositions of the whiskers before and after sputtering. Analysis of a standard (Sn foil with normal isotopic abundances) using both techniques gave nearly identical results. This confirmed that the isotopic differences observed in the whiskers after sputtering are real and not an artifact of the analytical techniques used.

The data suggests that when the whiskers formed on the matte tin double layer, the tin within the grain boundaries feeding the whiskers had not yet reached an equilibrium composition (i.e., the material was still Sn^{120} rich). Although the isotopic composition of the tin within the grain boundaries would change with time, the growth of the whiskers was faster than this compositional change which explains why each whisker had a uniform internal isotopic composition along its length. The internal isotopic composition could vary from whisker to whisker, however, depending on how long after plating the whisker formed. After formation of the whiskers was complete, the tin within the grain boundaries feeding the whiskers began to approach the equilibrium composition. Diffusion of this tin onto and along the surface of the whiskers occurred and was extremely rapid compared to diffusion into the lattice of the whiskers. The surface composition of the whiskers was in constant flux until the equilibrium composition was achieved. This would explain why the interior of each whisker on the matte tin double layer was enriched in Sn^{120} compared to the exterior of the whisker.

The isotopic compositions of whiskers that grew on the matte Sn^{120}/Sn^{118} double layer **close to the single layer/double layer interface** were different than the compositions of whiskers well removed from the interface. The amount of Sn^{118} detected was related to the distance of the whisker base from the adjacent single layer/double layer interface (Figure 51). Again, the isotopic compositions found on the whiskers prior to sputtering were uniform from the base of the whiskers to their tips (Table 7, Whiskers 3B, 3D and 3E). However, the compositions were not the same as the equilibrium composition expected within the matte tin plating after complete mixing of the two isotope layers has occurred. Undoubtedly, this was due to dilution of the tin diffusing over the surface of the whiskers by Sn^{120} diffusing over from the adjacent single layer. After sputtering, the isotopic compositions of the interiors of the whiskers were not identical to the pre-sputtering compositions and were not the same as the double layer equilibrium composition (Table 7). In most cases, the internal compositions of the whiskers were deficient in Sn^{118} compared to the surface compositions. Again, the data suggests that when these whiskers formed on the matte tin, the isotopic composition of the tin within the grain boundaries feeding the whiskers had not yet reached an equilibrium composition (i.e., the material was still Sn^{120} rich).

The isotopic compositions of whiskers that grew on the matte Sn^{120}/Sn^{118} single layer **close to the single layer/double layer interface** were also determined prior to and after sputtering. Again, the isotopic compositions found on the whiskers prior to sputtering were uniform from the base of the whiskers to their tips (Table 5 and Figure 46, Whiskers 2A, 3G, 3H, 3I, 3C and 3F). The amount of Sn^{118} detected was related to the distance of the whisker base from the adjacent single layer/double layer interface (Figure 51) which was the source of the Sn^{118}. After sputtering, the isotopic compositions of the interior of the whiskers were uniform from the base of the whiskers to their tips (Table 7, Whiskers 3G, 3H, 3I and 3F) and were also nearly identical to the pre-sputtering compositions (Figures 58 and 59). The data suggests that the isotopic composition of the tin within the grain boundaries feeding these whiskers did not change

rapidly with time thus allowing the internal and surface compositions of the whiskers to remain similar.

The isotopic compositions of several whiskers and nodules that grew on the bright Sn^{120}/Sn^{118} double layers were also quantified prior to and after sputtering. Unlike the matte tin plating, whiskers on the bright tin plating emanated from nodules which must have formed by long range diffusion of tin (since the plating directly under the nodules was not thick enough to provide the amount of tin contained within the nodules). As with the matte tin, the isotopic composition found on the whiskers prior to sputtering was uniform from the base of the whiskers to their tips (Table 8). The composition found on the surfaces of the whiskers and their corresponding nodules was close to the equilibrium composition expected within the bright tin plating after complete mixing of the two isotope layers has occurred (Tables 8 and 9). One might expect the nodules on the bright tin to have an isotopic composition identical to that of the double layer equilibrium composition if the nodules are indeed formed by the long range diffusion of tin. Any whiskers subsequently emanating from the nodules might likewise be expected to have an isotopic composition identical to that of its corresponding nodule. Sputtering and analysis of several whiskers/nodules gave conflicting results, however. Whisker 7 had nearly the same isotopic composition before and after sputtering (Table 8 and Figure 60). This whisker was fully formed at 23 days after plating when mixing of the double isotope layer was still incomplete. In contrast, Whisker 22 showed a decrease in the relative amount of Sn^{118} detected after sputtering (although the post-sputter composition was constant from the base of the whisker to its tip). The results obtained by sputtering the nodules were also inconsistent. The isotopic compositions of the sputtered nodules varied depending on where the line scans were drawn (Table 9 and Figures 61 and 62).

This study did not collect enough data from whiskers and nodules on the bright tin double layer to make any definitive conclusions concerning these conflicting observations.

CONCLUSIONS
The following conclusions can be draw from this study.

1. A layer of Sn^{120} over a layer of Sn^{118} showed significant interdiffusion in just a few days for both bright tin and matte tin. Mixing of the bright tin isotope layers was nearly complete at 66 days after plating while mixing of the matte tin isotope layers was far from complete at 117 days after plating. No dramatic changes in grain size within the platings were apparent in either case. The lattice diffusion coefficient calculated for the bright tin appeared to be larger than the literature values measured for a near perfect tin lattice.

2. Whiskers growing from the matte tin appeared to originate from the plating surface and not from the substrate/plating interface. The whiskers had a diameter equivalent to the grain size and no nodule growth prior to the formation of whiskers was observed. In contrast, whiskers on the bright tin plating grew from large nodules which must have formed by a recrystallization process.

3. Long range diffusion of Sn^{118} isotope parallel to the substrate was observed during TOF-SIMS analysis of whiskers growing on the matte Sn^{120} plating adjacent to a Sn^{118} source. Large amounts of Sn^{118} were detected in the whiskers but not in the plating itself. This suggests that the diffusion of Sn^{118} occurred through the grain boundaries (or over the plating surface) and not through the tin lattice.

4. Approximately three hundred days after plating, long range diffusion of Sn^{118} isotope parallel to the substrate was also observed during surface and depth profiling analyses of matte and bright Sn^{120} platings adjacent to a Sn^{118} source. In the matte tin case, the amount of Sn^{118} on the surface of the plating was greater than within the plating. This strongly suggests that the diffusion of Sn^{118} occurred through the grain boundaries (or over the plating surface) and not through the tin lattice.

5. The isotopic compositions of the surfaces of the tin platings appeared to be "frozen" possibly due to the formation of oxide layers which prevented further diffusion. If an oxide layer is indeed responsible for this observation, the data suggests that diffusion parallel to the substrate could still occur immediately under the oxide layer with subsequent diffusion into the lattice.

6. The isotopic compositions of the surfaces of all whiskers analyzed on the matte tin were relatively constant from the base of each whisker to its tip. Sputtering of the whiskers revealed that the isotopic composition inside a whisker could be different from its surface composition, however. These observations suggest that the internal composition of a whisker on matte tin was determined by the composition of the tin within the grain boundaries at the time of formation. After formation of a whisker, tin could still diffuse rapidly over the whisker surface and the surface composition would change as the tin within the grain boundaries approached an equilibrium isotopic composition.

REFERENCES

1. J.A. Brusse, G.J. Ewell, and J.P. Siplon, "Tin Whiskers: Attributes and Mitigation", *22nd Capacitor and Resistor Technology Symposium Proceedings*, March 25-29, 2002, pp. 67-80.

2. Dr. G.T. Galyon, "Annotated Tin Whisker Bibliography and Anthology, Version 1.2", NEMI Tin Whisker Modeling Project, November 2003.

3. V.K. Glazunova and N.T. Kudryavtsev, "An Investigation of the Conditions of Spontaneous Growth of Filiform Crystals on Electrolytic Coatings", J. of Applied Chemistry of the USSR (translated from *Zhurnal Prikladnoi Khimii*), Vol. 36, No. 3, March 1963, pp. 519-525.

4. N.A.J. Sabbagh and H.J. McQueen, "Tin Whiskers: Causes and Remedies", Metal Finishing, March 1975, pp. 27-31..

5. J.D. Eshelby, "A Tentative Theory of Metallic Whisker Growth", Phys. Rev., Vol. 91, 1953, pp. 755-756.

6. F.C. Frank, Phil. Mag., Vol. 44, 1953, pp. 854-860.

7. S. Amelinckx, W. Bontinck, W. Dekeyser and F. Seitz, "On the Formation and Properties of Helical Dislocations", Phil. Mag., Vol. 2, No. 15, March 1957, pp. 355-377.

8. R.R. Hasiguti, Acta Metallurgica., Vol. 3, 1955, pp. 200-201.

9. W.C. Ellis, D.F. Gibbons and R.G. Teuting in *Growth and Perfection of Crystals*, edited by R.H. Doremus, B.W. Roberts and David Turnbull, John Wiley & Sons, Inc., New York, 1958, pp. 102-120.

10. N. Furuta and K. Hamamura, Jap. J. of Appl. Physics, Vol. 8, No. 12, Dec. 1969, pp. 1404-1410.

11. U. Lindborg, "A Model for the Spontaneous Growth of Zn, Cd, and Sn Whiskers", Acta Met., Vol. 24, 1976, pp.181-186.

12. R. Kawanaka, K. Fujiwara, S. Nango and T. Hasegawa, "Influence of Impurities on the Growth of Tin Whiskers", Jap. J. of App. Physics, Part 1, Vol. 22, No. 6, June 1983, pp. 917-922.

13. D. Endicott and K.T. Kisner, "A Proposed Mechanism for Metallic Whisker Growth", *Proceedings of the AESF SUR/FIN Conference*, July 1984, pp. 1-20.

14. K.N. Tu, "Irreversible Processes of Spontaneous Whisker Growth in Bimetallic Cu-Sn Thin-Film Reactions", Physical Review B, Vol. 49, No. 3, 1994, pp. 2030-2034.

15. B.-Z. Lee and D.N. Lee, "Spontaneous Growth Mechanism of Tin Whiskers", Acta Metallurgica., Vol. 46, No. 10, 1998, pp. 3701-3714.

16. C. Xu, Y. Zhang, C. Fan, J.A. Abys, L. Hopkins and F. Stevie, "Understanding Whisker Phenomenon – Driving Force for the Whisker Formation", *IPC APEX 2002 Proceedings*, pp. S06-2-1 through S06-2-6.

17. Dr. I. Boguslavsky and P. Bush, "Recrystallization Principles Applied to Whisker Growth in Tin", *IPC APEX 2003 Proceedings*, pp. S12-4-1 through S12-4-9.

18. G. Galyon, "Integrated Recrystallization Theory for Whisker Formation", NEMI Workshop, TMS, March 2002, (cited in Handbook of *Lead-Free Solder Technology for Microelectronic Assemblies*, edited by K.J. Puttlitz and K.A. Stalter, Marcel Dekker, Inc., New York, 2004, pp. 893-896).

19. M.W. Barsoum, E.N. Hoffman, R.D. Doherty, S. Gupta and A. Zavaliangos, "Driving Force and Mechanism for Spontaneous Metal Whisker Formation", Physical Review Letters, Vol. 93, No. 20, 12 November, 2004, pp. 206104-1 through 206104-4.

20. H.-P. Kehrer and H.G. Kadereit, "Tracer Experiments on the Growth of Tin Whiskers", Applied Physics Letters, Vol. 16, No. 11, June 1970, pp. 411-412.

21. 45th Metal Finishing Guidebook Directory for 1977, Annual Edition, edited by N. Hall, Metals and Plastics Publications, Inc., Hackensack, N.J., 1977, p.p. 308-316.

22. T. Wirtz and H.-N. Migeon, "Cation Mass Spectrometry: Towards an Optimization of SIMS Analyses Performed in the MCs^+ Mode", Spectroscopy Europe, Vol. 15, No. 4, 2003, pp. 16-22.

23. P. Singh and M. Ohring, "Tracer Study of Diffusion and Electromigration in Thin Tin Films", J. Appl. Phys., Vol. 56, No. 4, August 1984, pp. 899-907.

24. P.G. Shewmon, *Diffusion in Solids*, McGraw-Hill Book Co., Inc., New York, 1963, p. 14.

25. J.D. Meakin and E. Klokholm, "Self-Diffusion in Tin Single Crystals", Transactions of the Metallurgical Society of AIME, Vol. 218, June 1960, pp. 463-466.

26. W. Lange and D. Bergner, Phys. Stat. Sol., Vol. 2, 1962, pp. 1410-1414.

27. C. Coston and N.H. Nachtrieb, "Self-Diffusion in Tin at High Pressure", J. Phys. Chem., Vol. 68, No. 8, August 1964, pp. 2219-2229.

28. F.H. Huang and H.B. Huntington, "Diffusion of Sb^{124}, Cd^{109}, Sn^{113}, and Zn^{65} in Tin", Phys. Rev. B, Vol. 9, No. 4, February 1974, pp. 1479-1488 (using average value cited in Reference 28).

29. B.D. Dunn, "A Laboratory Study of Tin Whisker Growth", ESA STR-223, European Space Agency, September 1987, pp. 40-41.

30. *Handbook of Lead-Free Soldering Technology for Microelectronic Assemblies*, edited by K.J. Puttlitz and K.A. Stalter, Marcel Dekker, Inc., New York, 2004, pp. 888-892.

31. Commission on Atomic Weights and Isotopic Abundances Report for the International Union of Pure and Applied Chemistry in *Isotopic Compositions of the Elements 1989*, Pure and Applied Chemistry, Vol. 70, 1998.

32. R.M. Fisher, L.S. Darken and K.G. Carroll, Acta Metallurgica., Vol. 2, 1954, pp. 368-373.

Table 1. Relative Percentage of Each Tin Isotope in the Anodes used for Electroplating

Isotope	Relative Percentages of Tin Isotopes	
	Sn^{120} Anode	Sn^{118} Anode
Sn^{124}	0.02	0.1
Sn^{122}	0.06	0.1
Sn^{120}	**99.6**	0.5
Sn^{119}	0.13	0.3
Sn^{118}	0.13	**97**
Sn^{117}	0.02	1.8
Sn^{116}	0.04	0.2
Sn^{115}	0.00	0.0
Sn^{114}	0.00	0.0
Sn^{112}	0.00	0.0
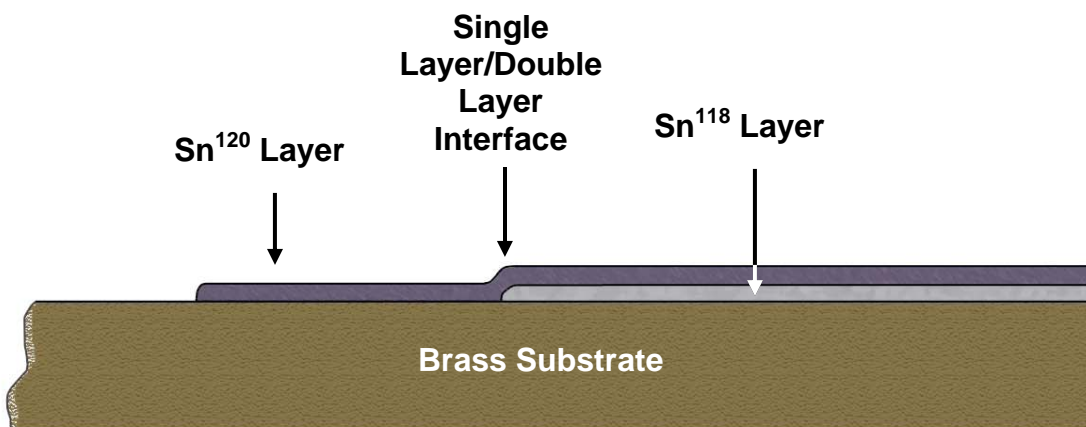
Figure 1. Sn^{120} Single Layer and Sn^{120}/Sn^{118} Double Layer on a Brass Coupon
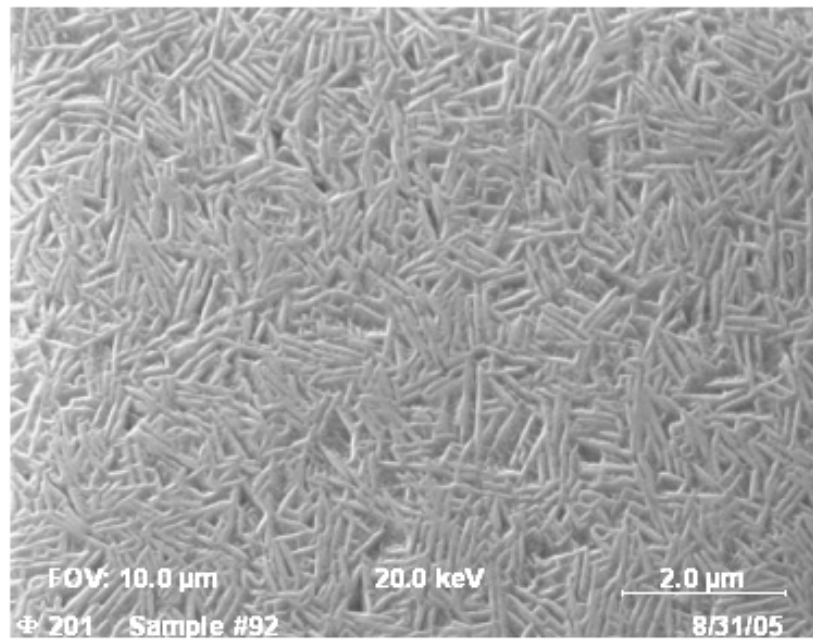
Figure 2. Surface Morphology of the Bright Tin Plating (3 Days after Plating)
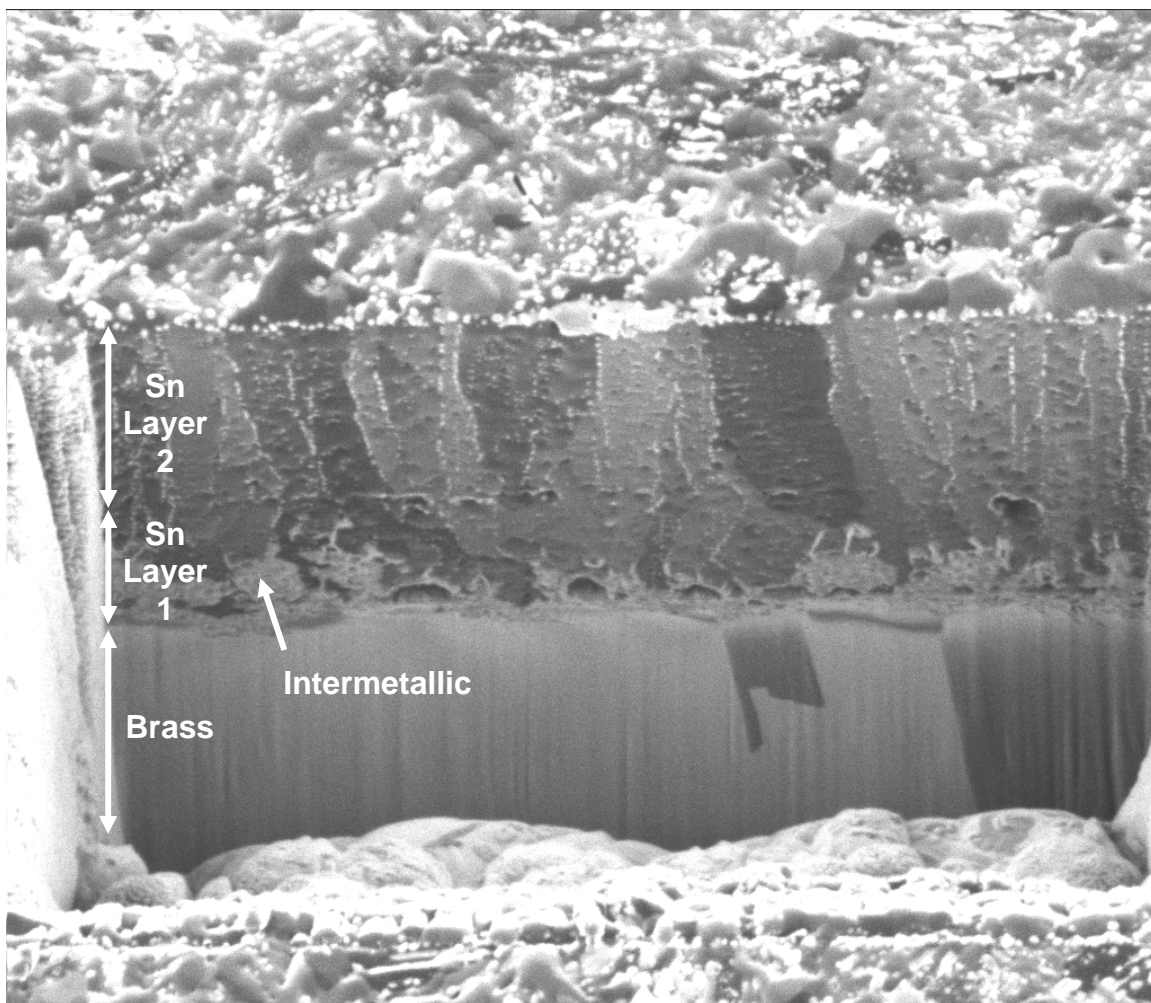
Figure 3. FIB Microsection of the Double Layer of Bright Tin Plating (Sample 90, 1.8 Microns Sn[120] over 1.3 Microns Sn[118], 109 Days after Plating)

13
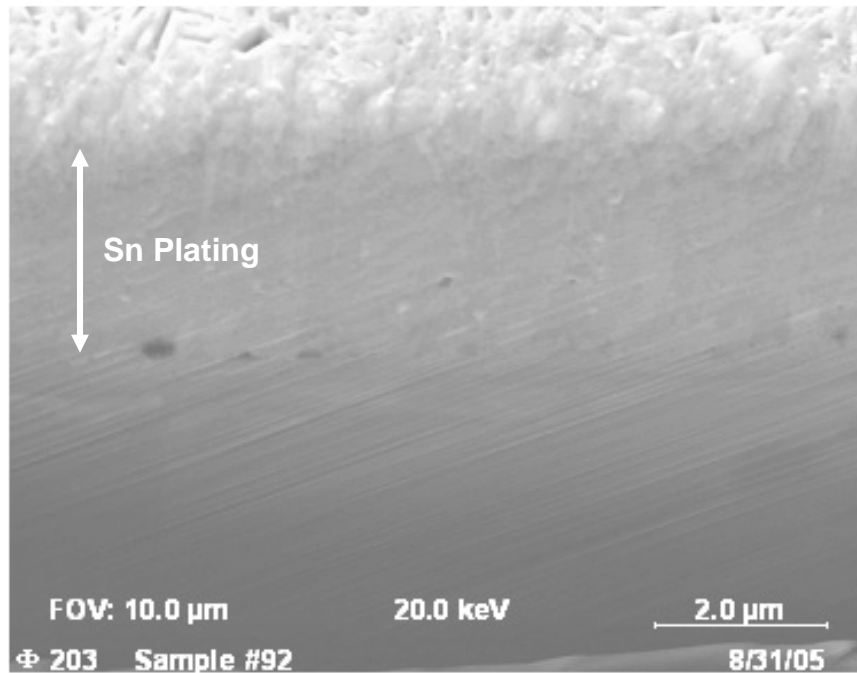
**Figure 4. SEM Image of an FIB Microsection of the Double Layer of Bright Tin Plating
(Sample 92, 1.2 Microns Sn[120] over 1.0 Microns Sn[118], 67 Days after Plating)**
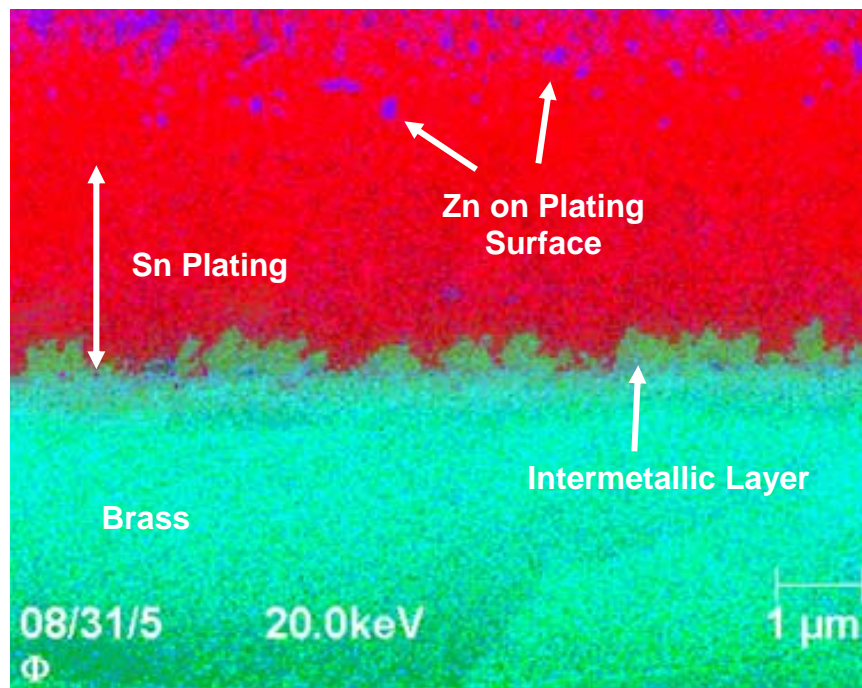
**Figure 5. Auger Elemental Map of the FIB Microsection from Figure 4
(Red=Sn; Green=Cu; Blue=Zn)**

14
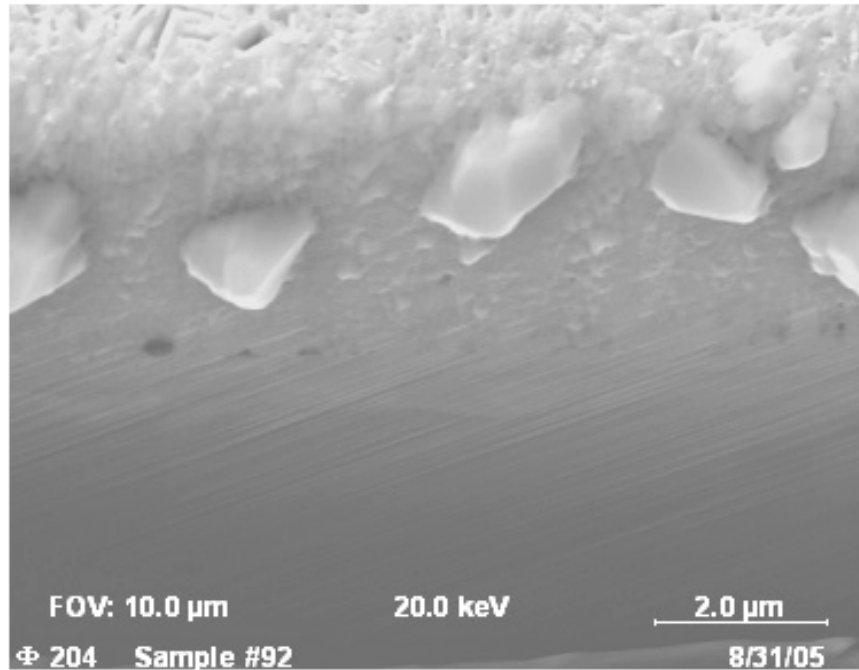
Figure 6. Nodules Forming 30 Minutes after the FIB Microsection was made (FIB Microsection from Figure 4)
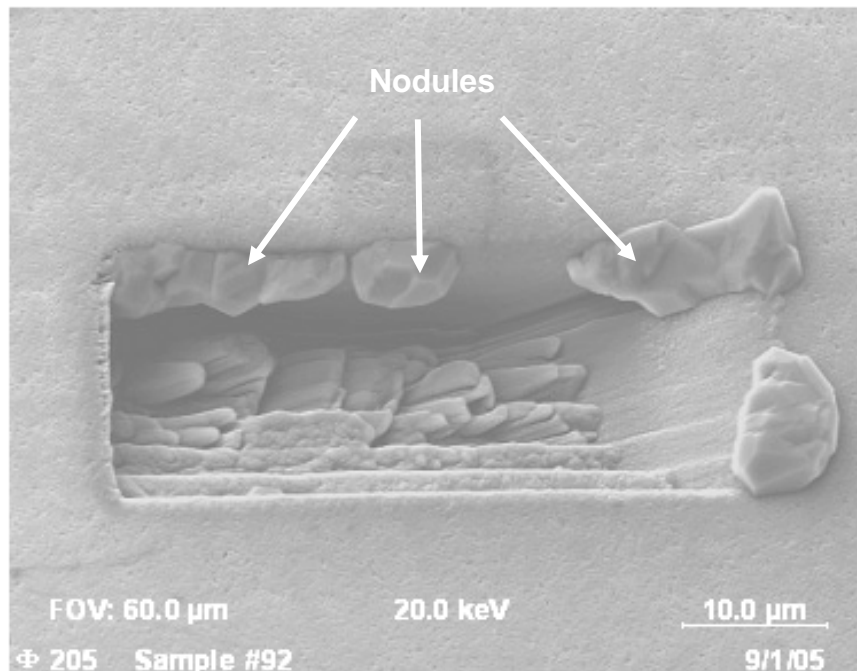
Figure 7. Nodules 18 Hours after the FIB Microsection was made (FIB Microsection from Figure 4)
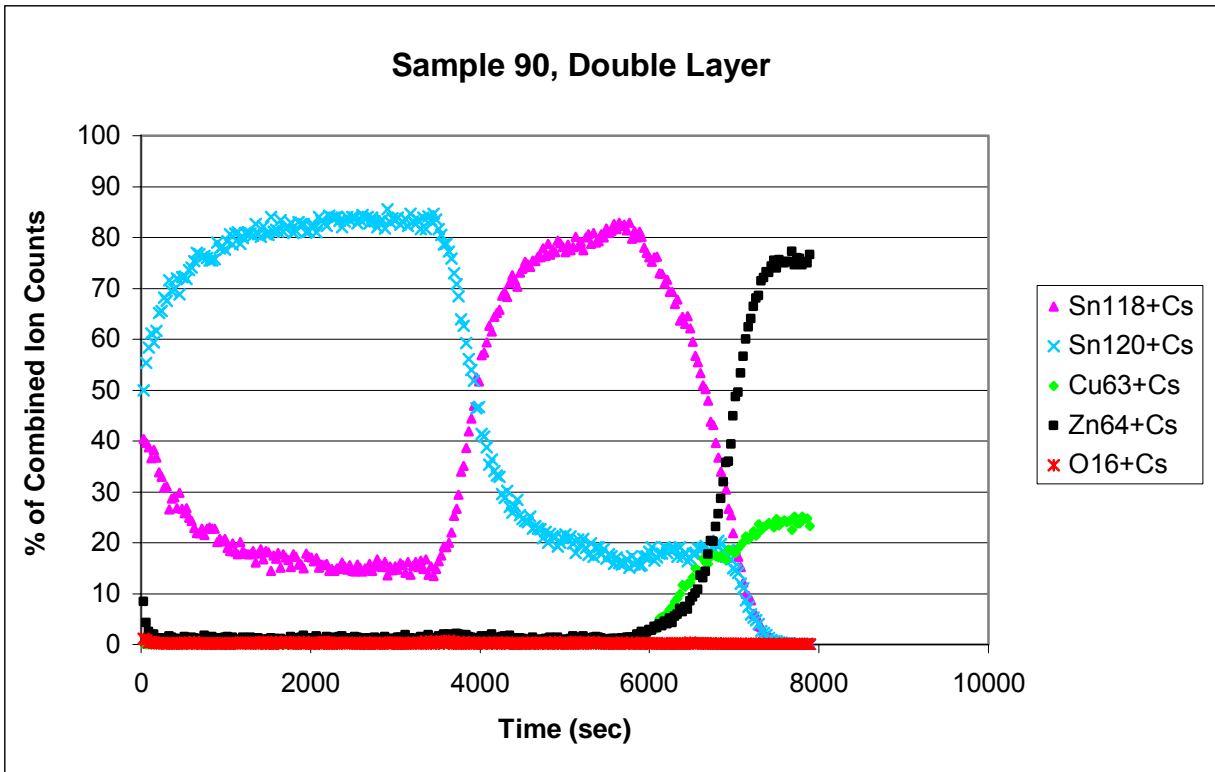
Figure 8. TOF-SIMS Depth Profile of the Double Layer of Bright Tin Plating (Sample 90, 1.8 Microns Sn^{120} over 1.3 Microns Sn^{118}, 3 Days after Plating)
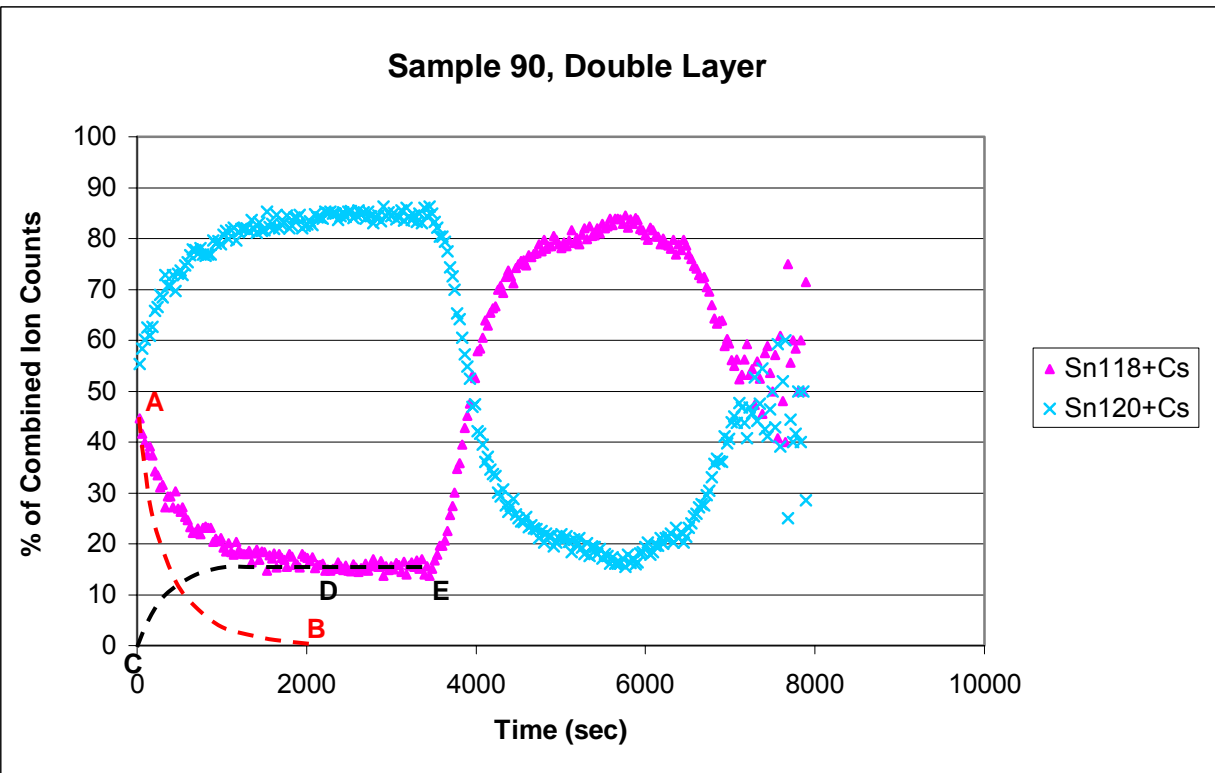
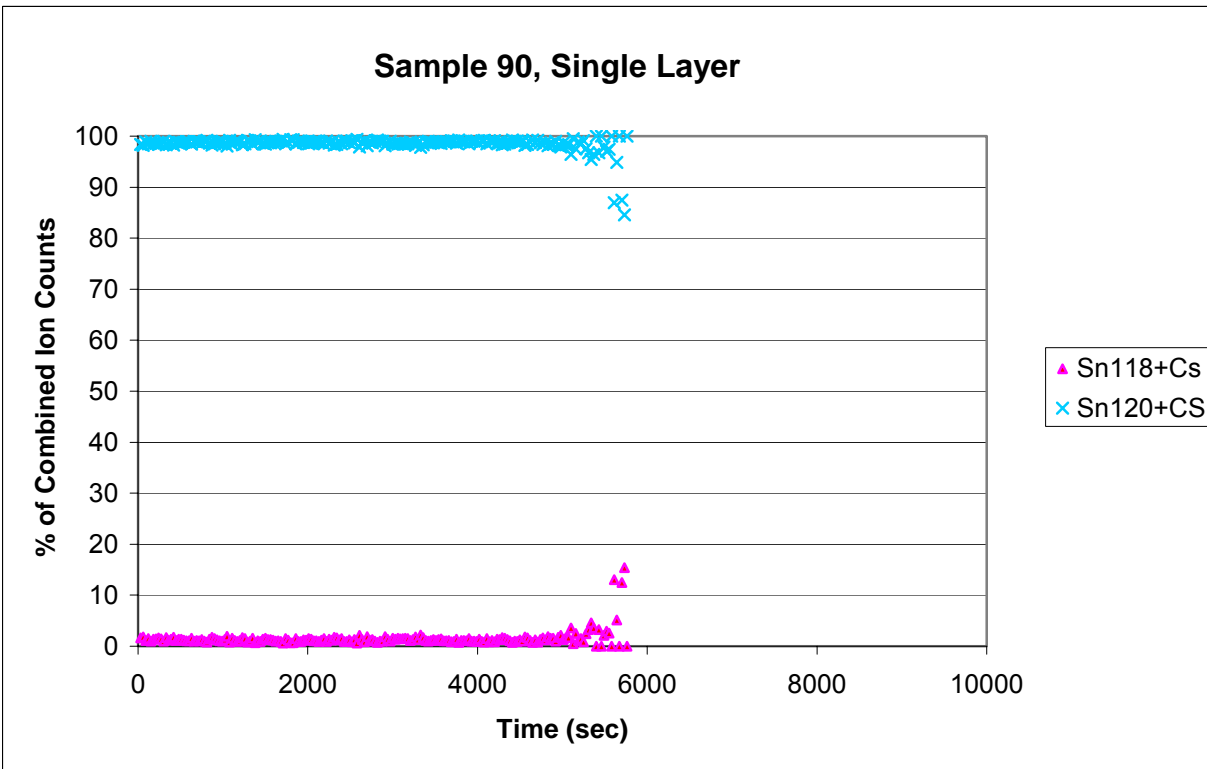**Figure 9. TOF-SIMS Depth Profile of the Double Layer of Bright Tin Plating showing Tin Isotopes Only (Sample 90, 1.8 Microns Sn^{120} over 1.3 Microns Sn^{118}, 3 Days after Plating). Line AB Represents Lattice Diffusion of Sn^{118} from the Surface. Line CDE Represents Lattice Diffusion of Sn^{118} into the Grains from the Grain Boundaries.**

16

Sn^{118} **Moving Up Grain Boundaries**

Brass Substrate

Sn^{120} **Grain**

Sn^{118} **Grain**

Plating Surface

Sn^{120} **Moving Down Grain Boundaries**

Depth Profile

%Sn^{120}

%Sn^{118}
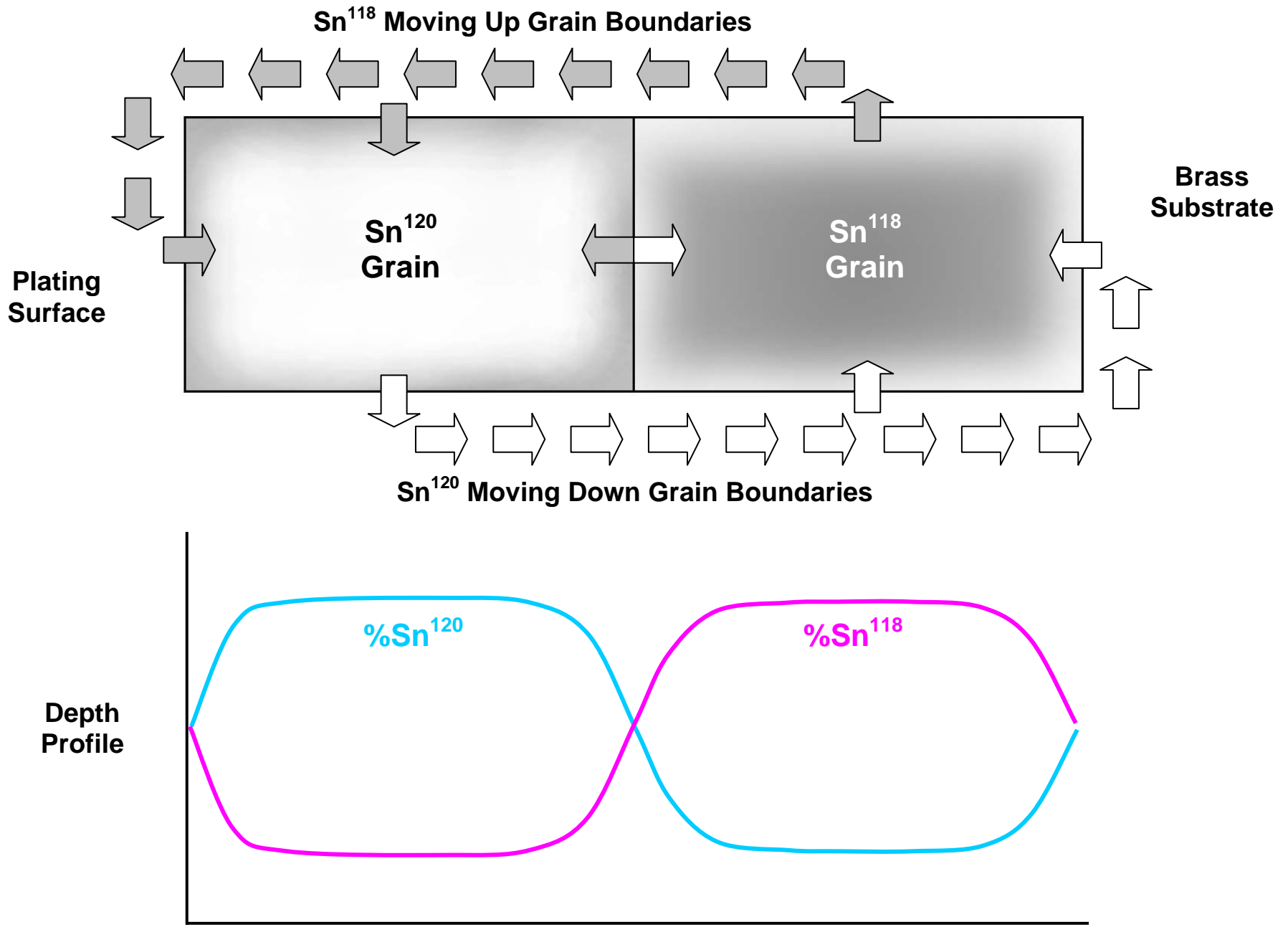
Figure 10. Schematic showing Diffusion of Tin along the Grain Boundaries and the Corresponding Depth Profile (Compare to Figure 9)

Table 2. Lattice Diffusion Coefficients of Common Metals

Metal	D at 25°C (cm^2/sec) (from Ref. 29)
Sn	1.8×10^{-18}
Zn	2.4×10^{-18}
Cd	1.0×10^{-15}
Cu	1.4×10^{-37}
Au	7.0×10^{-33}
Ag	7.5×10^{-34}
Cr	2.5×10^{-75}
Pt	6.2×10^{-52}

431.4 µm
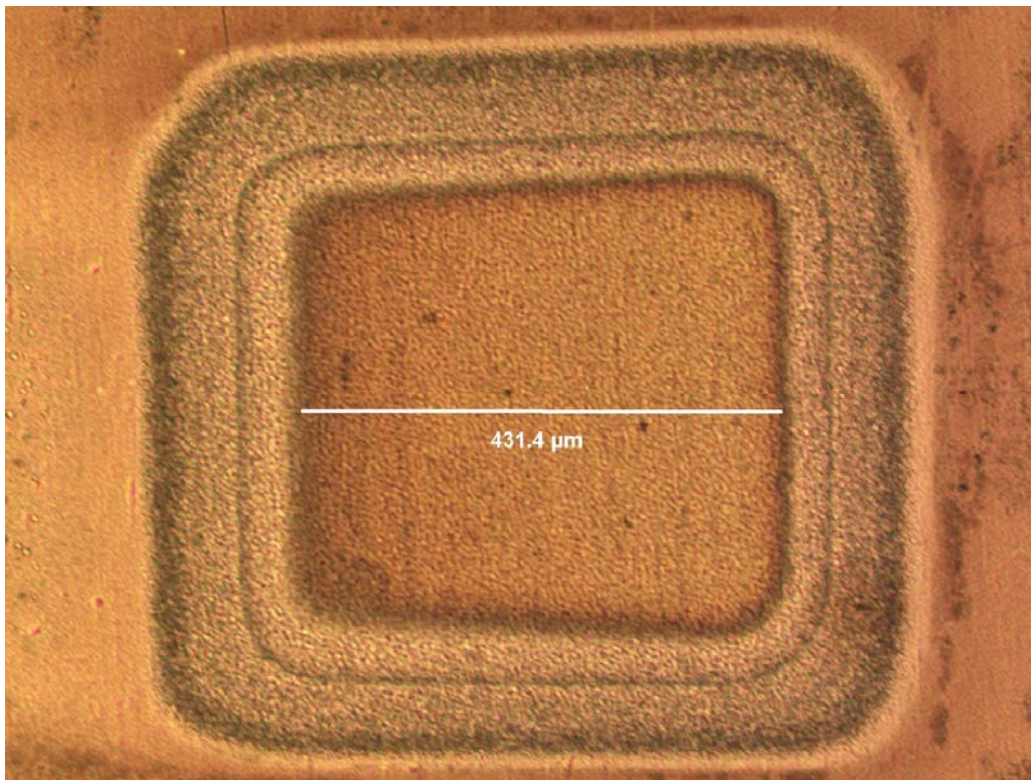
Figure 11. A Typical Depth Profile Crater
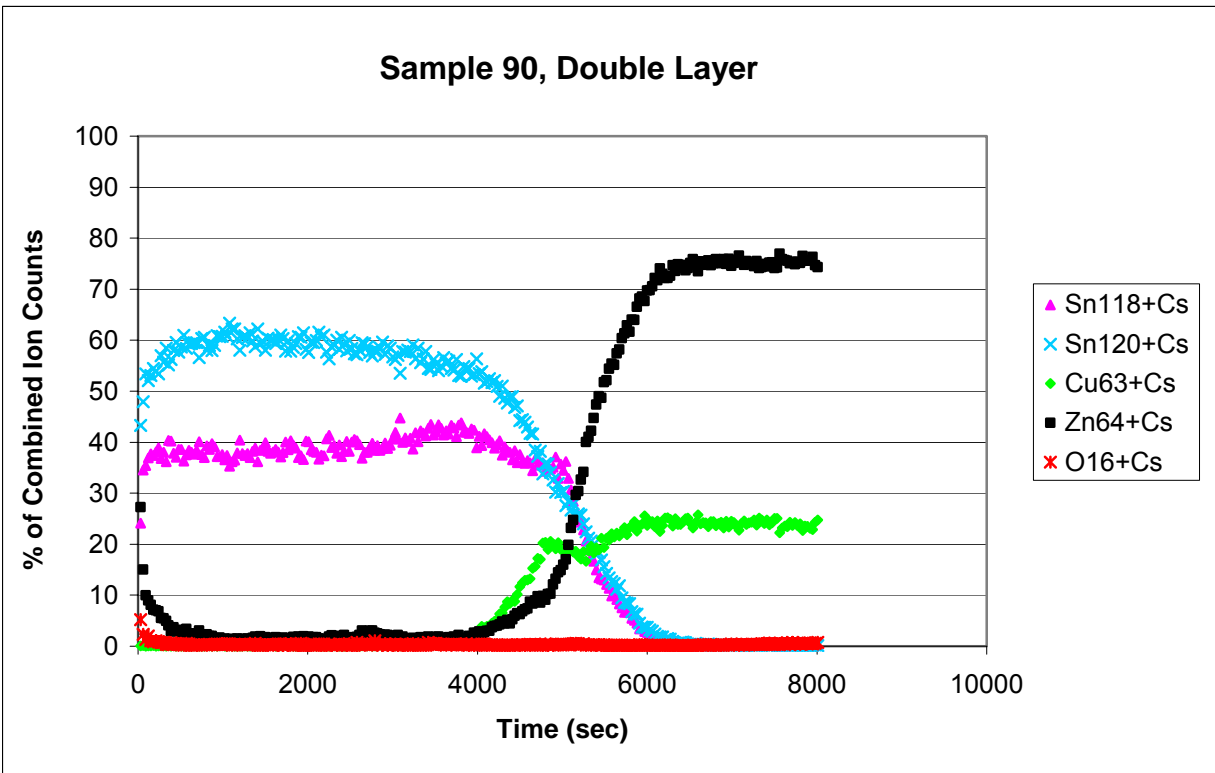
Figure 12. TOF-SIMS Depth Profile of the Double Layer of Bright Tin Plating (Sample 90, 1.8 Microns Sn^{120} over 1.3 Microns Sn^{118}, 66 Days after Plating)
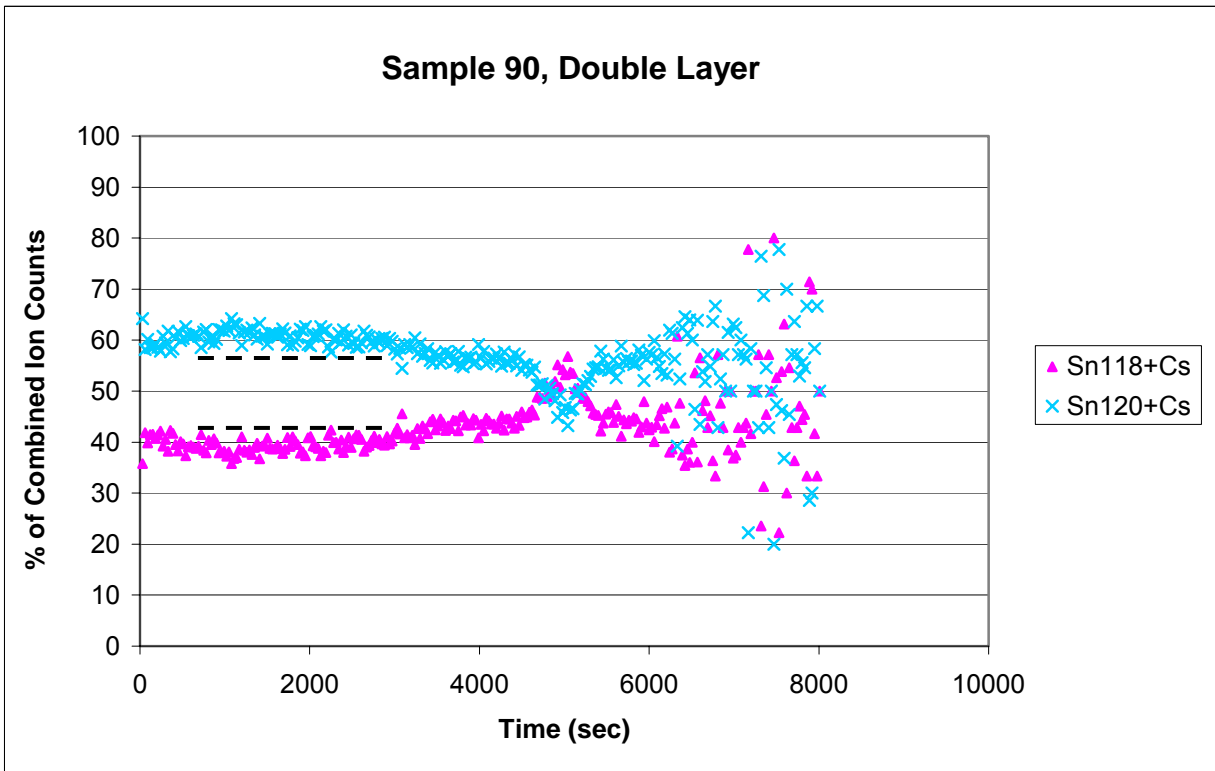
Figure 13. TOF-SIMS Depth Profile of the Double Layer of Bright Tin Plating showing Tin Isotopes Only (Sample 90, 1.8 Microns Sn^{120} over 1.3 Microns Sn^{118}, 66 Days after Plating). Dashed Lines show the Expected Relative Percent of Each Isotope when Diffusion is Complete (i.e., 57% Sn^{120} and 43% Sn^{118}).

19
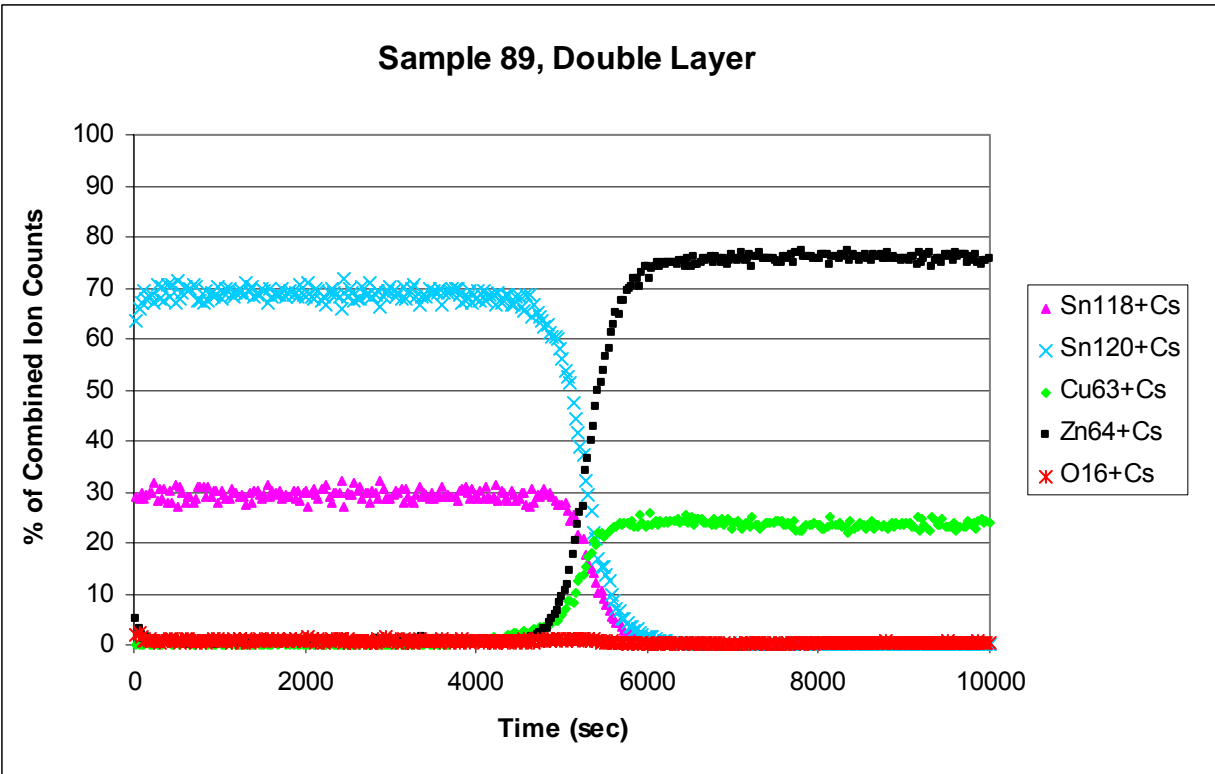
Figure 14. TOF-SIMS Depth Profile of the Double Layer of Bright Tin Plating (Sample 89, Approximately 1.8 Microns Sn^{120} over 0.8 Microns Sn^{118}, 187 Days after Plating)
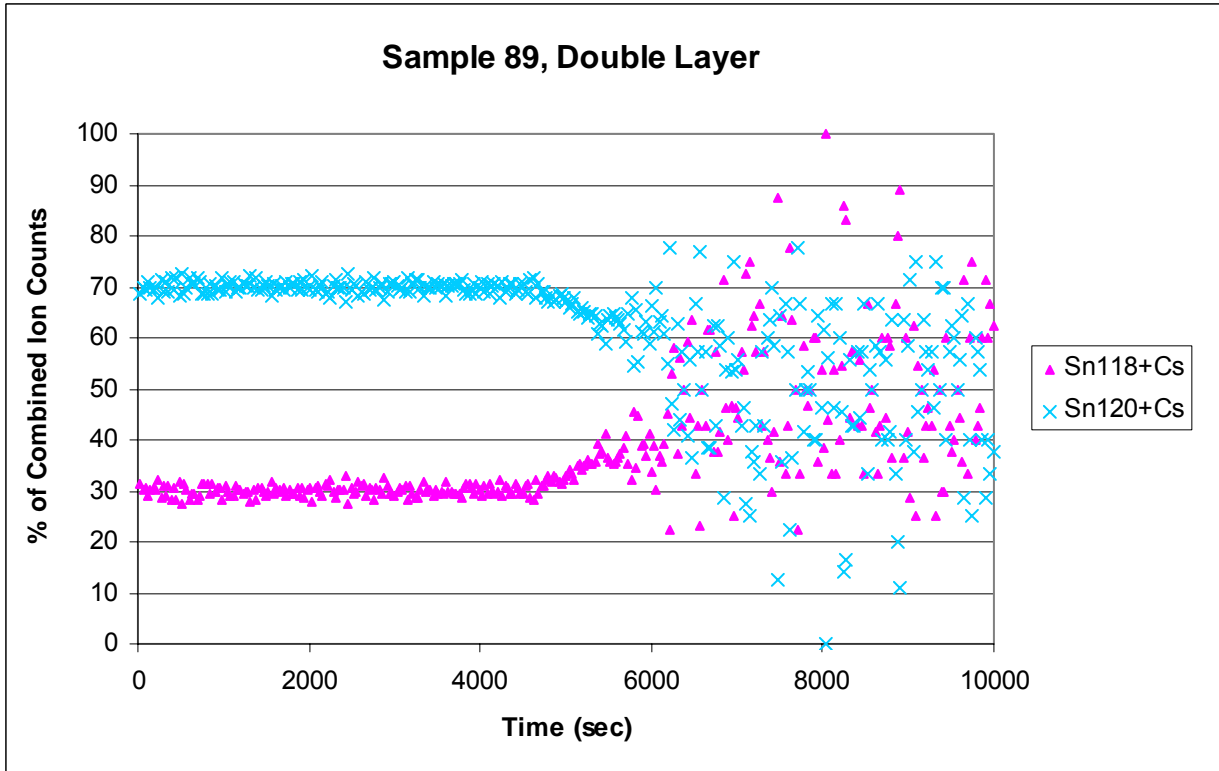
Figure 15. TOF-SIMS Depth Profile of the Double Layer of Bright Tin Plating showing Tin Isotopes Only (Sample 89, Approximately 1.8 Microns Sn^{120} over 0.8 Microns Sn^{118}, 187 Days after Plating)
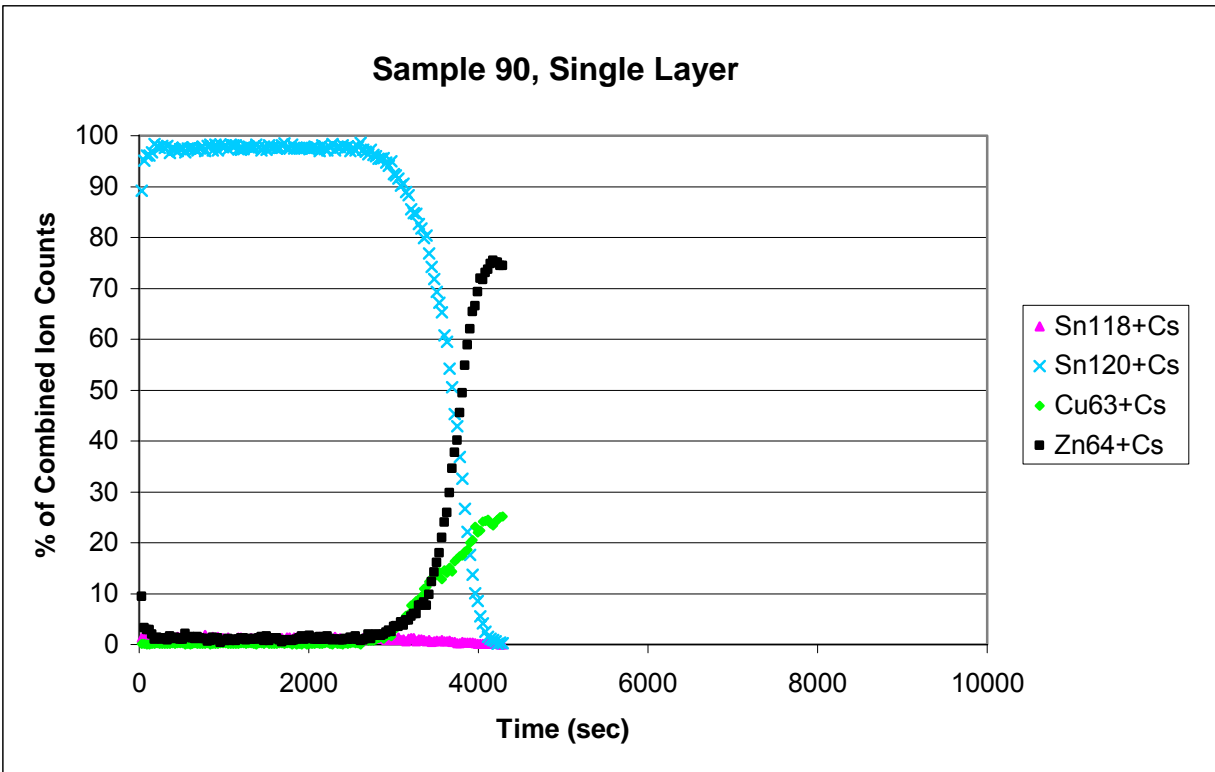
Figure 16. TOF-SIMS Depth Profile of the Single Layer of Sn[120] Bright Tin Plating (Sample 90, 1.8 Microns Sn[120], 3 Days after Plating, Analysis Location was 220 Microns from the Single Layer/Double Layer Interface)
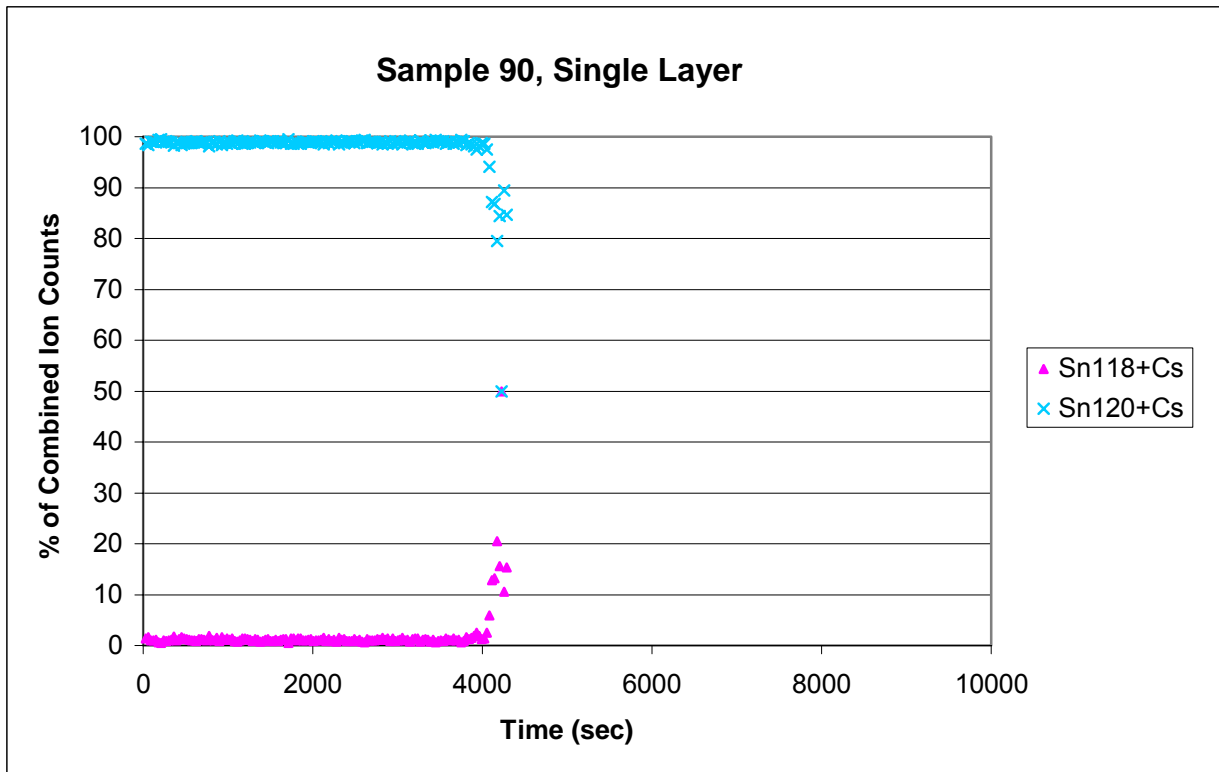
Figure 17. TOF-SIMS Depth Profile of the Single Layer of Sn[120] Bright Tin Plating showing Tin Isotopes Only (Sample 90, 1.8 Microns Sn[120], 3 Days after Plating, Analysis Location was 220 Microns from the Single Layer/Double Layer Interface)

21
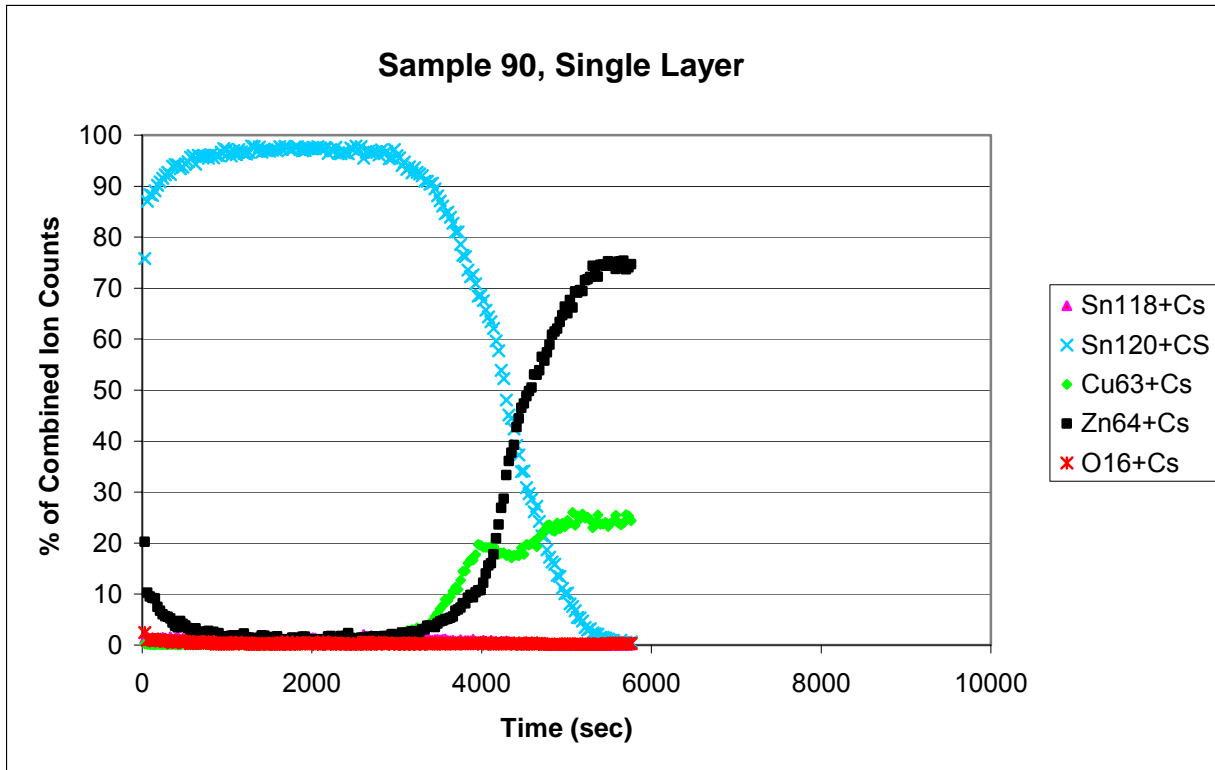
Figure 18. TOF-SIMS Depth Profile of the Single Layer of Sn^{120} Bright Tin Plating (Sample 90, 1.8 Microns Sn^{120}, 66 Days after Plating, Analysis Location was 280 Microns from the Single Layer/Double Layer Interface)

Figure 19. TOF-SIMS Depth Profile of the Single Layer of Sn^{120} Bright Tin Plating showing Tin Isotopes Only (Sample 90, 1.8 Microns Sn^{120}, 66 Days after Plating, Analysis Location was 280 Microns from the Single Layer/Double Layer Interface)
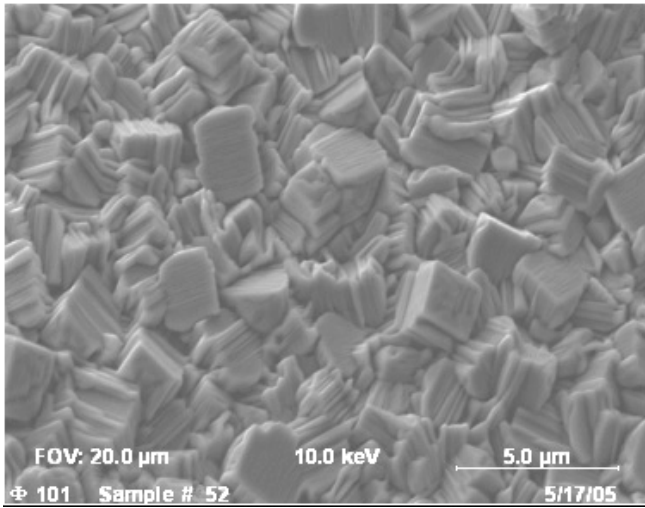
Figure 20. Surface Morphology of the Matte Tin Plating (10 Days after Plating)
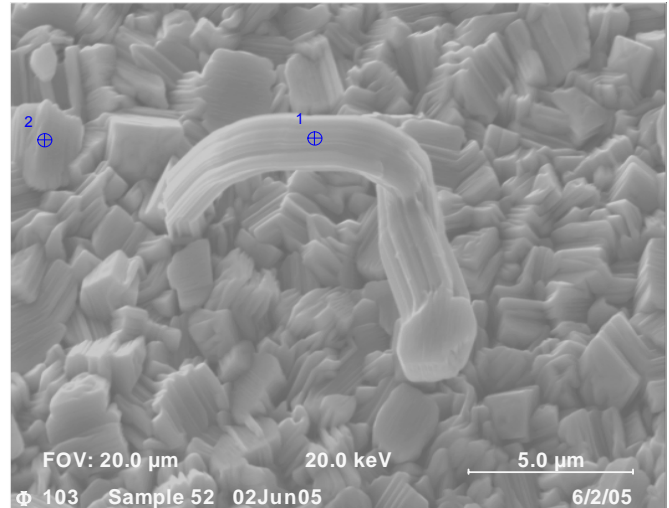
Figure 21. Whisker growing on the Matte Tin Plating (26 Days after Plating)
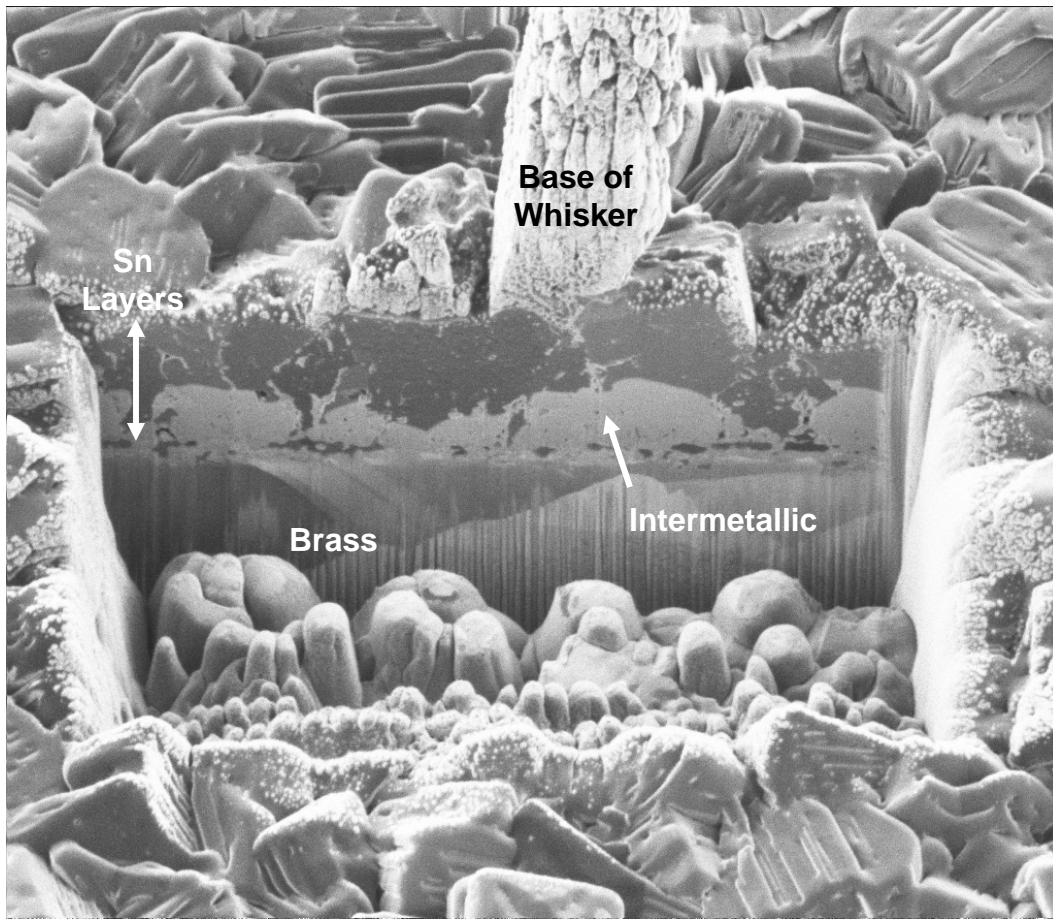
Figure 22. FIB Microsection of the Double Layer of Matte Tin Plating (Sample 52, 1.4 Microns Sn[120] over 1.6 Microns Sn[118], 158 Days after Plating)

23
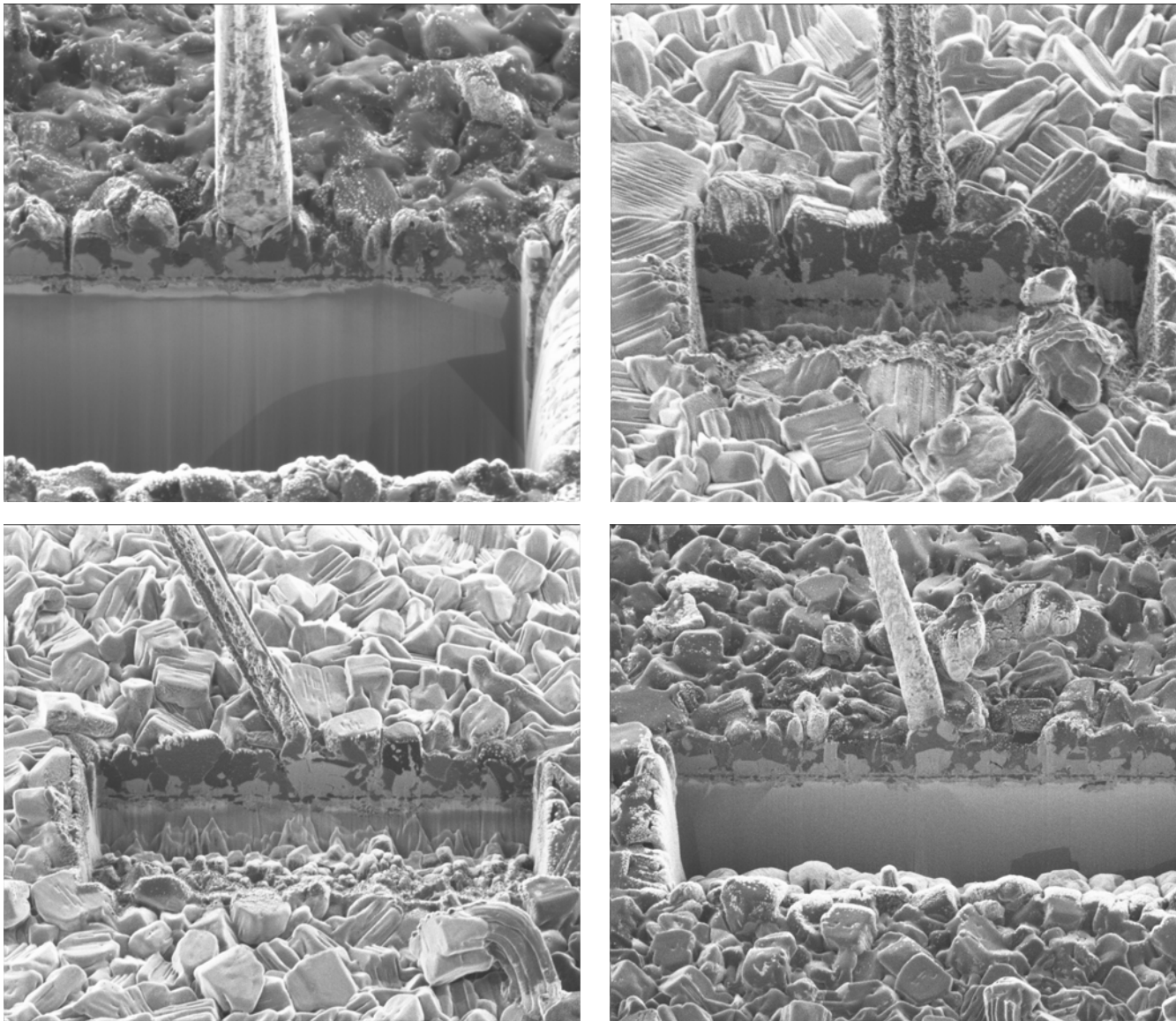
Figure 23. FIB Microsections of the Matte Tin Platings (158 Days after Plating)
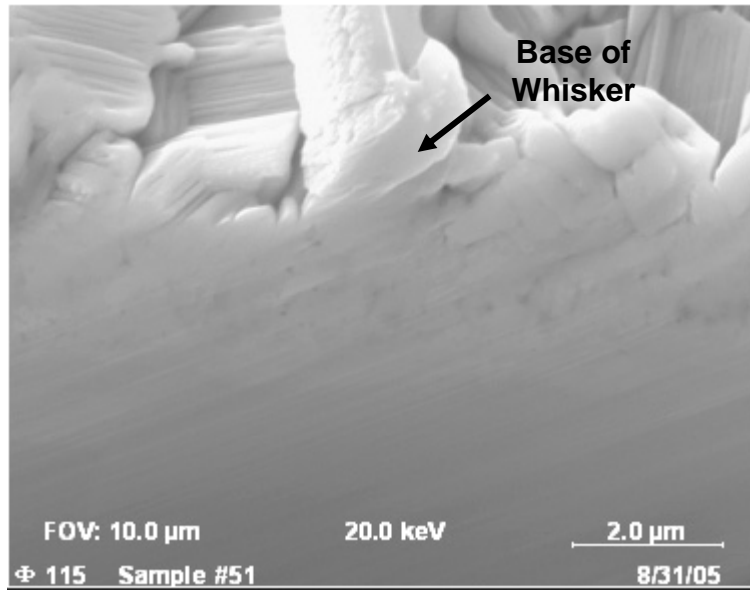
**Figure 24. SEM Image of FIB Microsection of the Double Layer of Matte Tin Plating
(Sample 51, 1.3 Microns Sn[120] over 1.6 Microns Sn[118], 116 Days after Plating)**
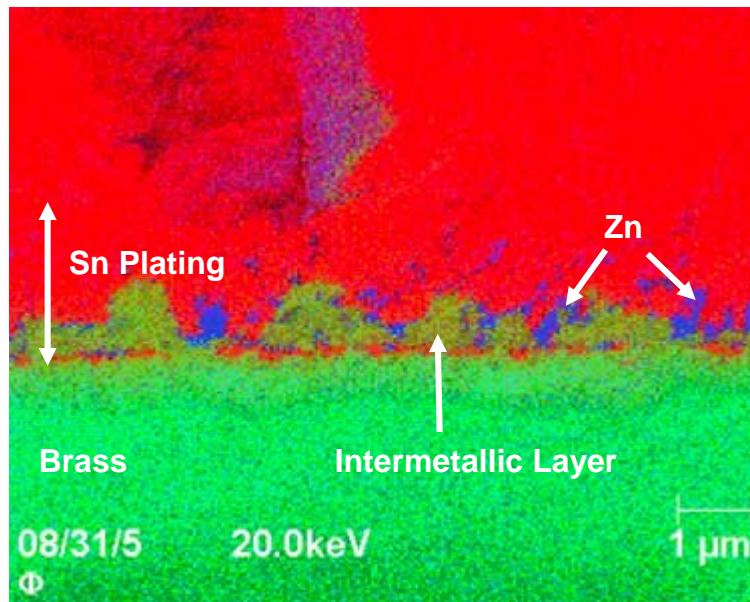
**Figure 25. Auger Elemental Map of FIB Microsection from Figure 24
(Red=Sn; Green=Cu; Blue=Zn)**
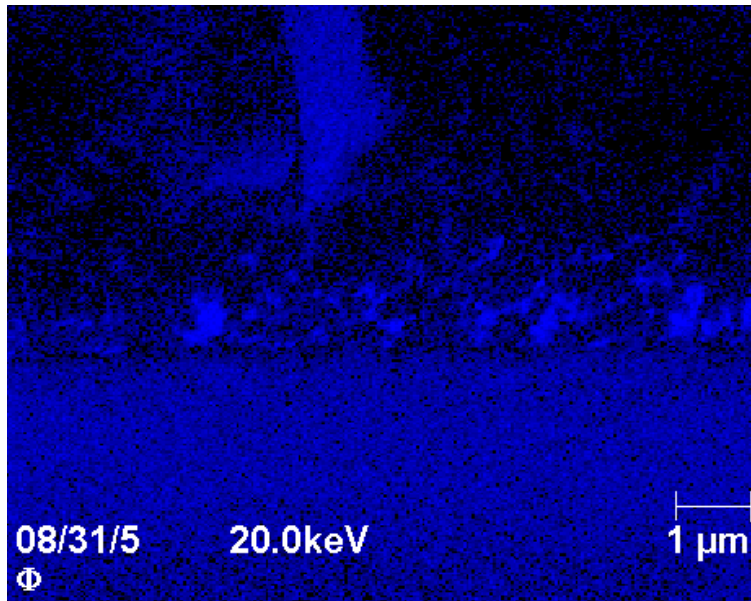
**Figure 26. Auger Elemental Map of FIB Microsection from Figure 24
Showing Zn Only**
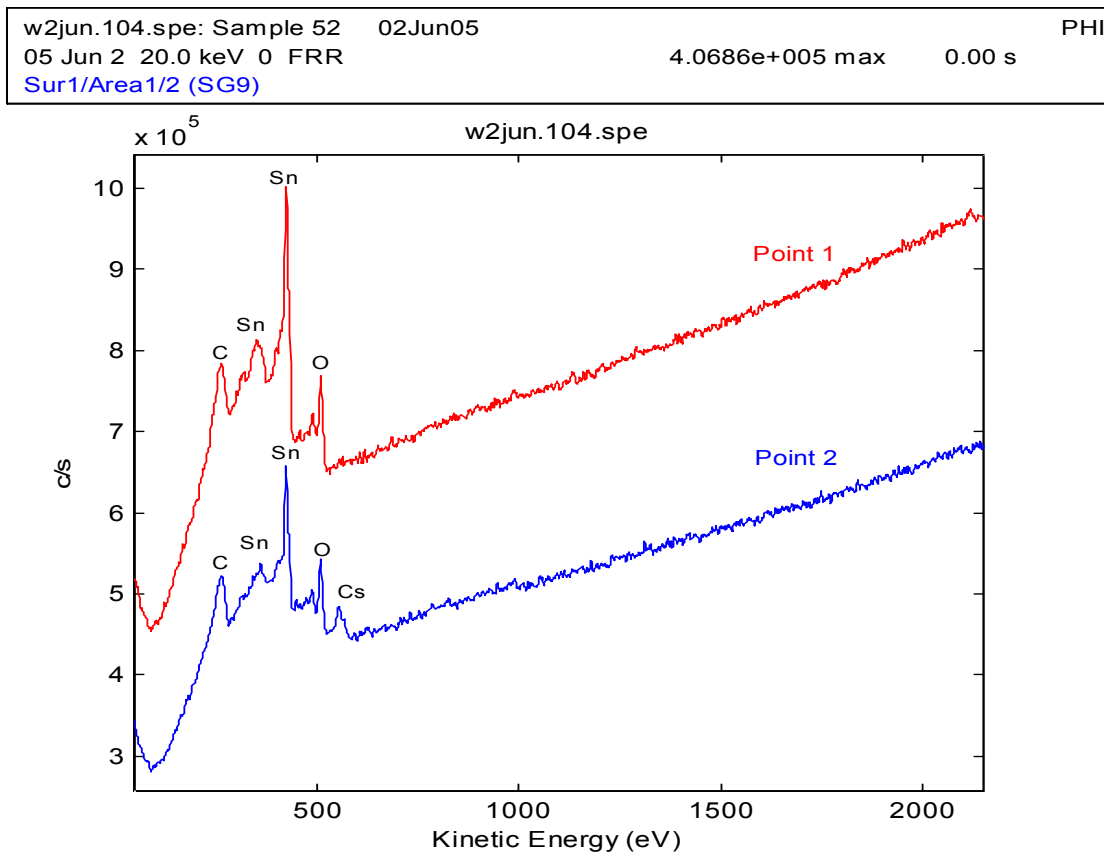
**Figure 27. Auger Analysis of the Whisker (Point 1) and the Adjacent
Plating (Point 2) from Figure 21**
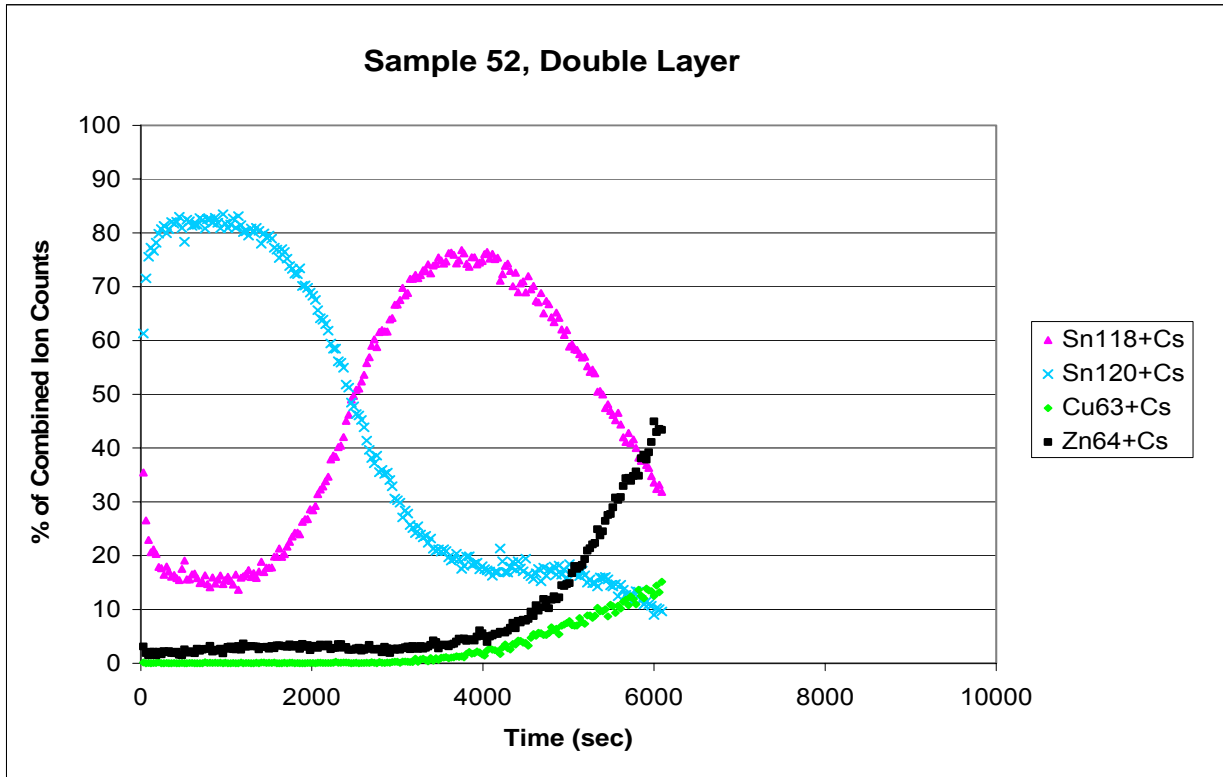
Figure 28. TOF-SIMS Depth Profile of the Double Layer of Matte Tin Plating (Sample 52, 1.4 Microns Sn^{120} over 1.6 Microns Sn^{118}, 10 Days after Plating)
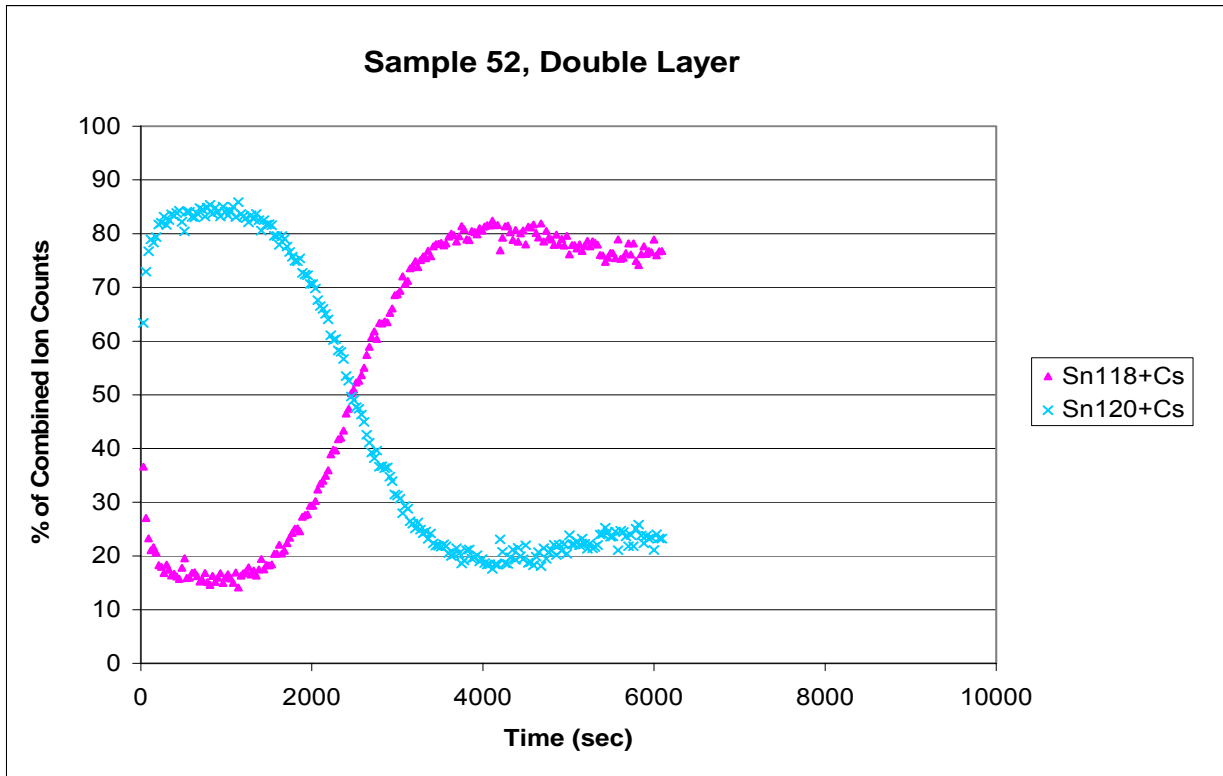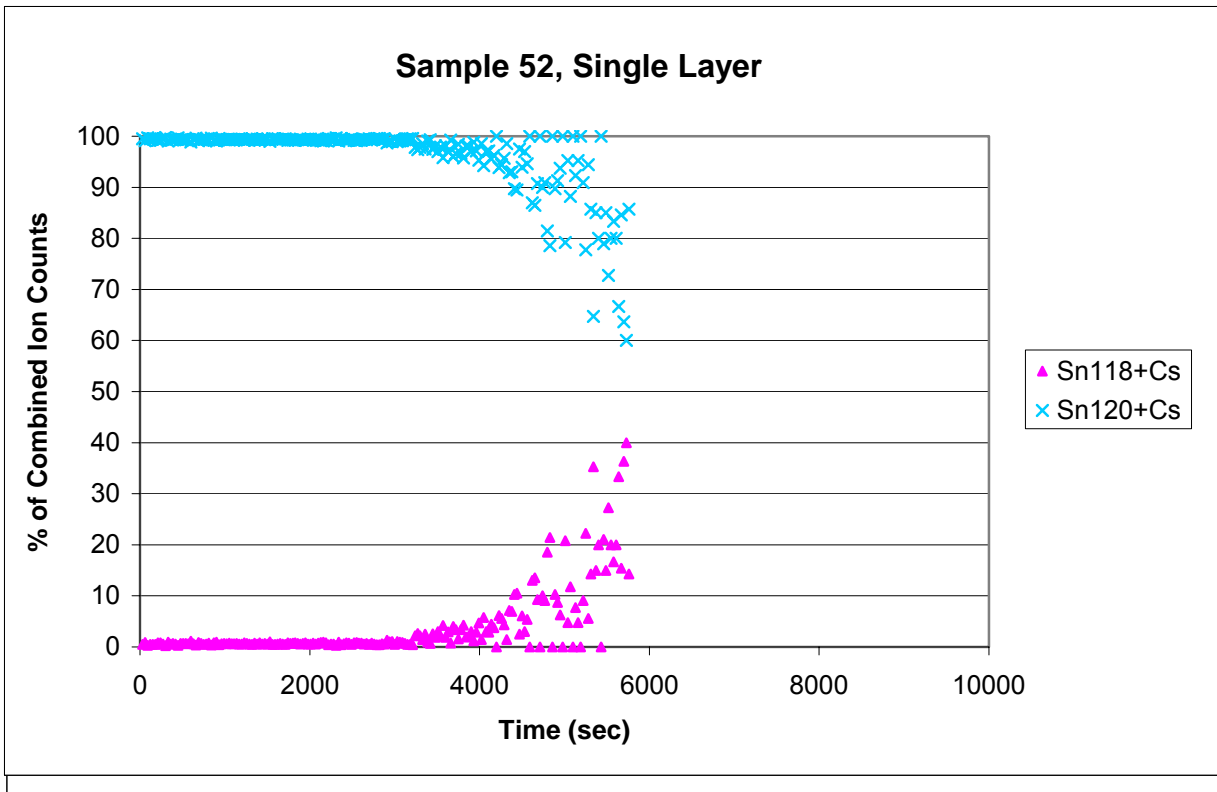

Figure 29. TOF-SIMS Depth Profile of the Double Layer of Matte Tin Plating showing Tin Isotopes Only (Sample 52, 1.4 Microns Sn^{120} over 1.6 Microns Sn^{118}, 10 Days after Plating)

27
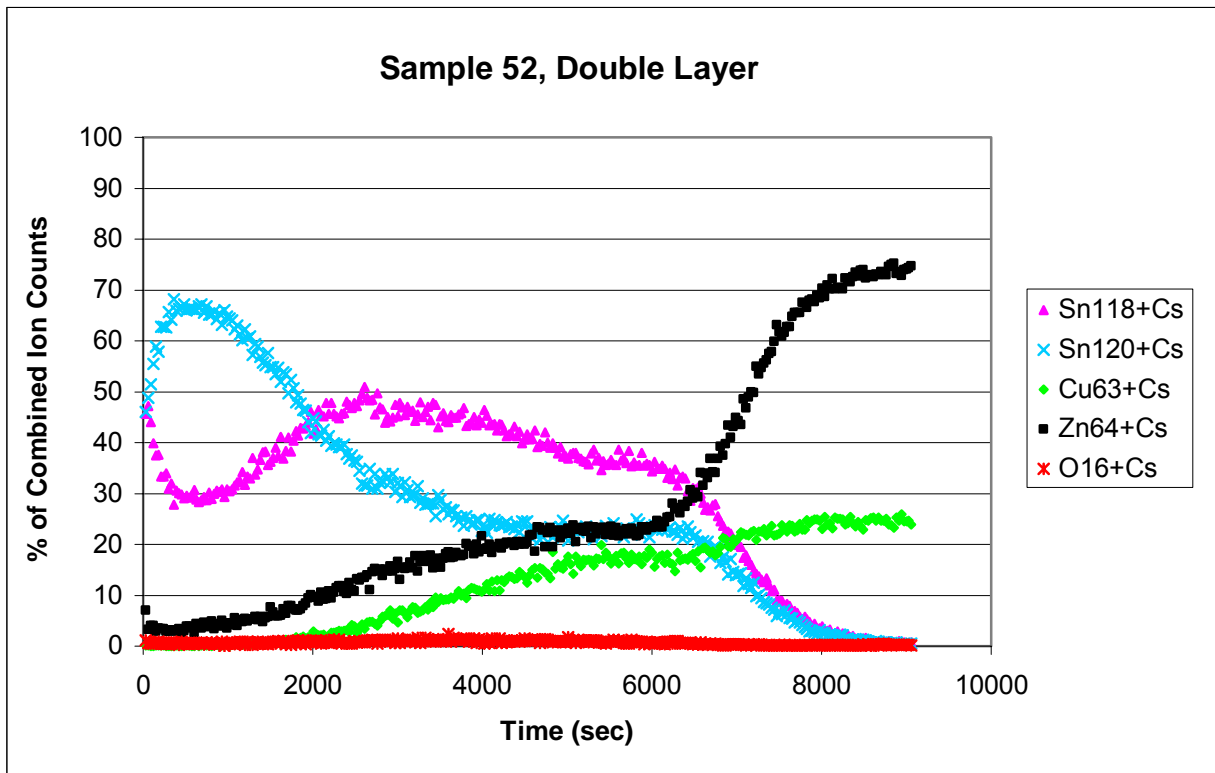
Figure 30. TOF-SIMS Depth Profile of the Double Layer of Matte Tin Plating (Sample 52, 1.4 Microns Sn[120] over 1.6 Microns Sn[118], 117 Days after Plating)
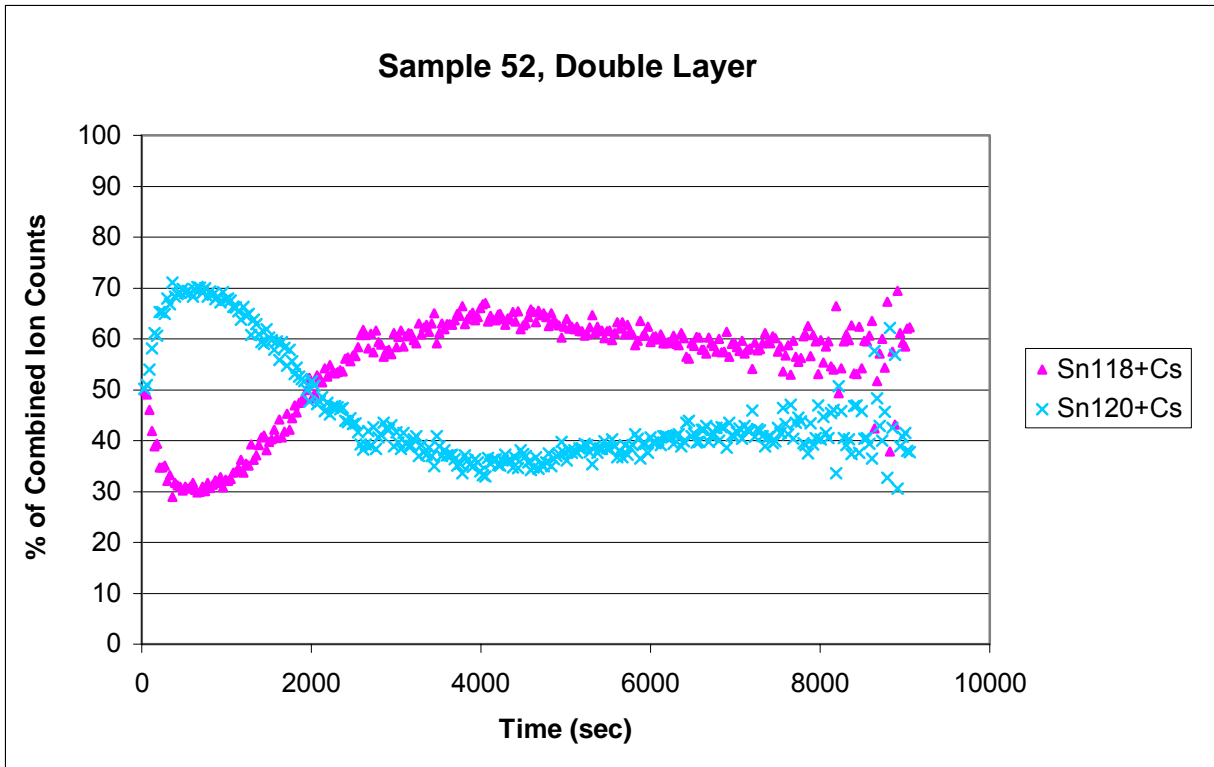
Figure 31. TOF-SIMS Depth Profile of the Double Layer of Bright Matte Plating showing Tin Isotopes Only (Sample 52, 1.4 Microns Sn[120] over 1.6 Microns Sn[118], 117 Days after Plating)
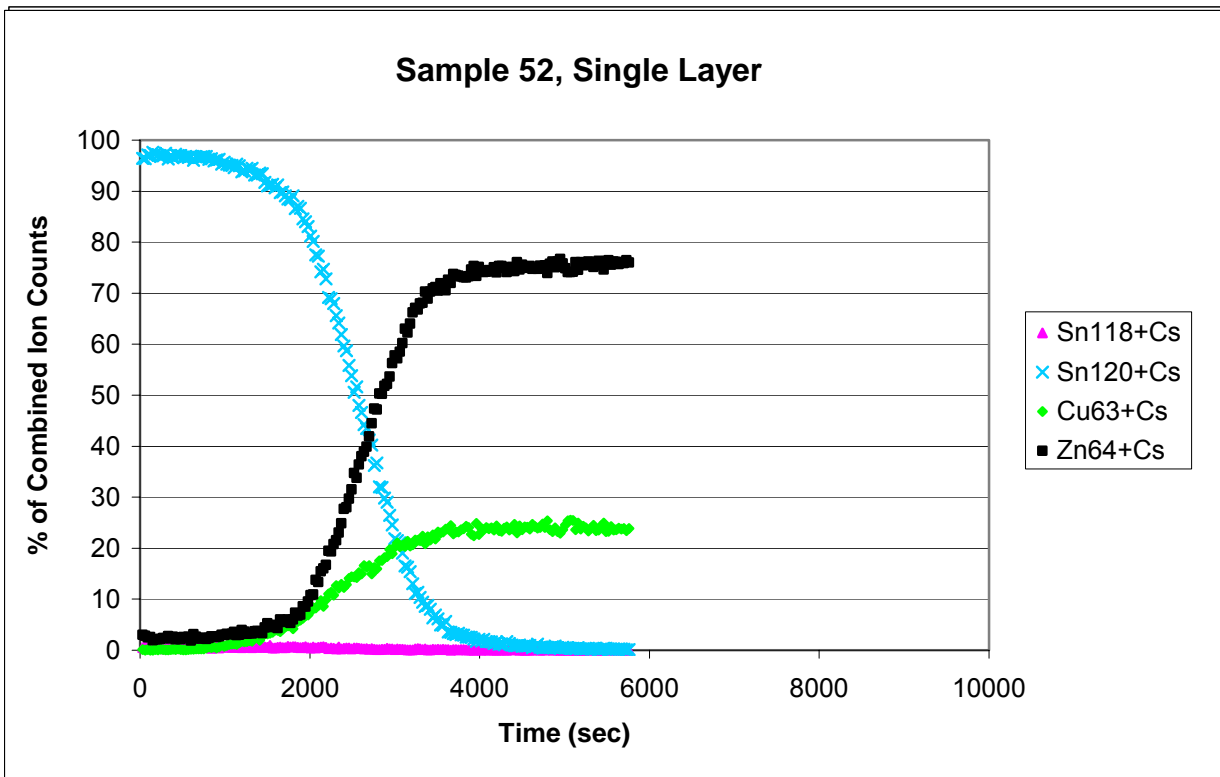
Figure 32. TOF-SIMS Depth Profile of the Single Layer of Sn^{120} Matte Tin Plating (Sample 52, 1.4 Microns Sn^{120}, 10 Days after Plating, Analysis Location was 2650 Microns from the Single Layer/Double Layer Interface)
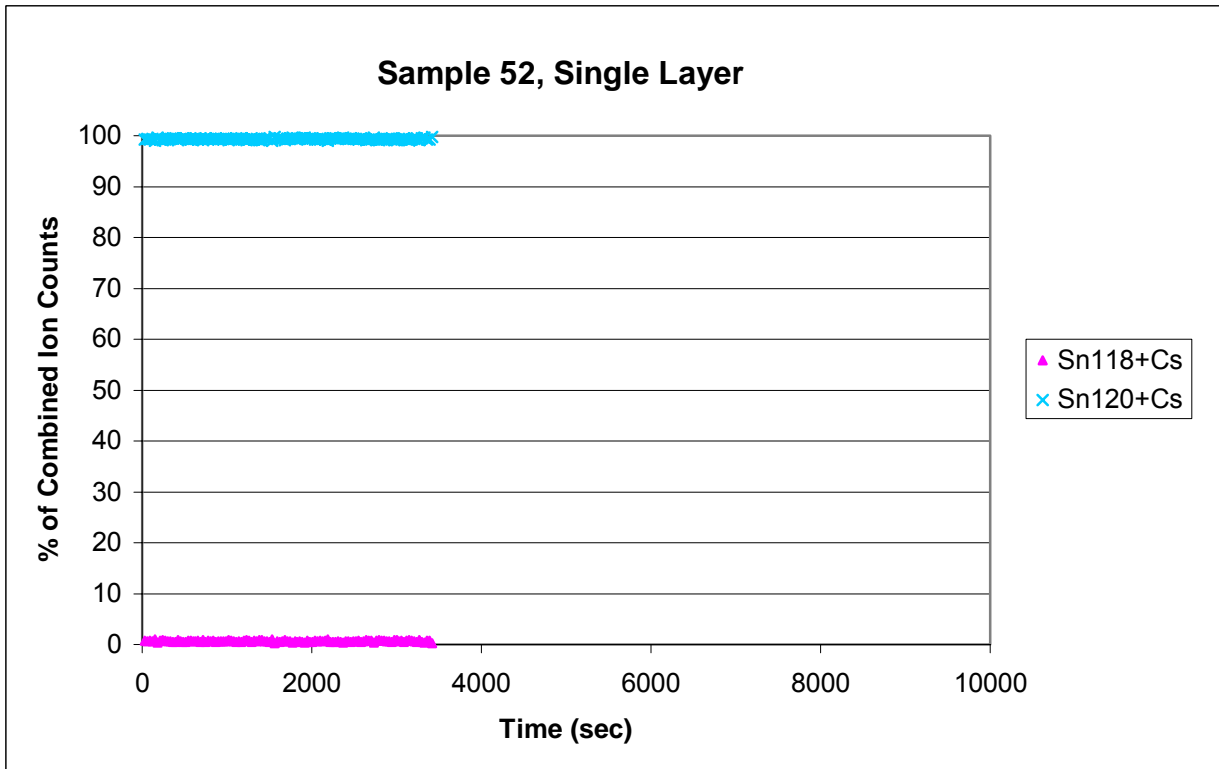

Figure 33. TOF-SIMS Depth Profile of the Single Layer of Sn^{120} Matte Tin Plating showing Tin Isotopes Only (Sample 52, 1.4 Microns Sn^{120}, 10 Days after Plating, Analysis Location was 2650 Microns from the Single Layer/Double Layer Interface)
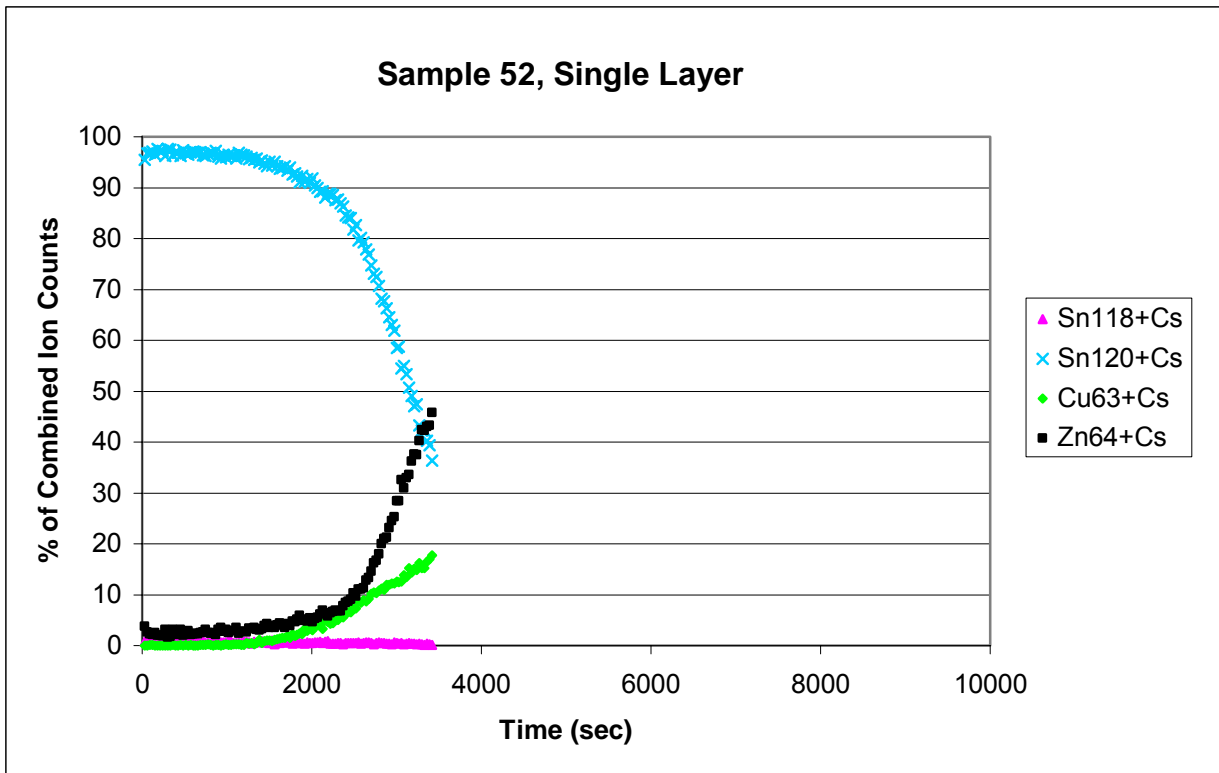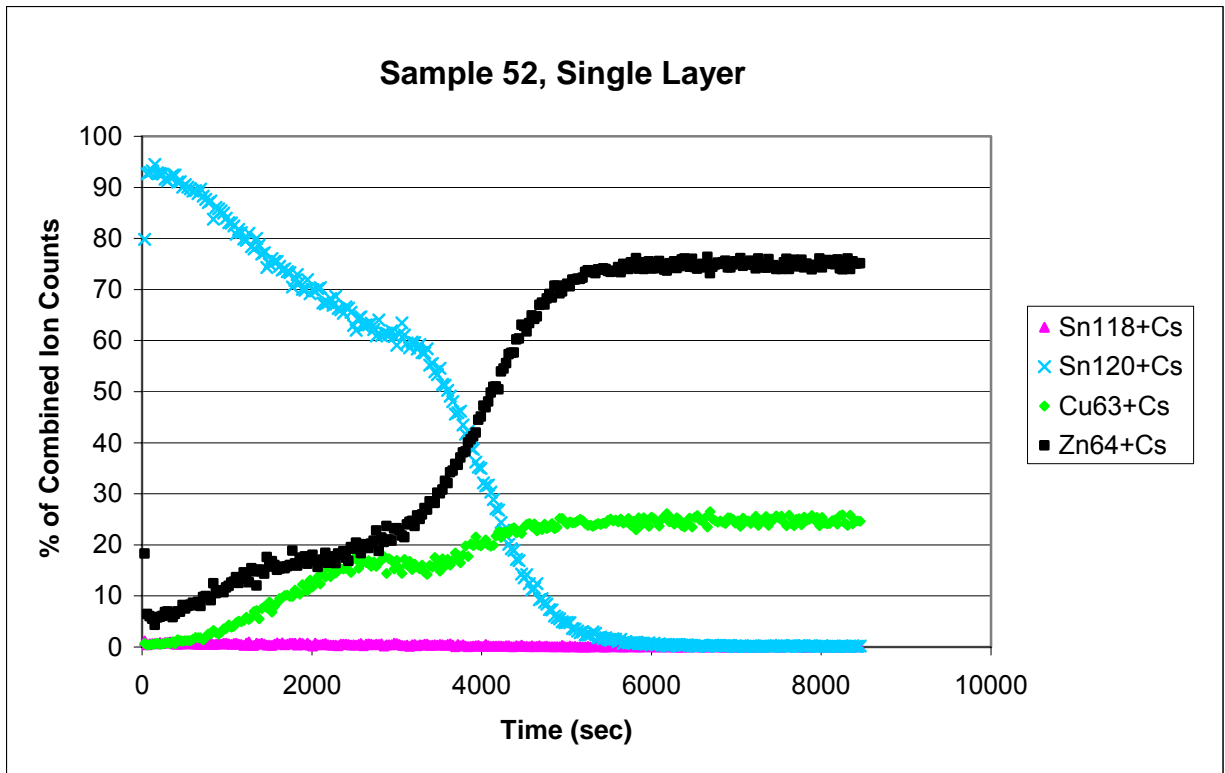
Figure 34. TOF-SIMS Depth Profile of the Single Layer of Sn^{120} Matte Tin Plating (Sample 52, 1.4 Microns Sn^{120}, 10 Days after Plating, Analysis Location was 290 Microns from the Single Layer/Double Layer Interface)
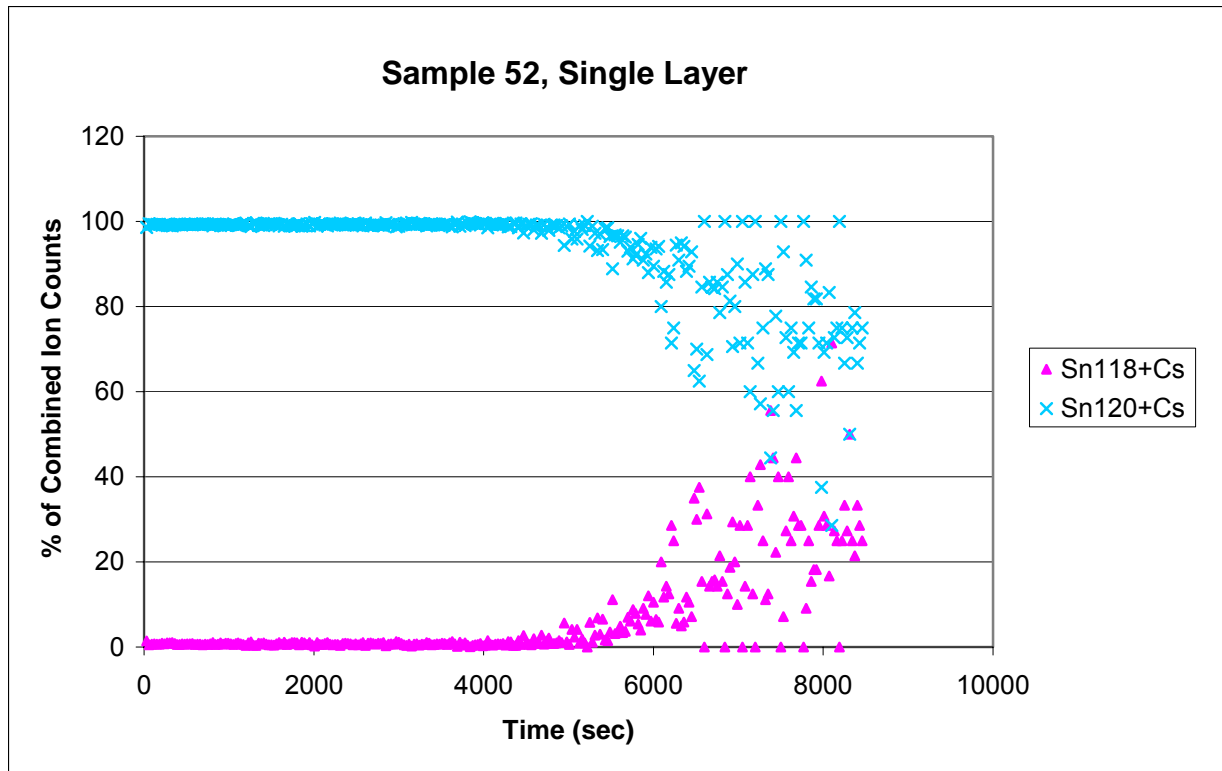

Figure 35. TOF-SIMS Depth Profile of the Single Layer of Sn^{120} Matte Tin Plating showing Tin Isotopes Only (Sample 52, 1.4 Microns Sn^{120}, 10 Days after Plating, Analysis Location was 290 Microns from the Single Layer/Double Layer Interface)

Figure 36. TOF-SIMS Depth Profile of the Single Layer of Sn^{120} Matte Tin Plating (Sample 52, 1.4 Microns Sn^{120}, 117 Days after Plating, Analysis Location was 315 Microns from the Single Layer/Double Layer Interface)
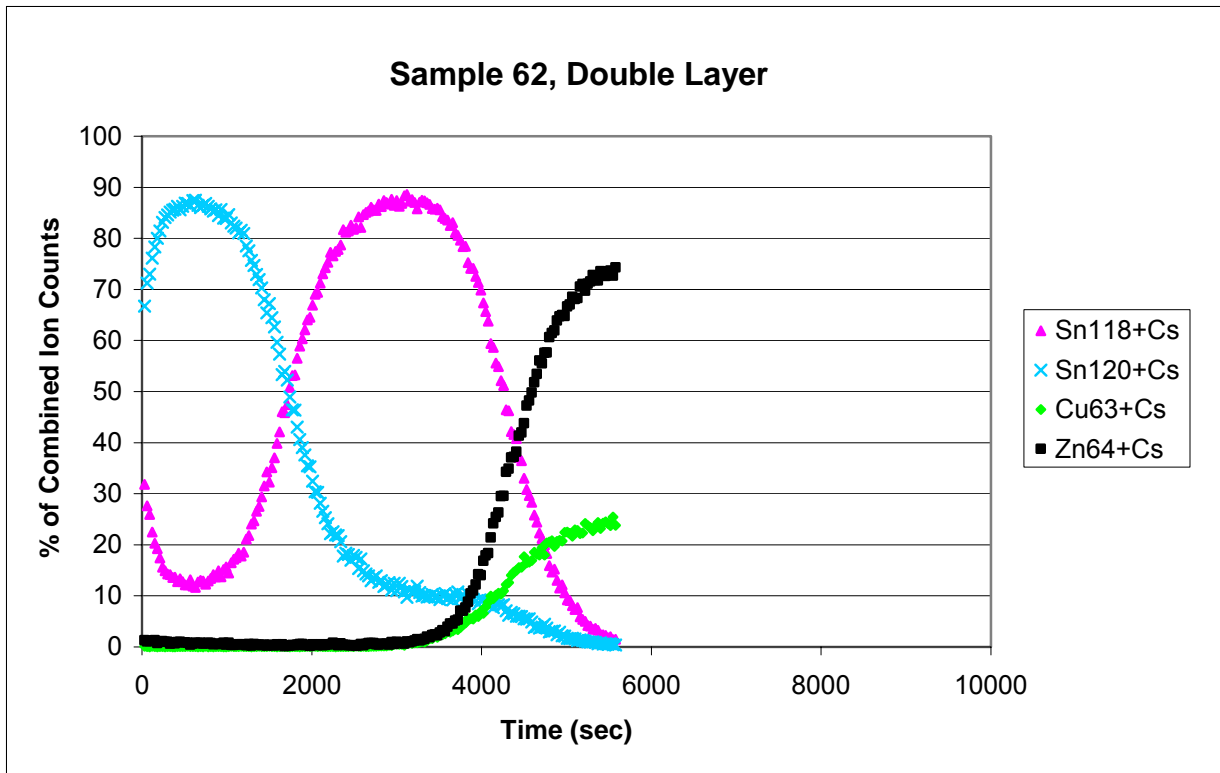

Figure 37. TOF-SIMS Depth Profile of the Single Layer of Sn^{120} Matte Tin Plating showing Tin Isotopes Only (Sample 52, 1.4 Microns Sn^{120}, 117 Days after Plating, Analysis Location was 315 Microns from the Single Layer/Double Layer Interface)

Figure 38. TOF-SIMS Depth Profile of the Double Layer of Matte Tin Plating (Sample 62, 0.8 Microns Sn^{120} over 1.2 Microns Sn^{118}, 3 Days after Plating)
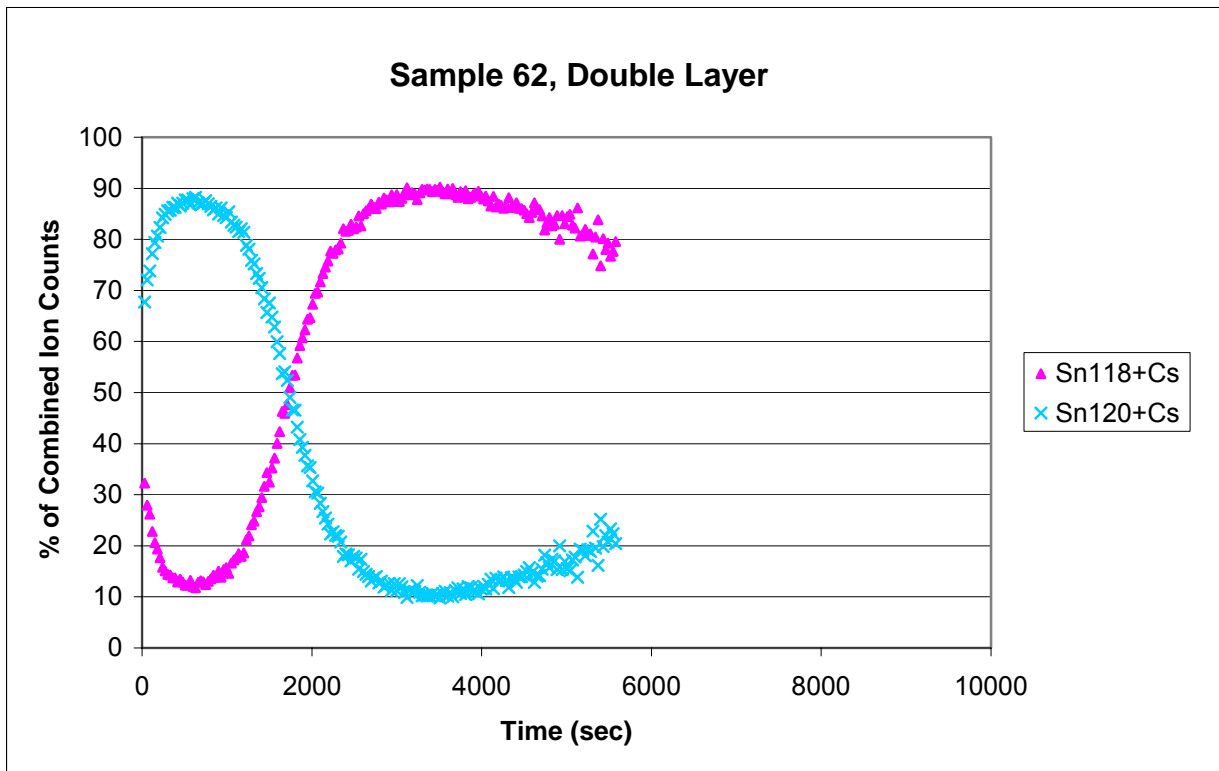

Figure 39. TOF-SIMS Depth Profile of the Double Layer of Matte Tin Plating showing Tin Isotopes Only (Sample 62, 0.8 Microns Sn^{120} over 1.2 Microns Sn^{118}, 3 Days after Plating)
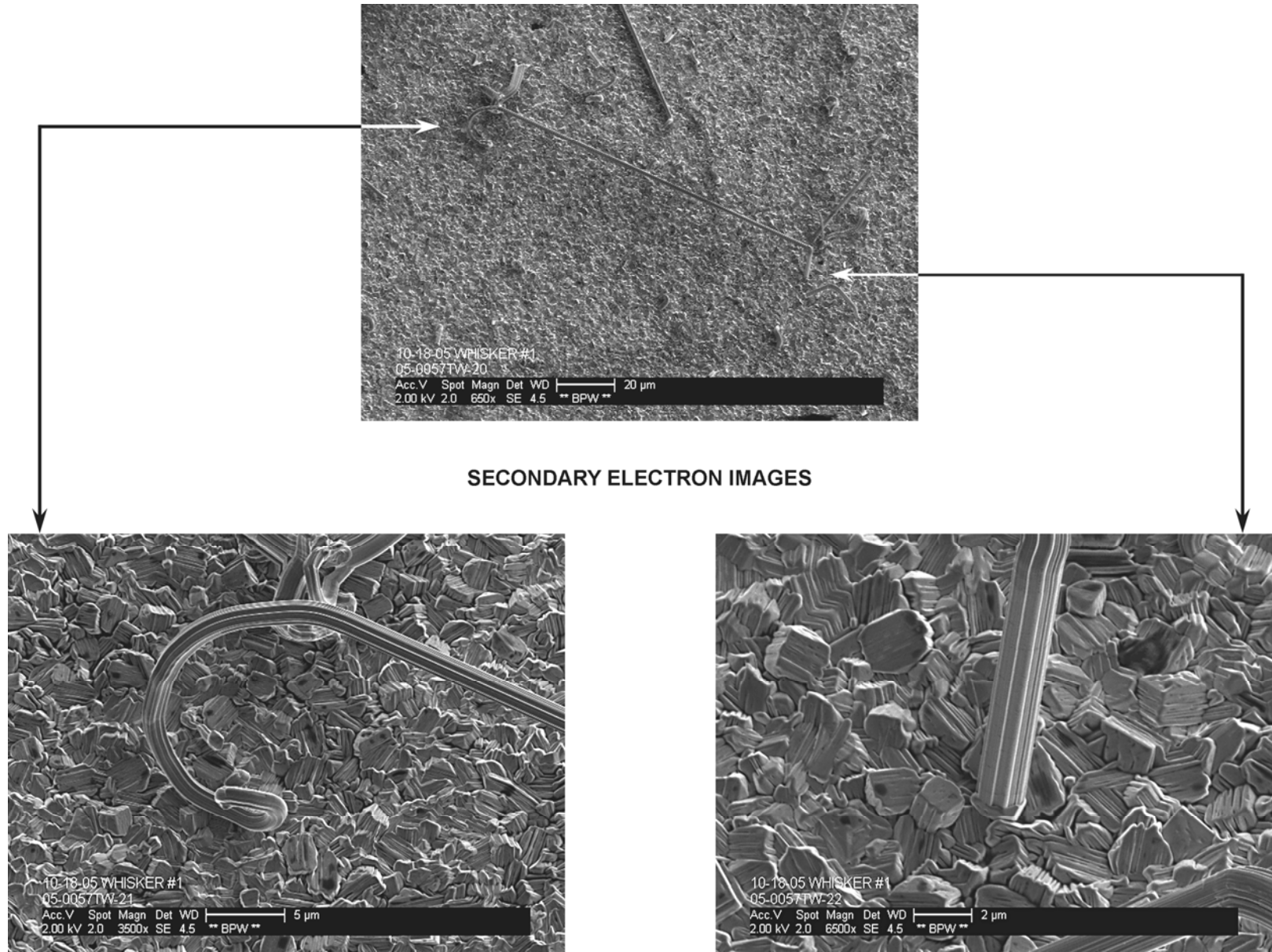
SECONDARY ELECTRON IMAGES

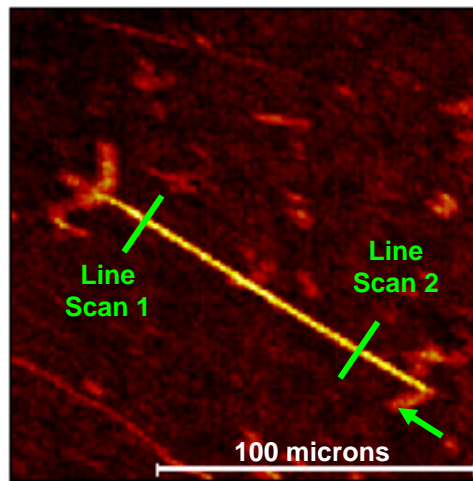**Figure 40. SEM Photo of Whisker 1 on the Sn^{120}/Sn^{118} Double Layer (Sample 62, Matte Tin Plating)**

Figure 41. TOF-SIMS Sn^{120} Positive Ion Image of Whisker 1 on the Sn^{120}/Sn^{118} Double Layer. The Green Arrow indicates the Base of the Whisker (Sample 62, Matte Tin Plating, 45 Days after Plating).
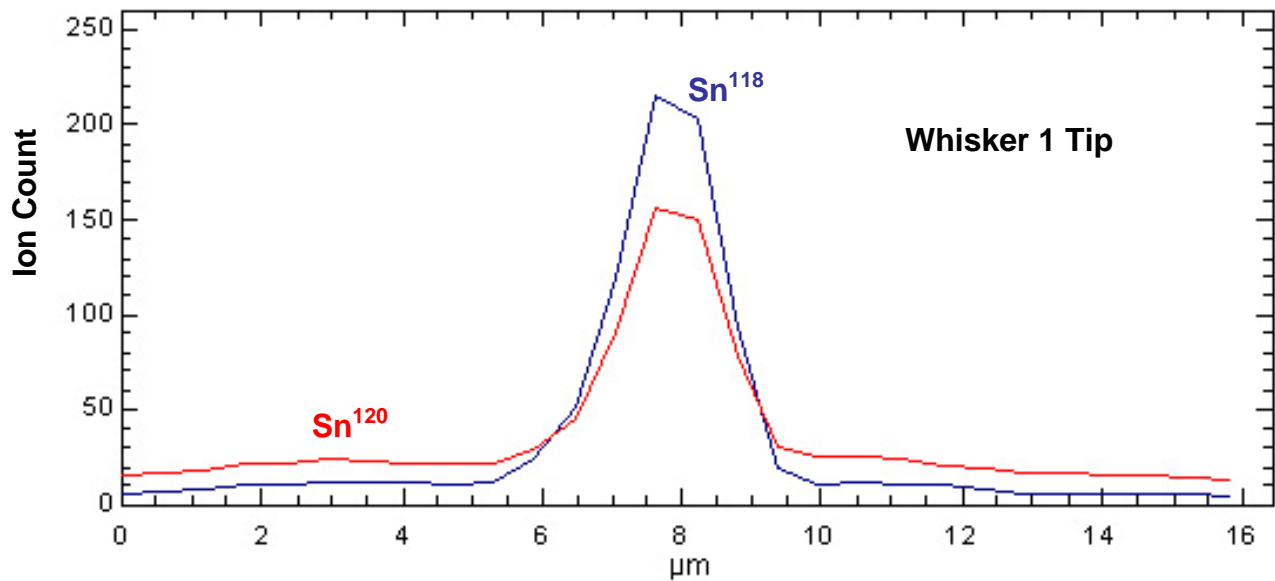

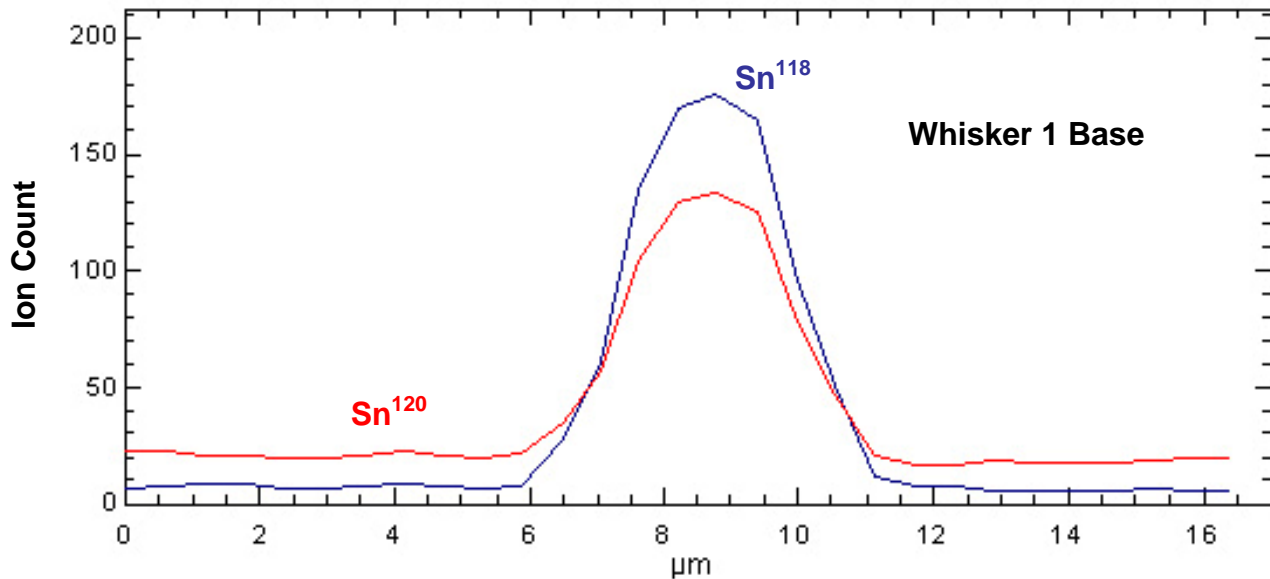**Figure 42. Line Scan 1 (for Sn^{120} and Sn^{118}) of Whisker 1 as shown in Figure 41**

Figure 43. Line Scan 2 (for Sn^{120} and Sn^{118}) of Whisker 1 as shown in Figure 41

34

Table 3. Tin Isotope Relative Percentages found on Whiskers on the Double Layer (Sn^{120} over Sn^{118}). The Absolute Error in the Measurements was estimated to be ±2 Percent.

Sample ID	Whisker ID	Plating Type	Expected Sn Isotope Relative Percentages in Sn^{120}/Sn^{118} Double Layer when Mixing is Complete		Sn Isotope Relative Percentages Found near Whisker Base		Sn Isotope Relative Percentages Found near Whisker Tip		Approx. Distance between Base and Tip Measurement Points (microns)	Approx. Distance of Whisker from Single Layer/Double Layer Interface (microns)	Comments
			$\%Sn^{120}$	$\%Sn^{118}$	$\%Sn^{120}$	$\%Sn^{118}$	$\%Sn^{120}$	$\%Sn^{118}$			
62	1	Matte	41	59	43	57	42	58	80	1400	Analyses Performed 44 Days after Plating; **Mixing of Double Layer was Incomplete.**
62	5A	Matte	41	59	38	62	37	63	20	5500	
62	5B	Matte	41	59	37	63	35	65	35	5500	
62	5C	Matte	41	59	37	63	36	64	45	5500	
52	17A	Matte	48	52	50	50	48	52	100	1100	Analyses Performed 117 Days after Plating; **Mixing of Double Layer was Incomplete (see Figure 31).**
52	17B	Matte	48	52	51	49	48	52	100	1100	
52	18	Matte	48	52	44	56	47	53	150	4700	
52	19A	Matte	48	52	47*	53*	48*	52*	320	5800	
52	19B	Matte	48	52	49*	51*	50*	50*	250	5800	
89	7	Bright	69	31	65	35	66	34	80	3200	Analyses Performed 66 Days after Plating; Mixing of Double Layer was Nearly Complete; However, Whisker 7 was Fully Formed 23 Days after Plating when Mixing of Double Layer was Incomplete.
89	11	Bright	69	31	nm	nm	64	36	20	3200	
89	21	Bright	69	31	66*	34*	70*	30*	55	3000	Analyses Performed 187 Days after Plating; Mixing of Double Layer was Complete (see Figure 15).
89	22	Bright	69	31	65	35	66	34	40	1650	

*Which end is the base and which end is the tip is unknown
nm = not measured

Table 4. Tin Isotope Relative Percentages found on Nodules on the Bright Tin Double Layer (Sn^{120} over Sn^{118})

| Sample ID	Nodule ID	Plating Type	Expected Sn Isotope Relative Percentages in Sn^{120}/Sn^{118} Double Layer when Mixing is Complete		Sn Isotope Relative Percentages Found on Nodule		Comments
			$\%Sn^{120}$	$\%Sn^{118}$	$\%Sn^{120}$	$\%Sn^{118}$	
89	Nodule at Base of Whisker 7	Bright	69	31	65	35	Analyses Performed 187 Days after Plating; Mixing of Double Layer was Complete (see Figure 15).
89	Nodule at Base of Whisker 22	Bright	69	31	67	33	
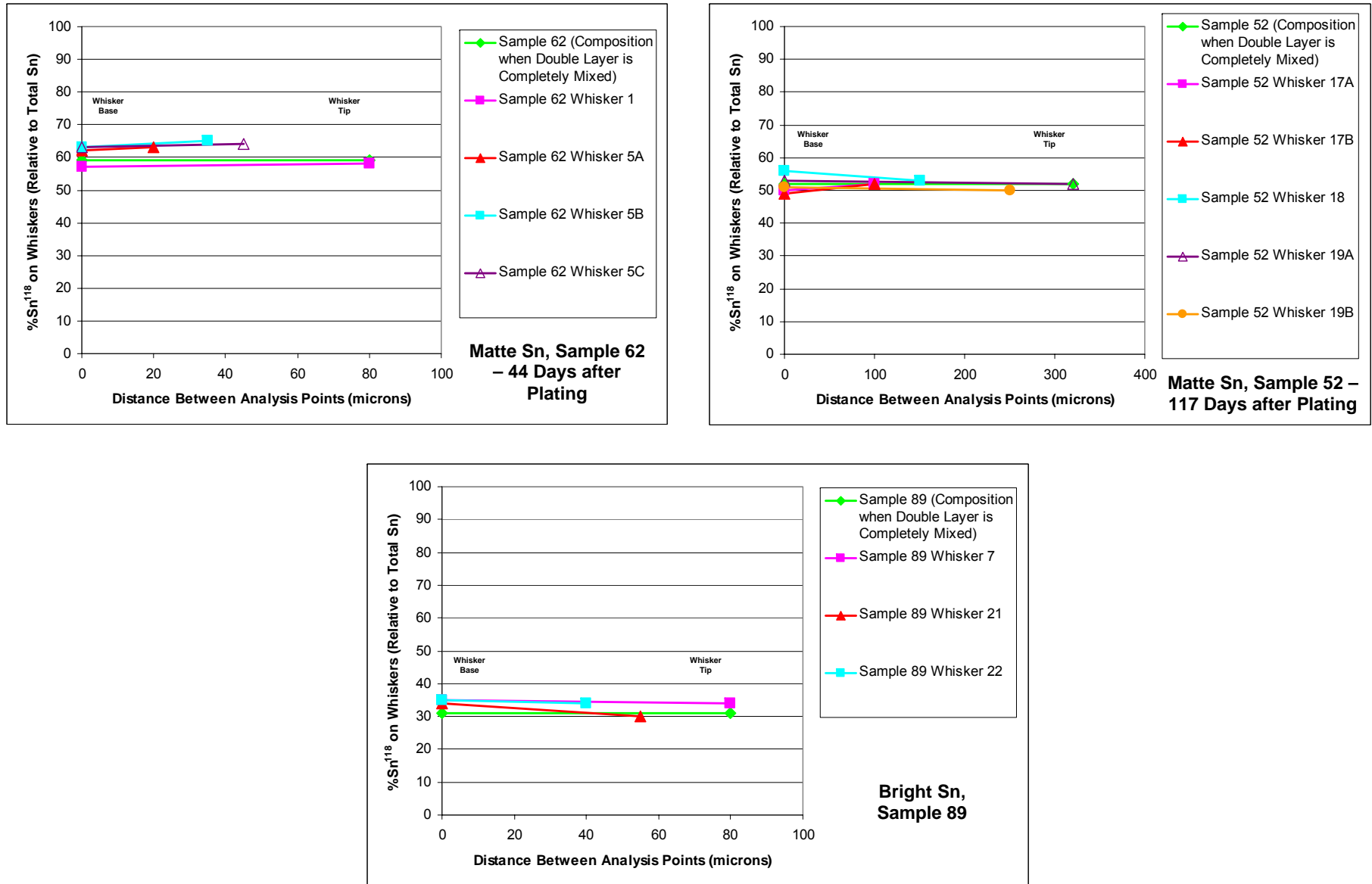
Figure 44. Percent of Sn[118] found on the the Base and the Tip of the Whiskers on the Double Isotope Layer (Data is from Table 3. Note: the Isotopic Composition is Relatively Constant along the Length of Each Whisker. Also, the Isotopic Compositions are Close to the Composition Expected from Complete Mixing of the Double Layer).
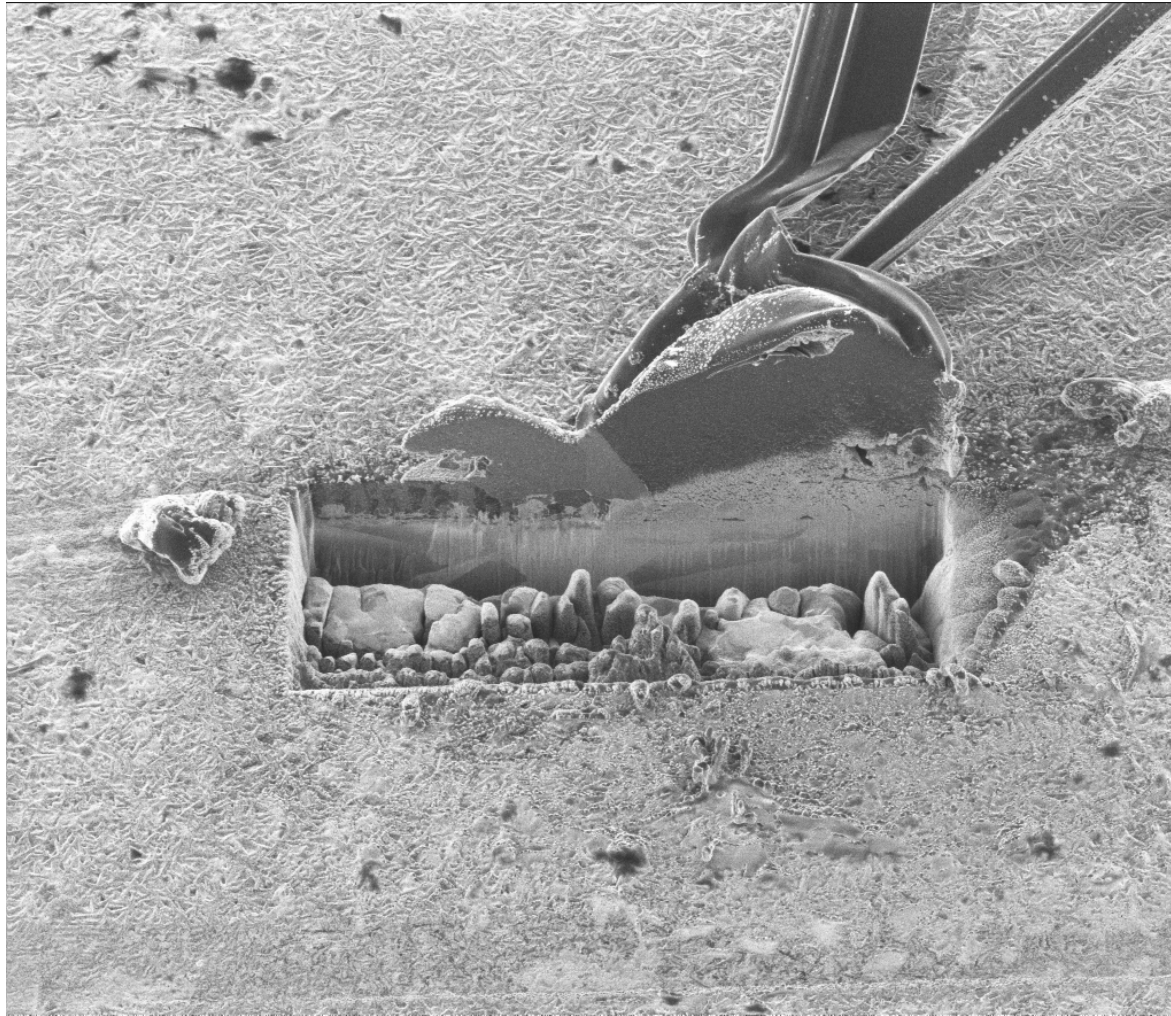
Figure 45. FIB Microsection of a Nodule on the Bright Tin Plating. Nodule was formed by Recrystallization of the Plating Grains (Sample 90, Single Layer, Note the Whiskers growing from the Nodule).

Table 5. Tin Isotope Relative Percentages found on Whiskers on the Sn^{120} Single Layer

| Sample ID	Whisker ID	Plating Type	Sn Isotope Relative Percentages Found near Whisker Base		Sn Isotope Relative Percentages Found near Whisker Tip		Approx. Distance between Base and Tip Measurement Points (microns)	Comments
			%Sn^{120}	%Sn^{118}	%Sn^{120}	%Sn^{118}		
62	2A	Matte	97	3	96	4	130	Analysis performed 45 Days after Plating.
62	3G	Matte	90	10	87	13	35	
62	3H	Matte	90	10	91	9	25	
62	3I	Matte	96	4	95	5	15	Analyses performed 108 Days after Plating.
62	3C	Matte	94	6	94	6	140	
62	3F	Matte	84	16	85	15	10	
89	9	Bright	99	1	99	1	95	Analysis performed 66 Days after Plating.
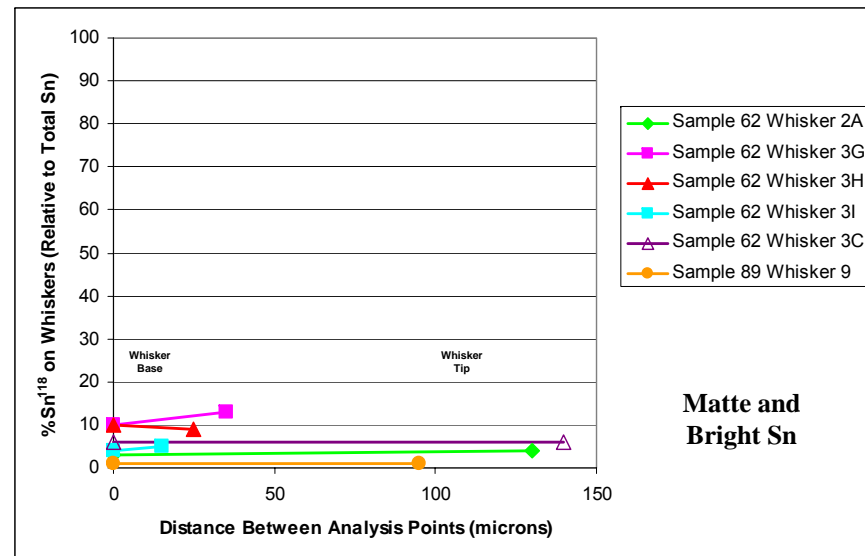
Figure 46. Percent of Sn^{118} found on the the Base and the Tip of the Whiskers on the Single Isotope Layer (Data from Table 5, Note: the Isotopic Composition is Relatively Constant along the Length of Each Whisker)
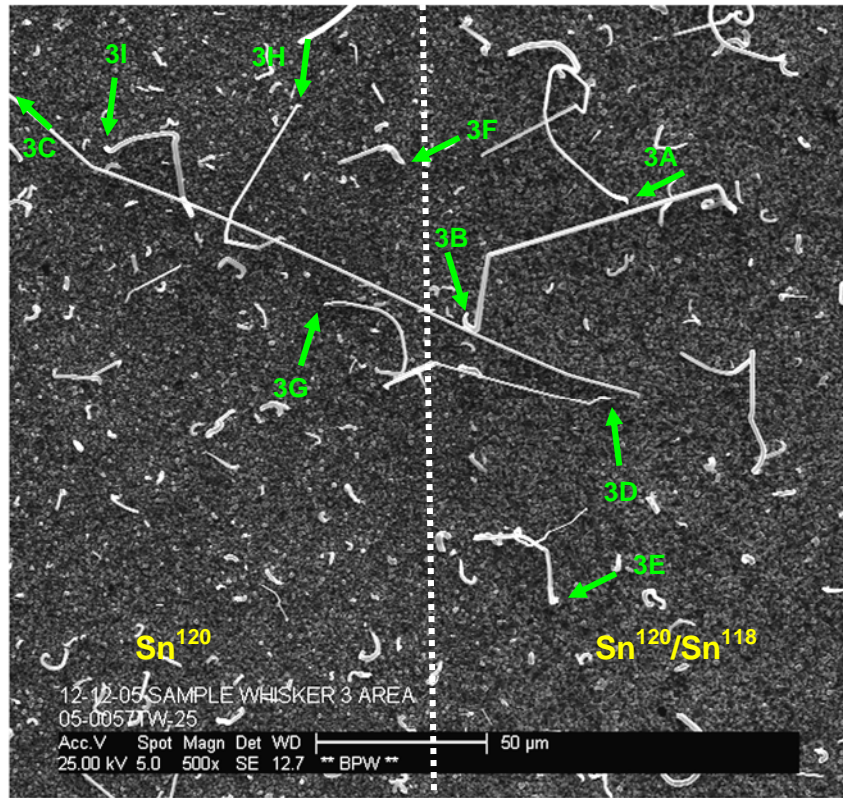
38

Figure 47. SEM Image of Tin Whiskers; a Green Arrow indicates the Base of the Whisker (Sample 62, Matte Tin Plating, the Dotted White Line marks the Interface between the Sn^{120} Single Layer and the Sn^{120}/Sn^{118} Double Layer, Photo taken 211 Days after Plating)
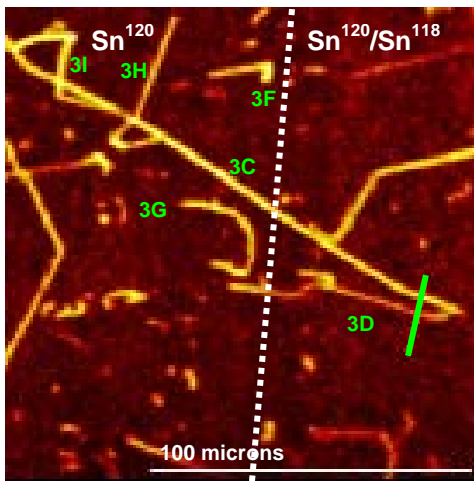

Figure 48. TOF-SIMS Sn^{120} Positive Ion Image of Area in Figure 47 (Sample 62, Matte Tin Plating, the Dotted White Line marks the Interface between the Sn^{120} Single Layer and the Sn^{120}/Sn^{118} Double Layer, 108 Days after Plating). Whiskers 3A, 3F, 3G and 3I were Fully Formed at 45 Days after Plating. The Green Line is a Line Scan.
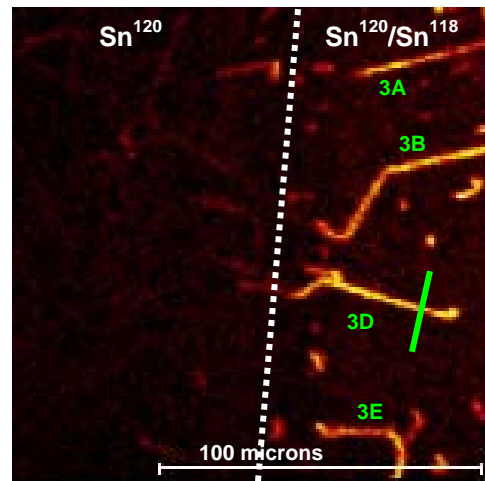
Figure 49. TOF-SIMS Sn^{118} Positive Ion Image of Area in Figure 47 (Sample 62, Matte Tin Plating, the Dotted White Line marks the Interface between the Sn^{120} Single Layer and the Sn^{120}/Sn^{118} Double Layer, 108 Days after Plating). The Green Line is a Line Scan.
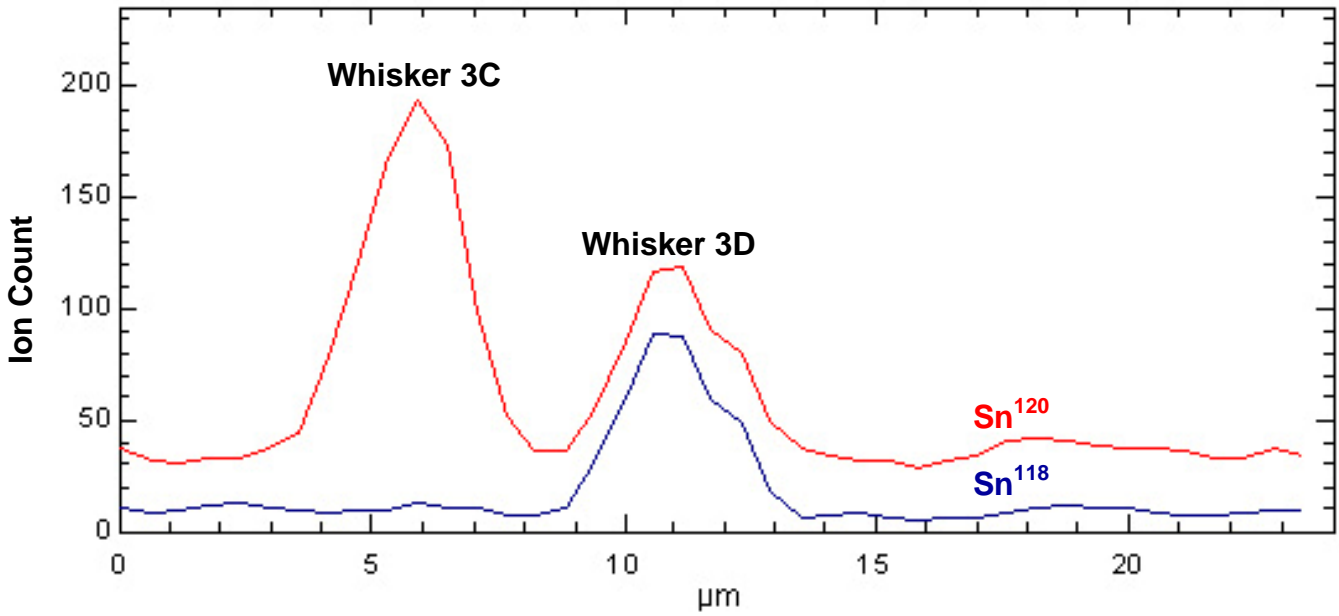
39

Figure 50. Sn^{120} Line Scan and Sn^{118} Line Scan of Whiskers 3C and 3D as shown in Figures 48 and 49
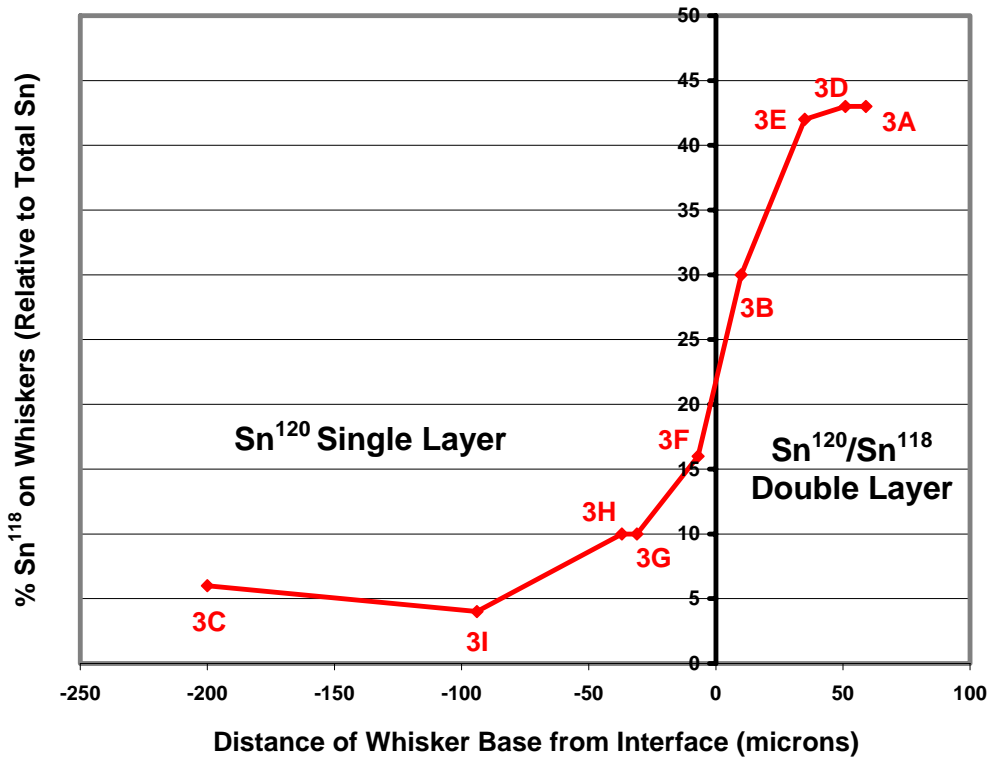
Figure 51. Relative Percent of Sn^{118} on Whiskers on Both Sides of the Interface between the Sn^{120} Single Layer and the Sn^{120}/Sn^{118} Double Layer (Sample 62, Matte Tin Plating, Data is for the Base of the Whiskers shown in Figure 47 at 108 Days after Plating)

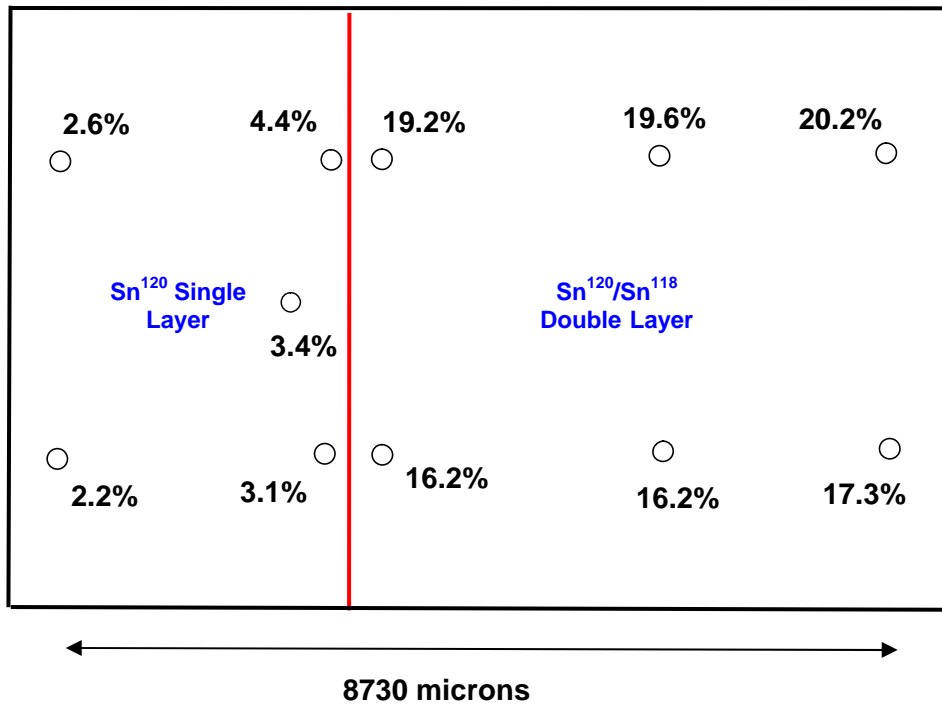2.6%   4.4%   19.2%   19.6%   20.2%

Sn^{120} Single Layer

3.4%

Sn^{120}/Sn^{118} Double Layer

2.2%   3.1%   16.2%   16.2%   17.3%

8730 microns

Figure 52. Relative Percent of Sn^{118} on the Matte Tin Plating Surface (Sample 63, Vertical Red Line marks the Interface between the Sn^{120} Single Layer and the Sn^{120}/Sn^{118} Double Layer, 299 Days after Plating). Absolute Experimental Error was ±0.3%.

Sn^{120} Single Layer

Sn^{120}/Sn^{118} Double Layer

3

4

1   2   51.9%   55.6%

1.6%   1.9%

5840 microns

Figure 53. Relative Percent of Sn^{118} on the Matte Tin Plating Surface after 270 Seconds of Sputtering (Sample 63, Vertical Red Line marks the Interface between the Sn^{120} Single Layer and the Sn^{120}/Sn^{118} Double Layer, 337 Days after Plating)

41

Figure 54. Relative Percent of Sn[118] on the Bright Tin Plating Surface (Sample 91, Vertical Red Line marks the Interface between the Sn[120] Single Layer and the Sn[120]/Sn[118] Double Layer, 254 Days after Plating). Absolute Experimental Error was ±0.3%.
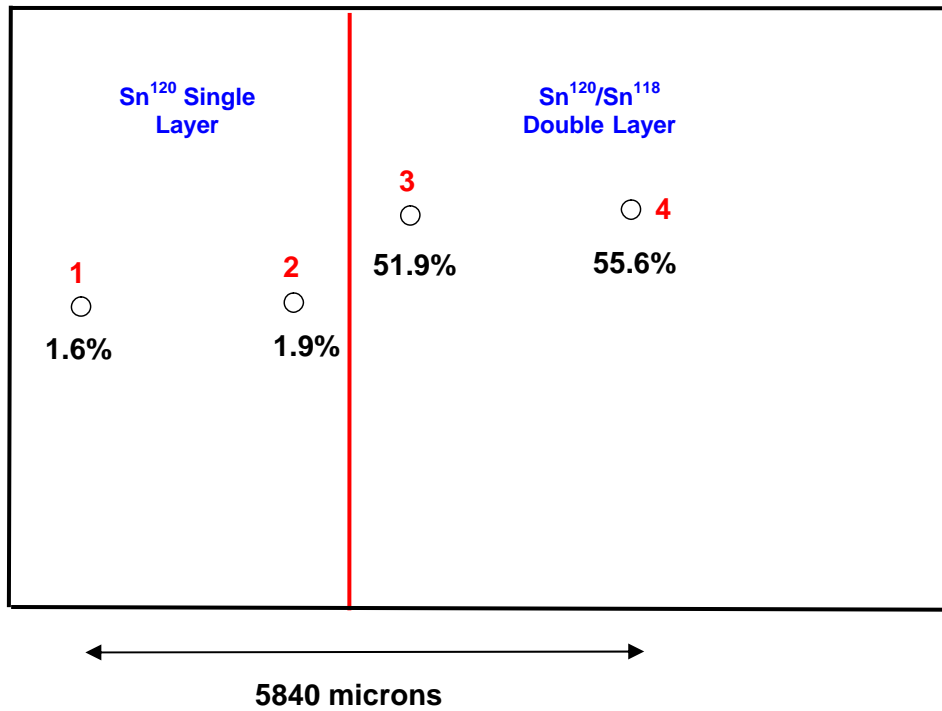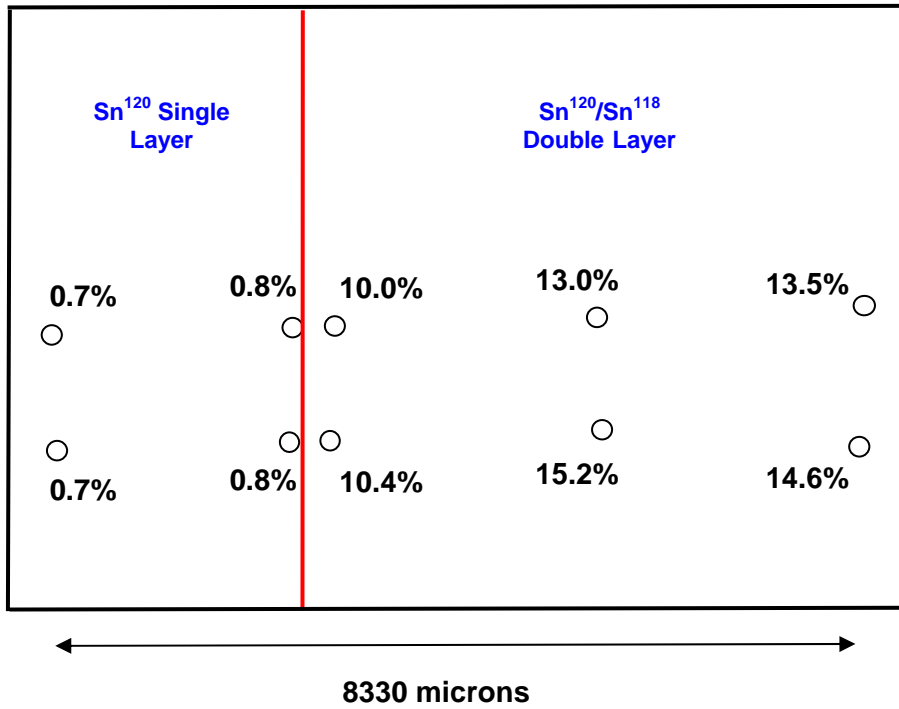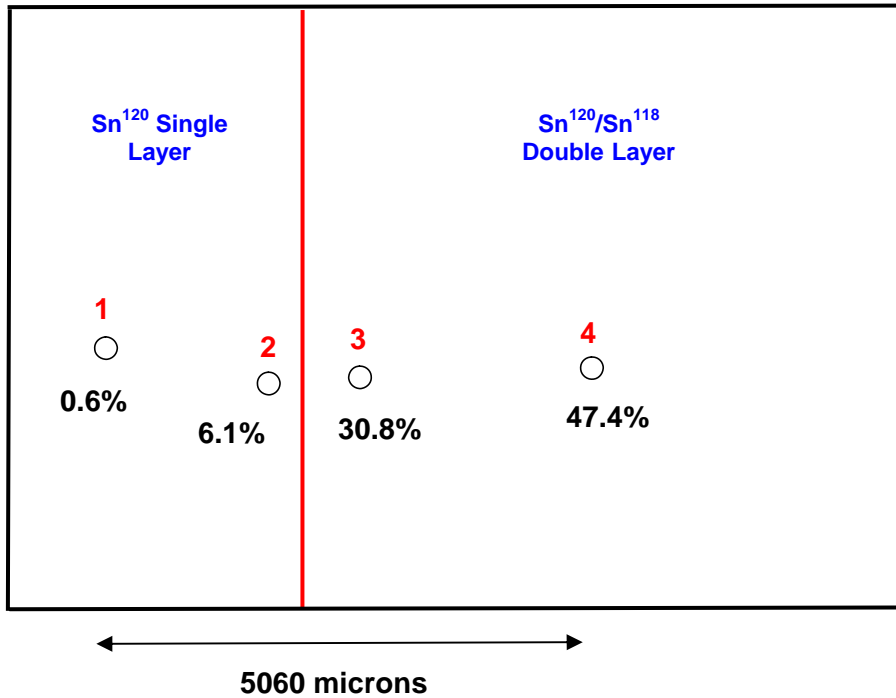

Figure 55. Relative Percent of Sn[118] on the Bright Tin Plating Surface after 270 Seconds of Sputtering (Sample 91, Vertical Red Line marks the Interface between the Sn[120] Single Layer and the Sn[120]/Sn[118] Double Layer, 296 Days after Plating)
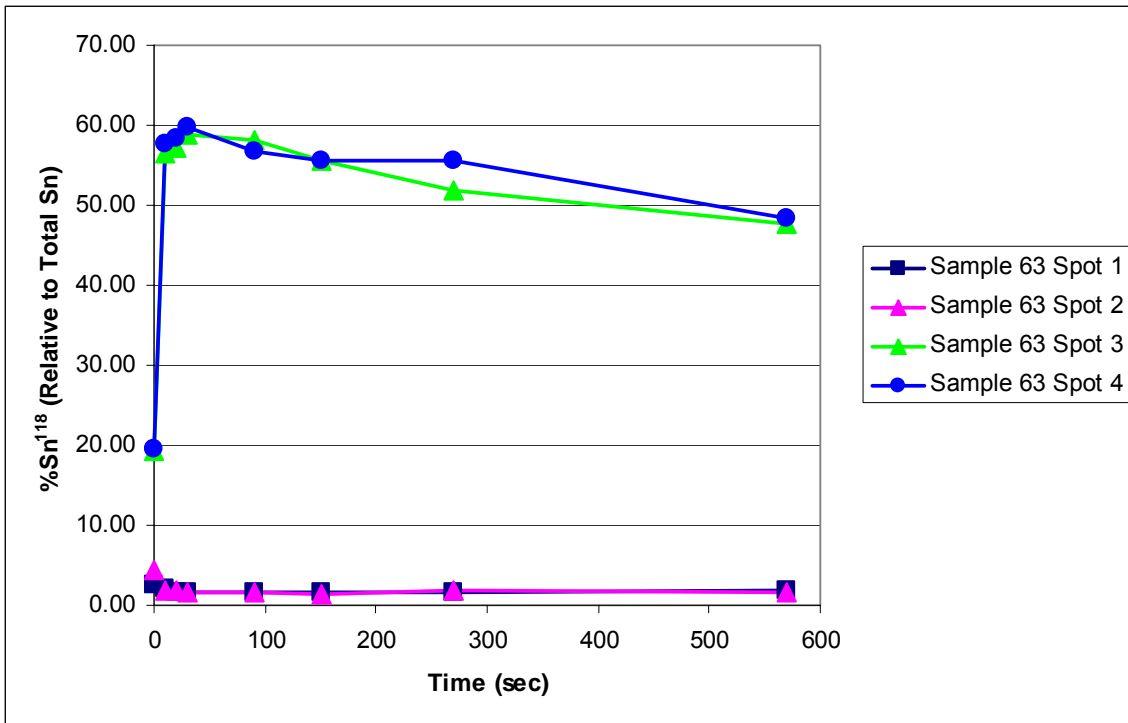
Figure 56. TOF-SIMS Depth Profiles of the Matte Tin Plating (Sample 63, Approximately 1.0 Microns Sn^{120} over 1.4 Microns Sn^{118}, 337 Days after Plating, See Figure 53 for Spot Locations, First Data Points are from Figure 52)
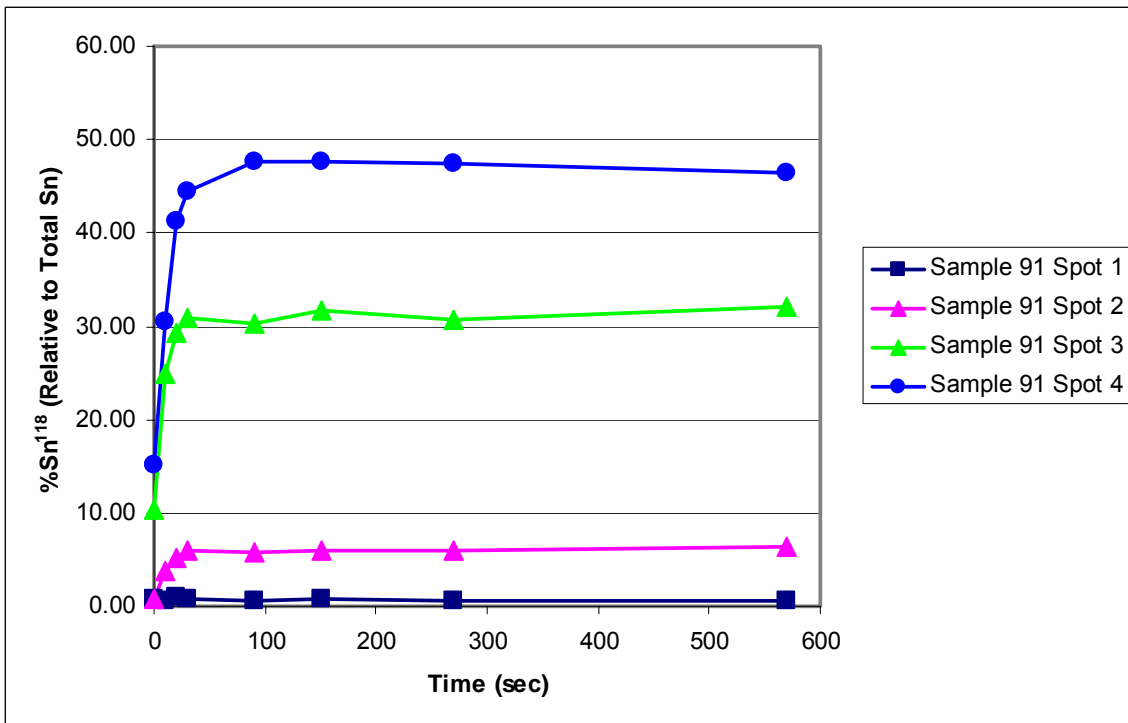

Figure 57. TOF-SIMS Depth Profiles of the Bright Tin Plating (Sample 91, Approximately 1.5 Microns Sn^{120} over 1.4 Microns Sn^{118}, 296 Days after Plating, See Figure 55 for Spot Locations, First Data Points are from Figure 54)

Table 6. Tin Isotope Relative Percentages found on the Surface of the Platings.
Absolute Experimental Error was ±0.3%.

Sample ID	Surface Area Analyzed	Plating Type	Time Elaspsed since Plating (days)	Expected Sn Isotope Relative Percentages in Sn^{120}/Sn^{118} Double Layer when Mixing is Complete		Sn Isotope Relative Percentages found on Plating Surface		Location of Area Analyzed
				$\%Sn^{120}$	$\%Sn^{118}$	$\%Sn^{120}$	$\%Sn^{118}$	
89	Sn^{120} Single Layer	Bright	187	69	31	99.5	0.5	Center of Single Layer
89	Sn^{120}/Sn^{118} Double Layer	Bright	187	69	31	84.1	15.9	Center of Double Layer
52	Sn^{120}/Sn^{118} Double Layer	Matte	10	48	52	83.7	16.3	Center of Double Layer
63	Sn^{120}/Sn^{118} Double Layer	Matte	3	42	58	83.3	16.7	Center of Double Layer

Table 7. Tin Isotope Relative Percentages found before and after Sputtering of Whiskers on Matte Tin.
The Absolute Error in the Measurements was estimated to be ±2 Percent.

Sample ID	Whisker ID	Plating	Plating Type	Expected Sn Isotope Relative Percentages in Sn^{120}/Sn^{118} Double Layer when Mixing is Complete		Pre-Sputter Analyses (45 days after plating for Whiskers 1, 5A, 5B, 5C; 108 days after plating for Whiskers 3B, 3D, 3E, 3F, 3G, 3H, 3I)				Pre-Sputter Analyses (254 days after plating)				Post-Sputter Analyses (282 days after plating)				Approx. Distance between Base and Tip Measurement Points (microns)
						Sn Isotope Relative Percentages Found near Whisker Base		Sn Isotope Relative Percentages Found near Whisker Tip		Sn Isotope Relative Percentages Found near Whisker Base		Sn Isotope Relative Percentages Found near Whisker Tip		Sn Isotope Relative Percentages Found near Whisker Base		Sn Isotope Relative Percentages Found near Whisker Tip		
				$\%Sn^{120}$	$\%Sn^{118}$	$\%Sn^{120}$	$\%Sn^{118}$	$\%Sn^{120}$	$\%Sn^{118}$	$\%Sn^{120}$	$\%Sn^{118}$	$\%Sn^{120}$	$\%Sn^{118}$	$\%Sn^{120}$	$\%Sn^{118}$	$\%Sn^{120}$	$\%Sn^{118}$	
62	1	Sn^{120}/Sn^{118} Double Layer	Matte	41	59	43	57	42	58	40	60	40	60	58 ▲	42 ▼	58 ▲	42 ▼	130
62	5A	Sn^{120}/Sn^{118} Double Layer	Matte	41	59	38	62	37	63	39	61	30	70	47 ▲	53 ▼	44 ▲	56 ▼	20
62	5B	Sn^{120}/Sn^{118} Double Layer	Matte	41	59	37	63	35	65	37	63	34	66	44 ▲	56 ▼	45 ▲	55 ▼	35
62	5C	Sn^{120}/Sn^{118} Double Layer	Matte	41	59	37	63	36	64	36	64	41	59	44 ▲	56 ▼	46 ▲	54 ▼	45
62	3B	Sn^{120}/Sn^{118} Double Layer*	Matte	41	59	70	30	65	35	73	27	72	28	82 ▲	18 ▼	72	28	40
62	3D	Sn^{120}/Sn^{118} Double Layer*	Matte	41	59	57	43	57	43	57	43	55	45	72 ▲	28 ▼	80 ▲	20 ▼	40
62	3E	Sn^{120}/Sn^{118} Double Layer*	Matte	41	59	58	42	61	39	54	46	56	44	70 ▲	30 ▼	72 ▲	28 ▼	30
62	3F	Sn^{120} Single Layer*	Matte	41	59	84	16	85	16	86	14	87	13	85	15	85	15	10
62	3G	Sn^{120} Single Layer*	Matte	41	59	90	10	87	13	88	12	87	13	91	9	87	13	30
62	3H	Sn^{120} Single Layer*	Matte	41	59	90	10	91	9	90	10	91	9	90	10	93	7	25
62	3I	Sn^{120} Single Layer*	Matte	41	59	96	4	95	5	96	4	nm	nm	96	4	94	6	20

* Near double layer/single layer interface
nm = not measured
▲ = increase compared to pre-sputter
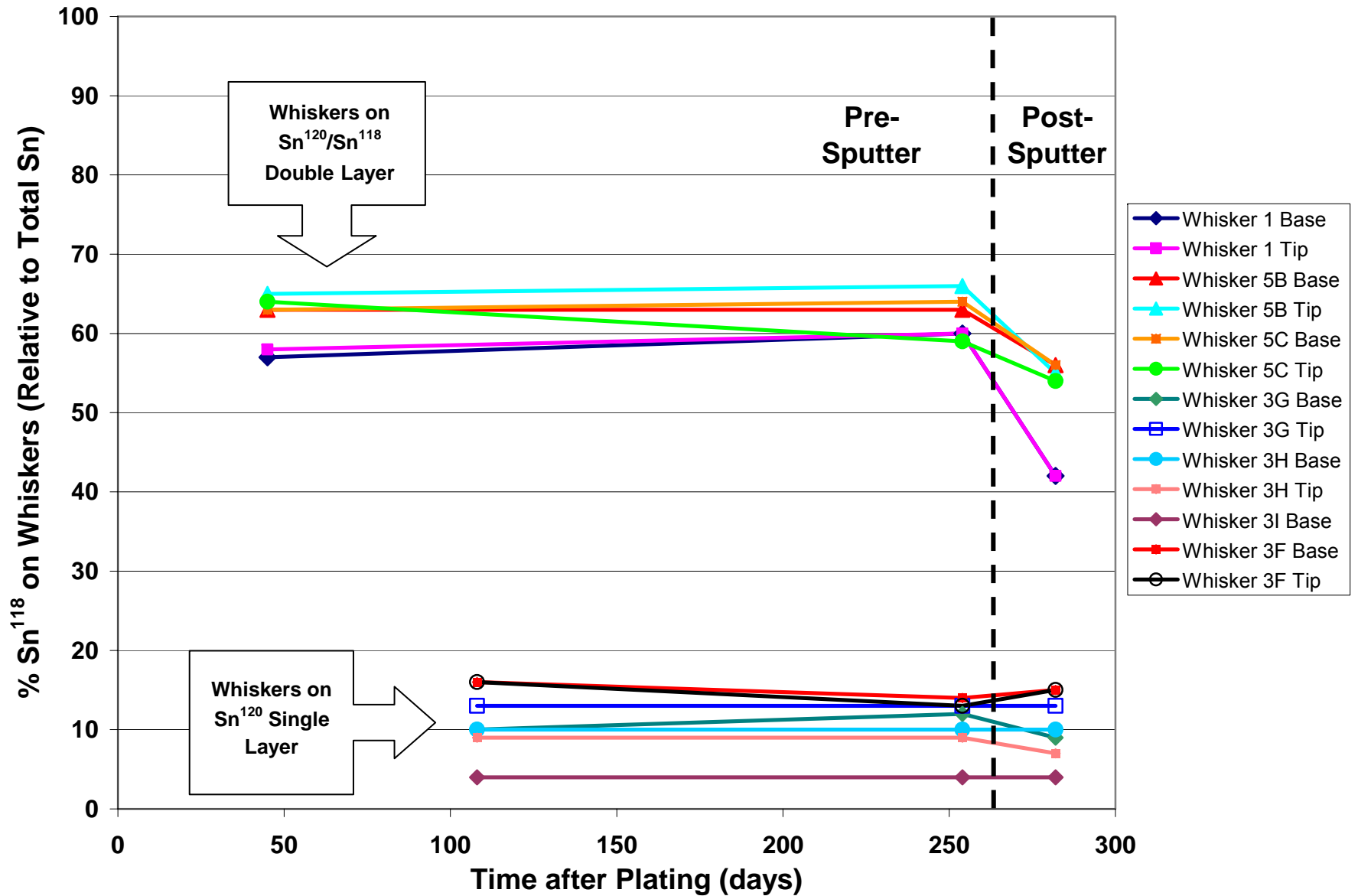▼ = decrease compared to pre-sputter

45

Figure 58. Relative Percentages of Sn^{118} found before and after Sputtering of Whiskers on Matte Tin (Sample 62, Data is from Table 7)
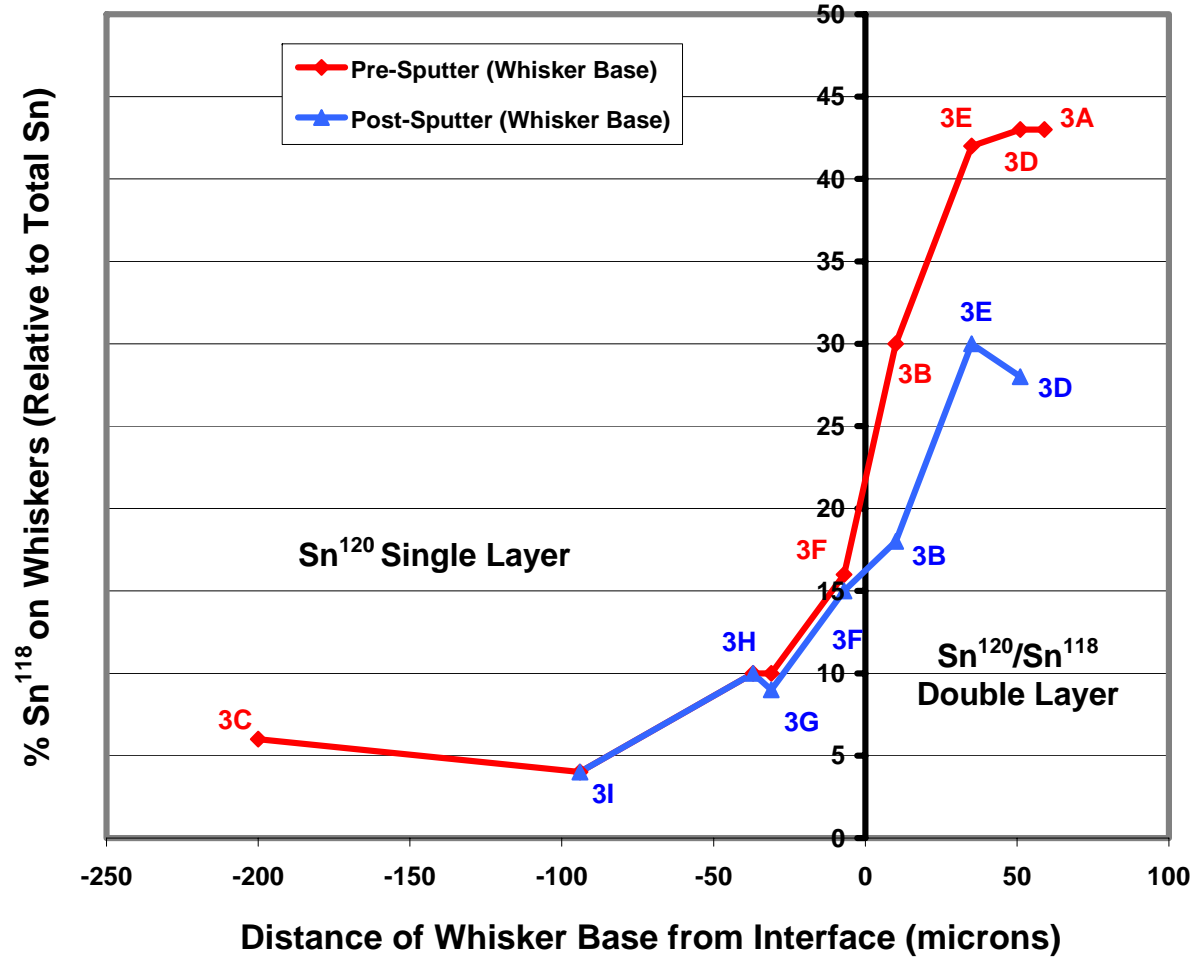
Figure 59. Relative Percentages of Sn[118] found before and after Sputtering of Whiskers on Both Sides of the Interface between the Matte Sn[120] Single Layer and the Matte Sn[120]/Sn[118] Double Layer (Data is for the Base of the Whiskers shown in Figure 47 at 108 Days after Plating and after Sputtering at 282 Days after Plating, see Table 7)

Table 8. Tin Isotope Relative Percentages found before and after Sputtering of Whiskers on the Bright Tin Double Layer (Sn^{120} over Sn^{118})

Sample ID	Whisker ID	Plating	Plating Type	Expected Sn Isotope Relative Percentages in Sn^{120}/Sn^{118} Double Layer when Mixing is Complete		Pre-Sputter Analyses (187 days after plating)				Post-Sputter Analyses (313 days after plating)				Approx. Distance between Base and Tip Measurement Points (microns)
						Sn Isotope Relative Percentages Found near Whisker Base		Sn Isotope Relative Percentages Found near Whisker Tip		Sn Isotope Relative Percentages Found near Whisker Base		Sn Isotope Relative Percentages Found near Whisker Tip		
				%Sn^{120}	%Sn^{118}	%Sn^{120}	%Sn^{118}	%Sn^{120}	%Sn^{118}	%Sn^{120}	%Sn^{118}	%Sn^{120}	%Sn^{118}	
89	7	Sn^{120}/Sn^{118} Double Layer	Bright	69	31	65	35	66	34	69	31	71	29	80
89	22	Sn^{120}/Sn^{118} Double Layer	Bright	69	31	65	35	66	34	79 ▲	21 ▼	81▲	19 ▼	20

▲ = increase compared to pre-sputter
▼ = decrease compared to pre-sputter

Table 9. Tin Isotope Relative Percentages found before and after Sputtering of Nodules on the Bright Tin Double Layer (Sn^{120} over Sn^{118})

| Sample ID	Nodule ID	Plating	Plating Type	Expected Sn Isotope Relative Percentages in Sn^{120}/Sn^{118} Double Layer when Mixing is Complete		Pre-Sputter Analyses (187 days after plating)		Post-Sputter Analyses (313 days after plating)	
						Sn Isotope Relative Percentages Found on Nodule		Range of Sn Isotope Relative Percentages Found on Nodule	
				%Sn^{120}	%Sn^{118}	%Sn^{120}	%Sn^{118}	%Sn^{120}	%Sn^{118}
89	Nodule at Base of Whisker 7	Sn^{120}/Sn^{118} Double Layer	Bright	69	31	65	35	68 to 60	32 to 40
89	Nodule at Base of Whisker 22	Sn^{120}/Sn^{118} Double Layer	Bright	69	31	67	33	75 to 64	25 to 36
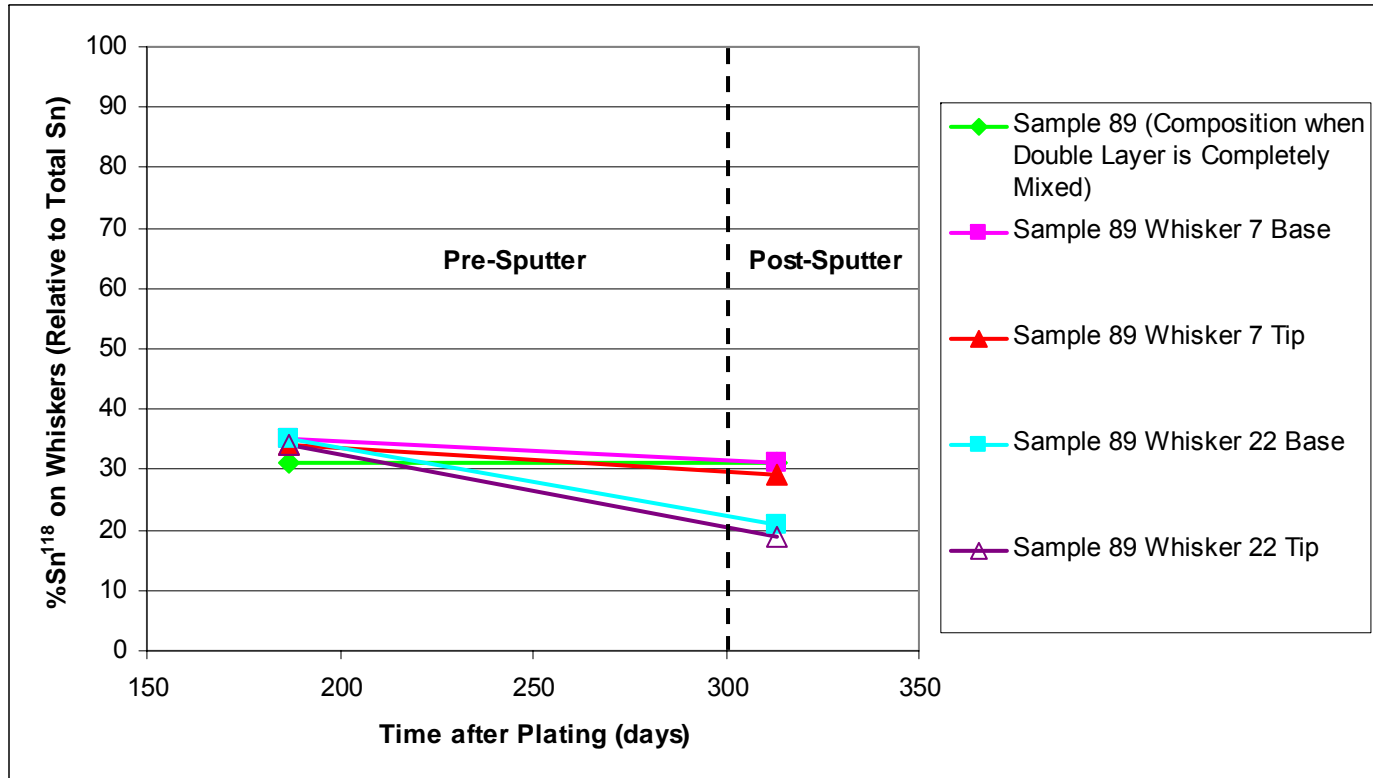
Figure 60. Relative Percentages of Sn^{118} found before and after Sputtering of Whiskers on the Bright Tin Double Layer (Sample 89, Data is from Table 8)
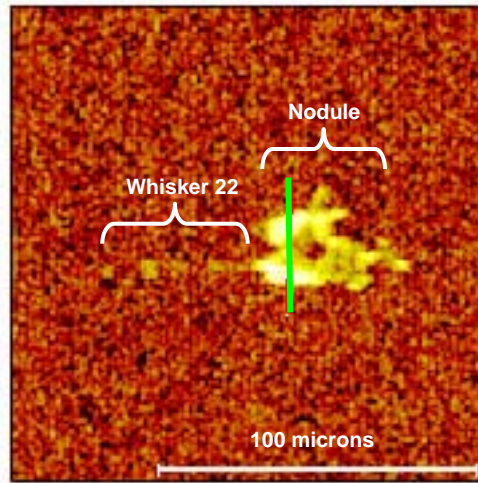
Figure 61. TOF-SIMS Sn^{120} Negative Ion Image of the Nodule at the Base of Whisker 22 after Sputtering (Sample 89, Bright Tin Plating). The Green Line is a Line Scan.
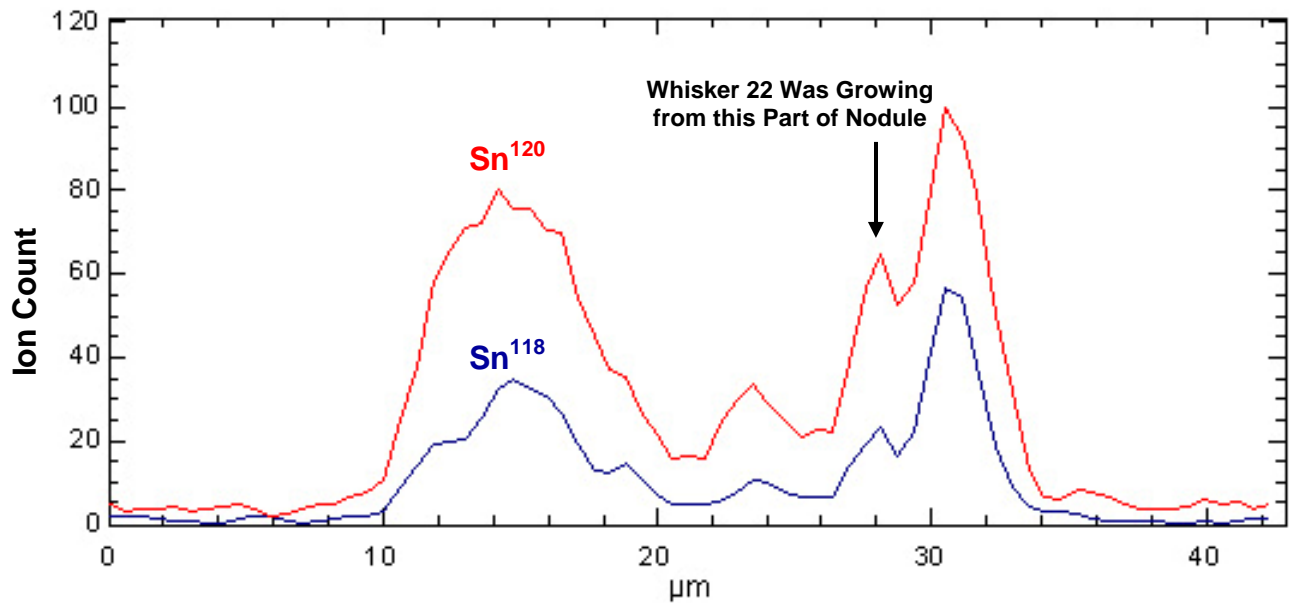

Figure 62. Sn^{120} Line Scan and Sn^{118} Line Scan of the Nodule at the Base of Whisker 22 after Sputtering (See Figure 61)